

72-4547

LENTZ, Ronald Raymond, 1943-
A NUMERICAL STUDY OF ELECTROMAGNETIC
SCATTERING FROM OCEAN-LIKE SURFACES.

The Ohio State University, Ph.D., 1971
Engineering, electrical

University Microfilms, A XEROX Company, Ann Arbor, Michigan

**A NUMERICAL STUDY OF ELECTROMAGNETIC
SCATTERING FROM OCEAN-LIKE SURFACES**

A DISSERTATION

**Presented in Partial Fulfillment of the Requirements for
the Degree Doctor of Philosophy in the Graduate
School of The Ohio State University**

By

Ronald Raymond Lentz, B.E.E., M.Sc.

**The Ohio State University
1971**

Approved by

Willie H. Peake
Adviser

**Department of
Electrical Engineering**

PLEASE NOTE:

**Some pages have light
and indistinct print.
Filmed as received.**

UNIVERSITY MICROFILMS.

ACKNOWLEDGMENTS

The author wishes to express his sincere gratitude to all those persons at the ElectroScience Laboratory and Computer Center who aided in the completion of this study. Special acknowledgment is extended to my advisor, Dr. William Peake, for his guidance and help. Finally, Dr. J. H. Richmond deserves thanks for many interesting conversations about computer techniques.

The work reported in this dissertation was supported in part by Contract NAS1-9998 between the National Aeronautics and Space Administration and The Ohio State University Research Foundation.

VITA

November 18, 1943 Born - Columbus, Ohio

June 1966..... B.E.E., The Ohio State University
Columbus, Ohio
Graduate Research Assistant, Antenna Laboratory,
The Ohio State University, Columbus, Ohio

September 1966 -
September 1970... National Science Foundation Traineeship,
The Ohio State University, Columbus, Ohio

1970..... Graduate Research Associate,
ElectroScience Laboratory,
The Ohio State University, Columbus, Ohio

LIST OF ILLUSTRATIONS

Figure		Page
1.	The scattering surface	3
2.	Ray tube geometry	6
3.	Specular point geometry	8
4.	Far field scattering geometry	11
5.	Geometry for specular point location	13
6.	Specular point shadowing	16
7.	Specular points on a sinusoidal surface	19
8.	Geometry for T.M. physical optics	22
9.	Geometry for T.E. physical optics	24
10.	Optically invisible surface currents	26
11.	Shadowing at the right end point	27
12.	Illustration of shadowed and illuminated zones	28
13.	Geometry for T.M. scattering	35
14.	Modification of true contour to a shortened contour	37
15.	Approximation of the surface current	39
16.	Breakdown of surface into segments of length DC	42
17.	Contour and tapering function used to test the shortened contour assumptions	49
18.	Scattered field with and without extended boundaries, T.M. case	50
19.	Geometry for wedge test	51

LIST OF ILLUSTRATIONS (Cont.)

Figure		Page
20.	Computed $ J_s $ on a wedge, T.M. case	52
21.	Wedge scattered fields, T.M. case	52
22.	Three dimensional geometry for T.E. integral equation	53
23.	Two dimensional geometry for T.E. integral equation	54
24.	Open contour	55
25.	Geometry for calculation of far field scattering, T.E. polarization	58
26.	Scattered field with and without extended boundaries, T.E. Case	62
27.	Computed $ J_s $ near corner of a 90° wedge, T.E. polarization	63
28.	Wedge scattered fields, T.E. case	63
29.	Scattering from $50 \cos(2\pi x/800)$ as calculated by I.E., P.O., and G.O.; T.M. polarization	66
30.	Scattering from $50 \cos(2\pi x/800)$ as calculated by I.E., P.O., and G.O.; T.E. polarization	67
31.	Limitation of scattering directions predicted by geometrical optics	68
32.	Scattered fields predicted by P.O., G.O., and I.E. methods for $H(x) = 5 \sin(2\pi x/200)$, T.M. polarization	70
33.	Scattered fields predicted by P.O., G.O., and I.E. methods for $H(x) = 5 \sin(2\pi x/200)$, T.E. polarization	71
34.	Scattered fields predicted by P.O., G.O., and I.E. methods for $H(x) = 15 \sin(2\pi x/200)$, T.M. polarization	72
35.	Scattered fields predicted by P.O., G.O., and I.E. methods for $H(x) = 15 \sin(2\pi x/200)$, T.E. polarization	73
36.	Scattered fields predicted by P.O., G.O., and I.E. methods for $H(x) = 25 \sin(2\pi x/200)$, T.M. polarization	74

LIST OF ILLUSTRATIONS (Cont.)

Figure		Page
37.	Scattered fields predicted by P.O., G.O., and I.E. methods for $H(x) = 25 \sin(2\pi x/200)$, T.E. polarization	75
38.	Agreement of geometrical and physical optics when they are incorrect	77
39.	Perturbation theory test	80
40.	Sea surface height spectrum	81
41.	Expected value of backscattered $ E_2^S ^2$ from ensemble	82
42.	Storing a symmetric matrix in a linear array	130

TABLE OF CONTENTS

	Page
ACKNOWLEDGMENTS.....	ii
VITA.....	iii
LIST OF ILLUSTRATIONS.....	iv
 Chapter	
I. INTRODUCTION.....	1
II. THE GEOMETRICAL OPTICS METHOD.....	6
A. <u>Geometrical Optics</u>	6
B. <u>Discussion of the Geometrical Optics Program</u>	13
C. <u>Using the Geometrical Optics Program</u>	18
III. THE PHYSICAL OPTICS METHOD.....	20
A. <u>The Physical Optics Approximation</u>	20
B. <u>Discussion of the Physical Optics Computer Programs</u>	26
C. <u>Comments on the Use of the Physical Optics Programs</u>	30
IV. THE INTEGRAL EQUATION METHOD.....	32
A. <u>Moment Methods</u>	32
B. <u>Integral Equation for Transverse Magnetic Polarization</u>	35
C. <u>Discussion of the Computer Program for Transverse Magnetic Polarization</u>	41
D. <u>Tests of the Transverse Magnetic Integral Equation Programs</u>	48
E. <u>Integral Equation for Transverse Electric Polarization</u>	53
F. <u>Discussion of the Computer Program for the Transverse Electric Polarization</u>	59
G. <u>Tests of the Transverse Electric Integral Equation Programs</u>	61
V. APPLICATIONS.....	65

TABLE OF CONTENTS (Cont.)

Chapter	Page
VI. SUMMARY AND CONCLUSIONS.....	83
Appendix	
A. COMPUTER PROGRAMS.....	85
B. SOLUTION OF SYSTEMS OF SIMULTANEOUS LINEAR EQUATIONS.	125
REFERENCES.....	132

CHAPTER I

INTRODUCTION

The scattering of electromagnetic waves from the ocean surface has been of great interest for some time. In this work the scattering from one dimensional sea-like random surfaces is examined by a variety of computational methods, with a view to establishing what practical limitations must be satisfied on such surface parameters as radius of curvature, mean squared height, etc., in order that the statistical properties of the scattered radiation may be calculated with reasonable accuracy. The results of the computations are then used to discuss the applicability of the several theoretical models for sea-surface scattering (geometrical optics, physical optics, perturbation theory and the composite model) and the prospect for direct calculation of the scattered fields from the actual sea surface.

During the past few years, theoretical and experimental work here and abroad (Refs. [1]-[7]) has led to an understanding of the mechanisms responsible for scattering and emission of microwaves by the ocean. For off-normal backscatter, the "Bragg-scatter" from capillary and short wavelength components of the ocean surface, which can be calculated by perturbation theory, has explained the angular

and polarization dependence of the microwave radar return. When combined with the known height spectrum (Ref. [8]) of the ocean surface, it explains the weak dependence of backscatter on electromagnetic wavelength and wind velocity. Near the specular direction, i.e., near normal incidence for backscatter, the scattering is controlled by the slope distribution of the large scale structure of the surface. This part of the scattering is calculated by geometrical optics, and explains the dependence of the emissivity of the surface on wind velocity.

Nevertheless, the many assumptions required in finding the scattered fields by the perturbation or geometrical optics approximations, particularly assumptions about the Gaussian character of the surface height statistics, and the applicability of the theoretical approximations to the actual sea surface, have led to considerable discussion about the validity of the various theoretical solutions (Ref. [9]). Since straightforward verification by measurement is not practical, partly because of difficulty in the measurement process itself and partly because of the difficulty in specifying exactly what the surface was when the measurement was being made, it is desirable to have a direct method for calculating the scattering from a specific realization of the ocean surface. Direct calculations will allow a realistic assessment of the validity of the various theories, without any assumptions about the statistical properties of the surface. If a statistical average of the scattered fields over an ensemble of surface representations is required, it can be obtained (albeit at

some cost.) by a direct summation of the scattered fields from the individual surface representations.

The specific surfaces considered here are cylindrical perfectly conducting surfaces as shown in Fig. 1. The surface generators are

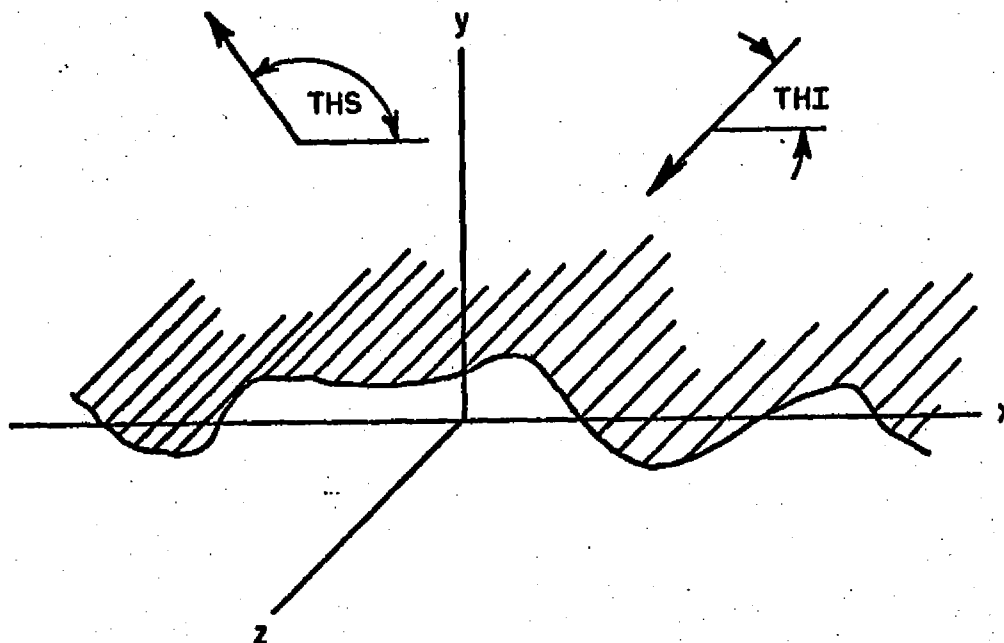


Fig. 1.--The scattering surface.

parallel to the z axis, and the surface elevation is specified by $y = H(x)$. The incident field is a plane wave whose direction of propagation lies in the x,y plane and makes an angle of TH_I with the positive x axis, while the observation direction makes an angle of TH_S with the positive x axis. Time dependence is assumed to be $e^{j\omega t}$ and has been suppressed throughout. All distances are measured in centimeters.

Three different methods for calculating the fields from such a surface are developed here. Although the details are discussed later it is desirable to outline each technique at this time.

The first approximate method is the geometrical optics technique (G.O.). For a given surface, and given scattering and incidence angles, the program locates the specular points on the surface (points where the local incidence angle equals the local scattering angle) and evaluates the radius of curvature at each specular point. The scattered far field is then found by summing the contribution from each of the specular points, including an extra 90° phase shift for the fields scattered from concave up portions of the surface. Shadowing of one section of the surface by another section may be taken into account.

The next approximation is the physical optics (P.O.) technique. For a given surface the scattered field is computed by integrating over the approximate surface current

$$(1) \quad \mathbf{J}_s = 2\hat{n} \times \mathbf{H}^i$$

where \hat{n} is the outward normal to the surface and \mathbf{H}^i is the incident magnetic field. Shadowing is always taken into account, as this is implicit in the physical optics formulation.

The last method developed here is based on a point matching solution to the integral equation satisfied by the true surface current \mathbf{J}_s . The scattered fields are then found by integrating over the surface currents. Test cases (e.g., the wedge problem) have shown this method to be by far the most accurate; hence it is used as a standard to which all others are compared. However, because of computer storage limitations, this program can not handle surfaces whose arclengths are greater than ~ 60 electrical

wavelengths, whereas the G.O. and P.O. programs can, in principle, handle surfaces of any length provided sufficient computer time is available.

In order to avoid edge effects, tapering of the incident field is necessary in the integral equation solutions. The same tapering has been applied in both the G.O. and P.O. solutions so that they can be directly compared to the exact fields. The tapering applied here is illustrated in Fig. 14 of Chapter IV.

In the succeeding chapters each of these methods will be described in detail. By comparing the results for a series of test surfaces, the limitations of each method are established.

CHAPTER II
THE GEOMETRICAL OPTICS METHOD

The first approach to examining the scattering from a one dimensional rough surface is the geometrical optics method. By this is meant that the scattered field is computed by finding the specular points on the surface, and associating with each such point a scattered field amplitude and phase which depend on the geometrical properties of the surface at the specular point.

A. Geometrical Optics

Conservation of energy flux along a ray path will provide us with the geometrical optics field strengths (Ref. [10]).

Consider the two dimensional ray tube shown in Fig. 2. If u_0 is the field strength at some reference point at a distance ρ from the caustic and u is the field strength at distance $\rho + \ell$ from the caustic, then the conservation of energy in the ray tube requires

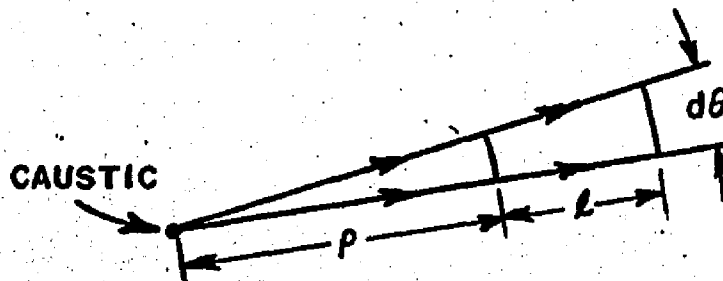


Fig. 2.--Ray tube geometry.

$$(2) \quad u_0^2 \rho \, d\theta = u^2 (\rho + \ell) \, d\theta$$

so that one may write

$$(3) \quad u(\ell) = u_0 \sqrt{\frac{\rho}{\rho + \ell}} e^{-jk\ell}.$$

The factor $e^{-jk\ell}$, with λ_e the electrical wavelength and

$$(4) \quad k = 2\pi/\lambda_e$$

accounts for the phase shift between ρ and $\rho + \ell$. Equation (3) fails at ℓ equal to $-\rho$. This location (at the confluence of the rays) is termed a caustic. Kay and Keller (Ref. [11]) have demonstrated that at points beyond the caustic (ℓ less than $-\rho$) Eq. (3) is still valid if a phase shift of $+90^\circ$ is introduced.

To use geometrical optics it is necessary to find all points on the scattering body at which the law of reflection is satisfied locally for the particular set of THI and THS under consideration. Once these points are located Eq. (3) is used to calculate the scattered field. Figure 3 shows the geometry for the calculation of the scattered field from one such specular point. By the law of reflection, the local incidence and scattering angles are equal and are marked ANG in the figure. The distances marked r_c and ρ are the radius of curvature and the distance from the specular point to the optical image of the source (i.e., the caustic distance) respectively. The distance ρ is given by a cylindrical mirror formula as

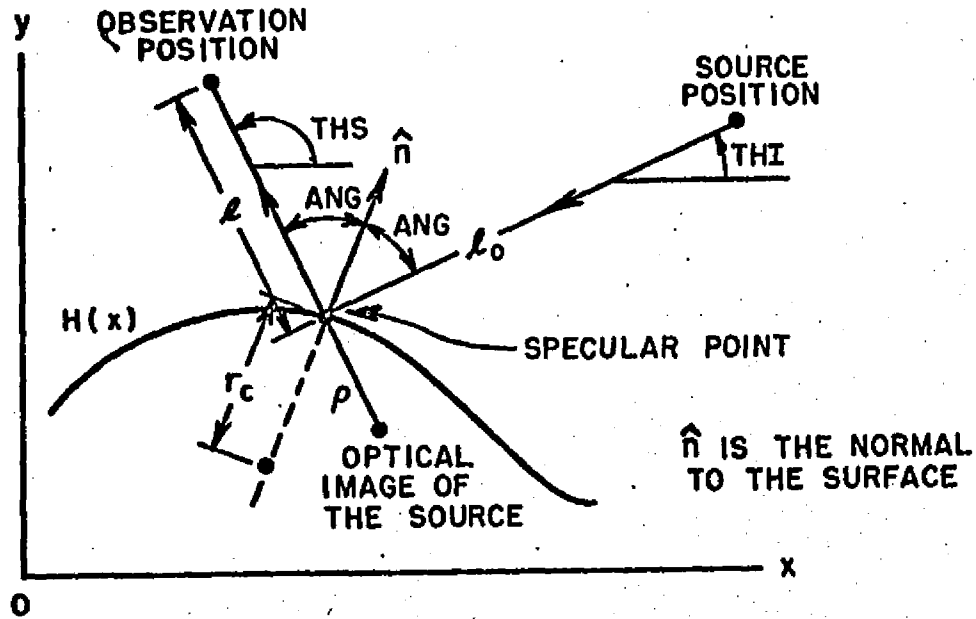


Fig. 3.--Specular point geometry.

$$(5) \quad \frac{1}{\rho} = \frac{2}{|r_c| \cos(\text{ANG})} + \frac{1}{\ell_0}.$$

In the cases considered here the distance to the line source, ℓ_0 , will be assumed to be infinite, hence

$$(6) \quad \rho = \frac{|r_c| \cos(\text{ANG})}{2}.$$

If the specular point is taken as the reference position then Eq. (3) gives u_s , the scattered field at the observation position

$$(7) \quad \begin{aligned} u_s &= R u_1 \sqrt{\frac{\rho}{\rho + \ell}} e^{-jk\ell} \\ &= R u_1 \sqrt{\rho} e^{-jk\ell} / \sqrt{\ell} \text{ for } \ell \gg \rho \text{ (far field)} \end{aligned}$$

where u_i is the incident field evaluated at the specular point and R is a reflection coefficient. If the electric field is parallel to the surface generators (T.M. case) and u_i is taken as the incident electric field, then u_s is taken as the scattered electric field with $R = -1$. If the magnetic field is parallel to the surface generators (T.E. case) and u_i is taken as the incident magnetic field, then u_s is the scattered magnetic field and $R = +1$. For dielectric scatterers the corresponding Fresnel reflection coefficients are to be used for R . This makes the geometrical optics program the easiest to convert from perfectly conducting bodies to penetrable bodies.

Up to this point the scattering surface has been assumed to be concave down at the specular point. If the body is concave up at the specular point then the caustic position is above the surface instead of below, the scattered rays pass through the caustic on the way to the observation point if the observer is in the far field, and thus a phase shift of +90 degrees must be introduced. The distant scattered fields may then finally be written

$$(8) \quad E_Z^S(\ell) = -E_Z^i \Big|_{\text{Specular Point}} \sqrt{\frac{|r_c| \cos(\text{ANG})}{2}} \frac{e^{-jk\ell}}{\sqrt{\ell}} \epsilon$$

for the T.M. case and

$$(9) \quad H_Z^S(\ell) = H_Z^i \Big|_{\text{Specular Point}} \sqrt{\frac{|r_c| \cos(\text{ANG})}{2}} \frac{e^{-jk\ell}}{\sqrt{\ell}} \epsilon$$

for the T.E. case, where ϵ is +1 if the surface is concave down at the specular point and +j if the surface is concave up at the specular point.

On an actual surface there may be several specular points contributing to the total scattered field, so it is important to preserve the phase relationships among them. Phase reference is taken at the origin, and an incident wave of unit amplitude is assumed, i.e.,

$$(10) \quad E_z^i = e^{-j\bar{k} \cdot \bar{R}} \quad (\text{T.M. case})$$

$$(11) \quad H_z^i = e^{-j\bar{k} \cdot \bar{R}} \quad (\text{T.E. case})$$

where

$$(12) \quad \bar{k} \cdot \bar{R} = \frac{2\pi}{\lambda_e} (-x \cos(\text{THI}) - H(x) \sin(\text{THI})).$$

With the aid of the geometry shown in Fig. 4, the scattered far field is found from Eqs. (8) and (9), with $\epsilon = \epsilon_1 + \epsilon_2$, where

$$(13) \quad \epsilon_2 = -\bar{R} \cdot \hat{D}_s = -x \cos(\text{THS}) - H(x) \sin(\text{THS}),$$

and

$$(14) \quad \hat{D}_s = \cos(\text{THS})\hat{x} + \sin(\text{THS})\hat{y}$$

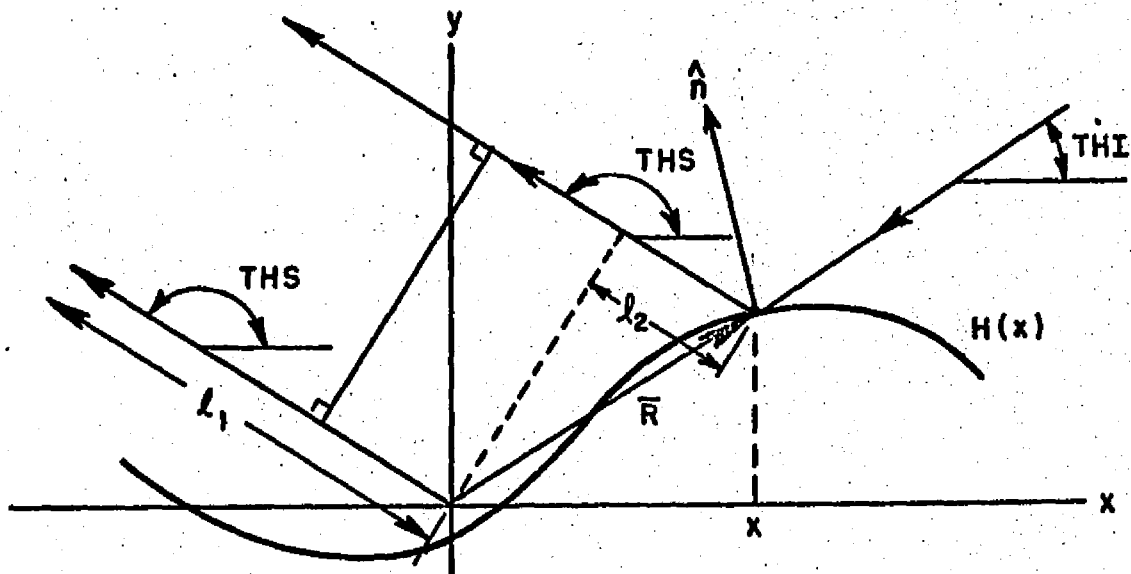


Fig. 4.--Far field scattering geometry.

is the unit vector in the scattering direction. Since $l_1 \gg l_2$, Eq. (8) becomes, for the T.M. case

$$(15) \quad E_z^S(l_1) = - \sqrt{\frac{|r_c| \cos(\text{ANG})}{2}} \frac{e^{-jk l_1}}{\sqrt{l_1}} e^{jkQ(x)}$$

where

$$(16) \quad Q(x) = x (\cos(\text{THI}) + \cos(\text{THS})) + H(x) (\sin(\text{THI}) + \sin(\text{THS})).$$

Similarly, for the T.E. case

$$(17) \quad H_z^S(l_1) = \sqrt{\frac{|r_c| \cos(\text{ANG})}{2}} \frac{e^{-jk l_1}}{l_1} e^{jkQ(x)}$$

The total scattered field in the THS direction is the sum of the fields scattered by each of the specular points. The numerical values of the scattered fields as calculated by the programs of Appendix A, and plotted in the various figures of Chapter V are denoted by E_Z^S and H_Z^S , and have been normalized with respect to the actual fields $E_Z^S(\rho_1), H_Z^S(\rho_1)$ by

$$(18) \quad \begin{Bmatrix} E_Z^S \\ H_Z^S \end{Bmatrix} = \sqrt{\rho_1} e^{jk\rho_1} \begin{Bmatrix} E_Z^S(\rho_1) \\ H_Z^S(\rho_1) \end{Bmatrix} .$$

It is clear that Eqs. (15) and (17) fail if the radius of curvature is infinite at the specular point. This is because the source was assumed at infinity, i.e., $\rho_0 \rightarrow \infty$. If ρ_0 were to be held finite then from Eq. (5)

$$(19) \quad \lim_{r_c \rightarrow \infty} = \rho_0$$

and the singularity in Eqs. (15) and (17) would not occur. In addition to the singularities caused by an infinitely distant source, there are a number of other shortcomings of the G.O. approximation. Among them are: a failure to account for wedge diffraction effects (radius of curvature goes to zero), a failure to account for diffraction from shadow boundaries into shadowed regions (Ref. [12]), a failure to properly predict the scattered fields if the surface

features subtend only a few Fresnel zones (Ref. [13]), and finally a failure to predict any scattered field if no specular point exists on the body.

Implicit in the geometrical optics technique is the concept of shadowing, that is, a specular point cannot contribute to the scattered field unless it can be seen by both the source and the observer. The program developed here can account for shadowing of this type.

B. Discussion of the Geometrical Optics Program

For geometrical optics calculations the first order of business is the location of the specular points. Figure 5 shows the geometry.

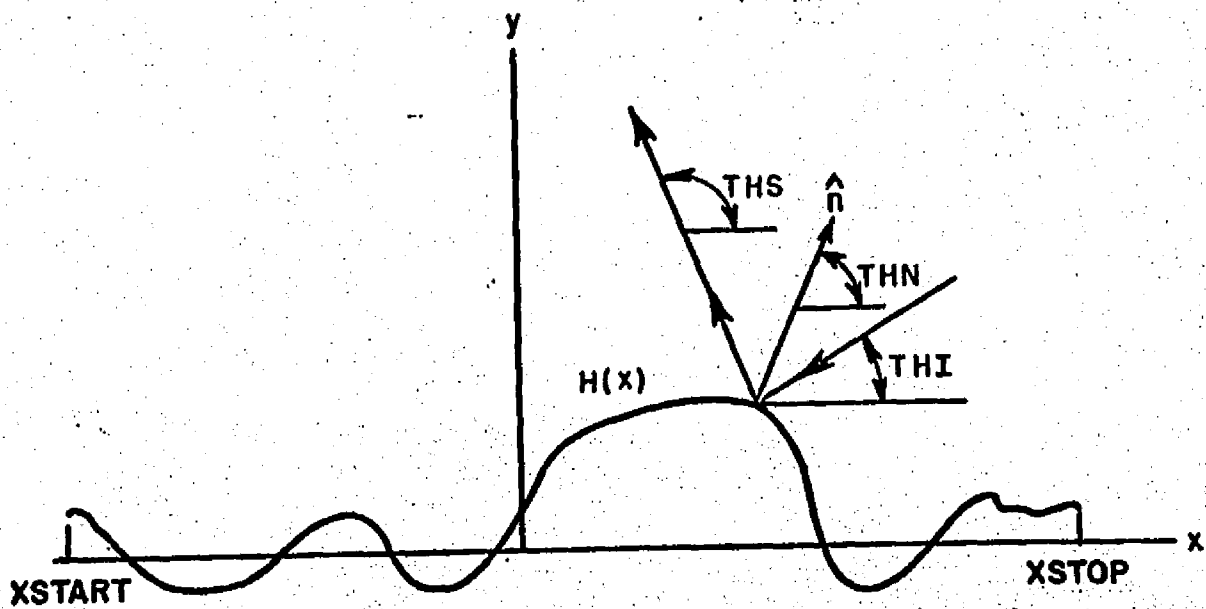


Fig. 5.--Geometry for specular point location.

The surface height profile is described by $H(x)$ and the regions under investigation lies between X_{START} (X_{START}) and X_{STOP} . θ_{HI} and θ_{HS} have already been defined; θ_{HN} (θ_{HN} (THETA of the NORMAL)) is the angle between the normal (\hat{n}) to the surface and the positive x axis.

Clearly

$$(20) \quad \text{THN}(x) = \pi/2 + \text{Tan}^{-1} (dH(x)/dx).$$

The law of reflection gives $(x, H(x))$ as a specular point when

$$(21) \quad \text{THS} - \text{THN}(X) = \text{THN}(X) - \text{THI}$$

i.e.,

$$(22) \quad (\text{THS} + \text{THI})/2 = \text{THN}(X).$$

The program calculates the function

$$(23) \quad E(X) = (\text{THS} + \text{THI})/2 - (\pi/2 + \text{Tan}^{-1} (dH(X)/dx))$$

for many points in the interval $(X\text{STRT}, X\text{STOP})$ and when this function changes sign a specular point has been located. The collection of points so located is stored in an array $XN(J)$. To save running time two searches are made, first a coarse grain search and then, in the neighborhood of each specular point, a finer grain pass is made.

The search must satisfy two requirements. First, it must be fine enough to locate all specular points; this requires that the surface must be sampled often enough to get an adequate description of its structure. For example if the surface were described by a Fourier series then one would expect that sampling every twentieth of the minimum mechanical wavelength would be sufficient. Secondly, the specular positions must be located to within a small fraction of an electrical wavelength so that the phase relationships among the various specular points are correctly maintained. In the light of

these considerations a first search might be made at a step size of (the minimum mechanical wavelength)/20. The fine grain search would then be made with a step size of say $(\lambda_e/20.0)$ or (1st step size/2.0) whichever is the smallest. In the program, the coarse step size is called DLTA (DELTA X) and the fine step size is called DLTA00. The local angle of incidence for each specular point is stored in an array ANG(J). This angle is used in the computation of the scattered field and is shown in Fig. 5. Once a complete pass is made over the surface, the scattered fields are computed. It should be noted that whenever any one of THI, THS, H(X) is changed, the complete pass must be made again.

The actual program, given in Appendix A, makes the scattered field computation for two cases:

- 1) all specular points contributing,
- 2) scattering from concave up specular points neglected when calculating the scattered field.

The second case, clearly incorrect, was an attempt to see how the computed fields would correspond to the results of certain statistical theories which neglect the concave up specular points. In the program the electric field calculated from the first case is called ESCNS (ELECTRIC FIELDS SCATTERED WITH NO SHADOWING) and from the second case ESCDNS (ELECTRIC FIELD SCATTERED FROM CONCAVE DOWN POINTS WITH NO SHADOWING).

Geometrical optics allows shadowing to be taken into account without much extra effort. The three types which may occur (specular point not illuminated by source, specular point not visible

to observer, both) are shown in Fig. 6. Each point in the array of specular points, XN , is examined for inbound shadowing in the following way. A line is passed through the specular point XN_j , $H(XN_j)$ with slope $\tan(\text{THI})$. The equation of the line is

$$(24) \quad YI(X) = \text{Tan}(\text{THI})x + (H(XN_j) - \text{Tan}(\text{THI}) XN_j)$$

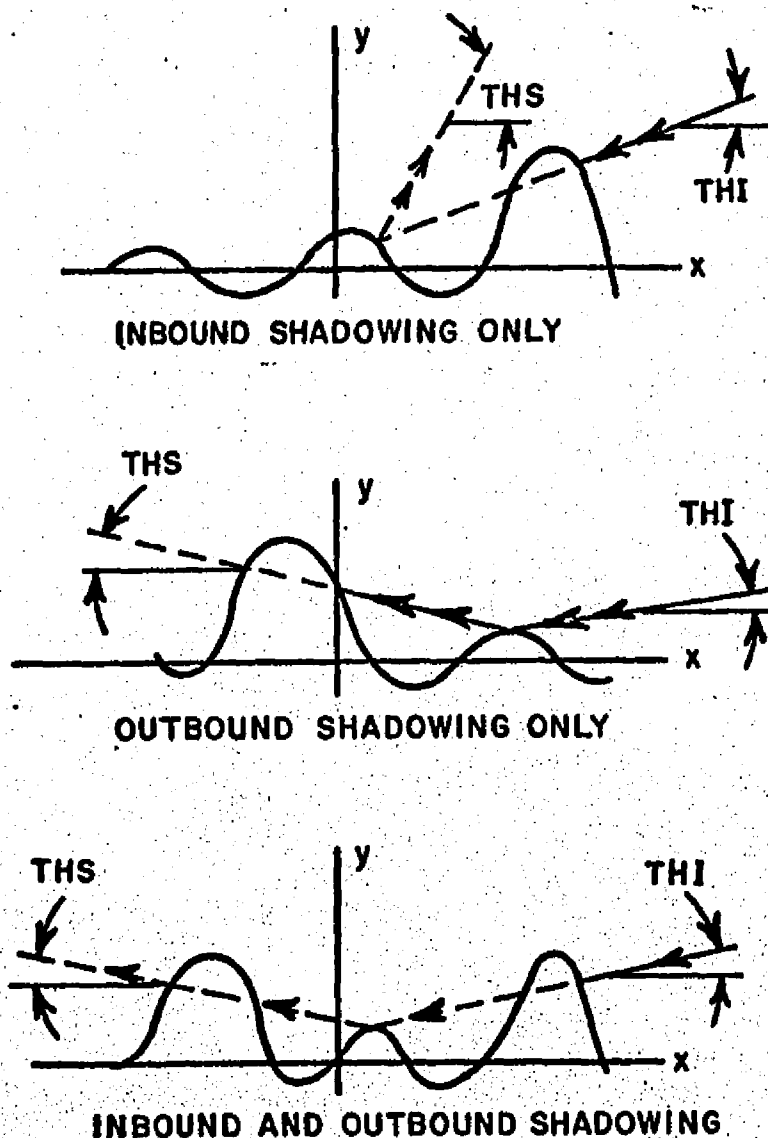


Fig. 6.--Specular point shadowing.

Then x is incremented in the proper direction until one of the following occurs. The first possibility is that at some point x , $YI(x)$ becomes greater than the maximum value that $H(x)$ can attain for any value of x in the interval $XSTRT, XSTOP$. This value of $H(x)$ is called $HMAX$ and must be supplied for each surface being considered. If the surface is a sum of sinusoids then $HMAX$ is equal to the sum of the individual magnitudes. The second possibility is that at some point the value of x is incremented out of the interval ($XSTRT, XSTOP$) being considered. The third and final possibility is that at some point x the line $YI(x)$ intersects the surface profile $H(x)$. When the first or second case occurs the specular point is not shadowed. In the third case the specular point is inbound shadowed and for that particular j , $XN(j)$ is set equal to a number much larger than $XSTOP$. This allows XN_j to be skipped when the contribution from each of the specular points is being computed. A very similar test is applied for outbound shadowing.

When both the inbound and the outbound shadowing tests are completed the array of specular point positions contains values which are either in the range $XSTRT < X < XSTOP$ or $XN_j >> XSTOP$. The scattered field is calculated as in the case where shadowing is neglected except that when $XN_j > XSTOP$ the field from this specular point is not put into the sum. The scattered field with shadowing accounted for is called ESCWS (ELECTRIC FIELD SCATTERED WITH SHADOWING) and the scattered field calculated with only concave down non-shadowed specular points contributing is called ESCD.

C. Using the Geometrical Optics Program

While the storage requirement is minimal, the running time of this program depends largely on the step sizes which have to be used during the search for the specular points, and the number of scattering angles. This means that as the length of the surface increases, the time per pass required to find the specular points goes up and the number of passes over the surface also increases, since to see detail in the scattered field pattern the scattering angle must be examined at a larger number of points (finer grain). The half-power beamwidth of a uniformly illuminated aperture of width $X_{STOP}-X_{STRT}$,

$$(25) \quad \text{beamwidth} \approx \frac{0.88 \lambda_e}{X_{STOP} - X_{STRT}} \text{ radians}$$

affords a crude estimate of the fineness of the grain which must be taken. The increment in THS should be less than a fifth of this.

The program has been checked for several cases, two of which will now be mentioned. The simplest check was the comparison with hand calculations for a surface described by

$$(26) \quad H(x) = 50 \cos(2\pi x/800)$$

with x in the range $(-200, 200)$. This surface has only one specular point or none at all depending upon TH1 and THS. Another check was performed for a sinusoidal surface like the one shown in Fig. 7.

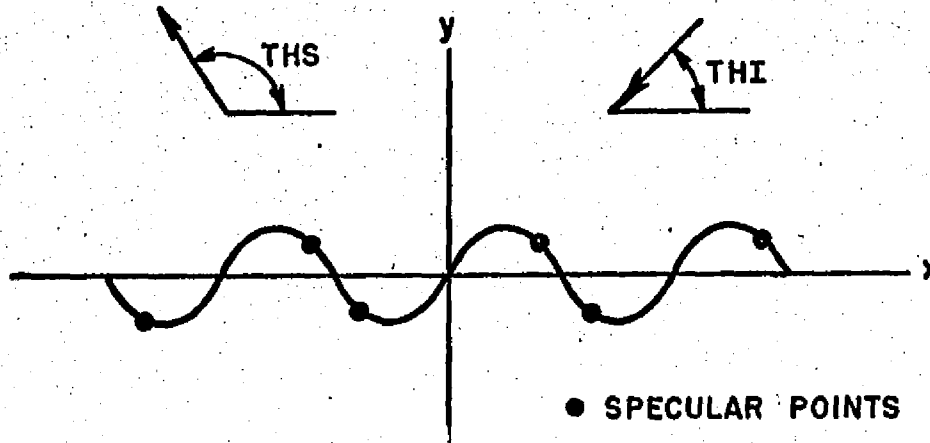


Fig. 7.--Specular points on a sinusoidal surface.

In this case the specular return comes from a collection of regularly spaced points which look like a pair of linear arrays of point sources. The program found the specular points and calculated the total scattered field correctly.

CHAPTER III
THE PHYSICAL OPTICS METHOD

The next complexity of approximation to the scattered fields to be considered here is given by the physical optics method.

A. The Physical Optics Approximation

Physical optics (P.O.), (Ref. [14]), approximates the true surface currents on a perfectly conducting body by the currents

$$(27) \quad \mathbf{J}_s = \begin{cases} 2\hat{\mathbf{n}} \times \mathbf{H}^i & \text{on the portions of the surface which are} \\ & \text{illuminated} \\ \mathbf{0} & \text{on the portions of the surface which are} \\ & \text{shadowed} \end{cases}$$

where $\hat{\mathbf{n}}$ is the outward normal to the surface and \mathbf{H}^i is the incident magnetic field evaluated at the surface. These approximate currents are then used in the radiation integral to calculate the scattered fields. The P.O. surface current is exact if the scattering body is perfectly conducting half space and the incident field is a plane wave. As the surface curvature decreases the P.O. currents depart more and more from the true currents; as the curvature at some point on Nor do the scattered fields predicted by P.O. satisfy the reciprocity theorem except for backscattering. Nevertheless, the P.O. method has a significant advantage over G.O. in that the fields remain

bounded even if the radius of curvature of the surface becomes infinite. Hence the flat facets of a surface can be approximately handled.

Whether or not P.O. provides any more useful results than G.O. is a question of long standing, and the answer seems to depend upon the geometry of the scattering body (Ref. [15]). For the kind of surfaces considered here it will appear that P.O. gives a good approximation to the scattered fields over a significantly wider range of surface characteristics than G.O. It is important to note that in this work the far field radiation integral over the physical optics currents is evaluated numerically to give the scattered fields. Unlike a number of rough surface scattering theories (Ref. [16]), no stationary phase approximation to the far field radiation integral is used. It is well known (Ref. [17]) that when the stationary phase approximation must be made, one obtains the G.O. result and there is then no difference between the two approaches.

The far-zone scattered fields will now be calculated using the physical optics currents. In the T.M. case, (see Fig. 8) the incident electric field is a z polarized plane wave of unit magnitude and the incident magnetic field is

$$(28) \quad \vec{H}^i = e^{+jk(x\cos(\theta_{HI}) + H(x)\sin(\theta_{HI}))} [-\sin(\theta_{HI})\hat{x} + \cos(\theta_{HI})\hat{y}]/\eta$$

where η is the impedance of free space. Using Ref. [18] and the fact that the tangential electric field vanishes on the surface, the scattered electric field is given by

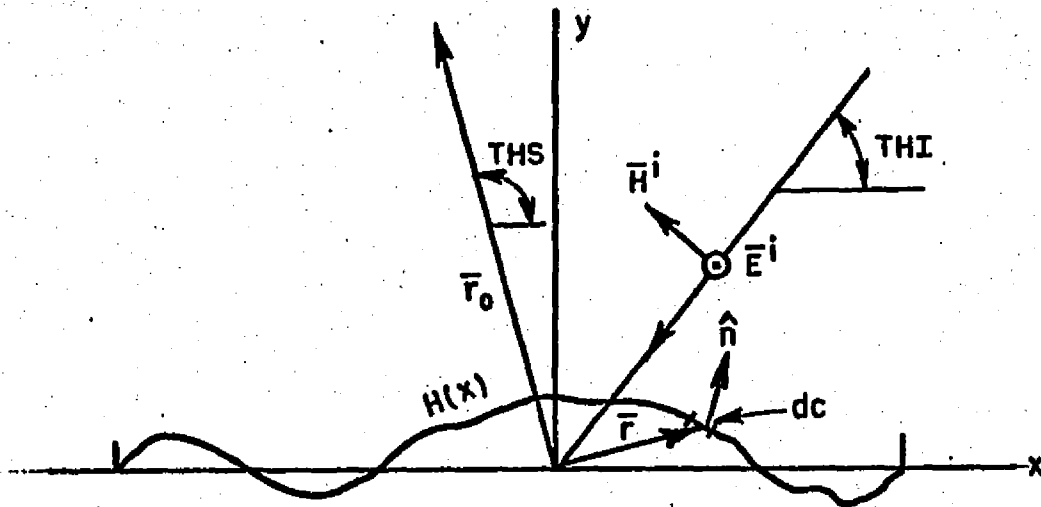


Fig. 8.--Geometry for T.M. physical optics.

$$(29) \quad E^S(\bar{r}_0) = -\frac{j\omega\mu_0}{2\pi} \int_{C_{ill}} \int_{-\infty}^{\infty} (\hat{n} \times \bar{H}^i) \frac{e^{-jk|\bar{r}-\bar{r}_0|}}{|\bar{r}-\bar{r}_0|} dz dc$$

where \bar{r}_0 is the position vector to the observation point, \bar{r} is the position vector of a point on the surface and \hat{n} is the unit outward normal to the surface. The notation C_{ill} indicates that the integration is to be carried out only over those portions of the contour which are optically illuminated.

Since \bar{H}^i and \hat{n} are independent of z one can show, by using an appropriate integral representation for the Hankel function (Ref. [19]), that the scattered field is

$$(30) \quad \bar{E}^S(\bar{\rho}_0) = - \frac{k\eta}{4} \int_{c_{111}} (2\hat{n}_x \bar{H}^1) H_0^{(2)}(k|\bar{\rho} - \bar{\rho}_0|) dc$$

where all variables are confined to the x,y plane

$$(31) \quad \bar{\rho}_0 = x_0 \hat{x} + y_0 \hat{y}$$

$$(32) \quad \bar{\rho} = x \hat{x} + y \hat{y}$$

and $H_0^{(2)}(x)$ is the Hankel function of the second kind and zero order. Using the large argument approximation for $H_0^{(2)}(x)$, the far field scattered electric field becomes

$$(33) \quad \bar{E}_z^S(\bar{\rho}_0) = - \left(\frac{2}{\pi k}\right)^{1/2} \frac{k}{2} e^{j\frac{\pi}{4}} \frac{e^{-jk|\bar{\rho}_0|}}{\sqrt{|\bar{\rho}_0|}} \int_{c_{111}} \sin(\pi H - \tan^{-1}(\dot{H})) e^{jkQ(x)} \sqrt{1+(\dot{H})^2} dx$$

where $H(x)$ describes the surface height profile,

$$(34) \quad \dot{H} = \frac{dH}{dx}$$

and $Q(x)$ is given by Eq. (16). As before, the factor

$$e^{-jk|\bar{\rho}_0|} / \sqrt{|\bar{\rho}_0|}$$

has been suppressed in both the computed and reported values of the scattered electric field, so that the actual field $E_z^S(\bar{\rho}_0)$ is related to the print out value E_z^S by

$$(35) \quad E_z^S = E_z^S(\bar{\rho}_0) \sqrt{|\bar{\rho}_0|} e^{+jk|\bar{\rho}_0|}$$

When the incident magnetic field is \hat{z} directed (transverse electric case) it is convenient to work with the scattered magnetic field. The latter is found from Ref. [20]

$$(36) \quad 4\pi \bar{H}^S(\bar{r}_0) = 2 \int_{-c_{i11}}^{\infty} \int_{-\infty}^{\infty} (\hat{n} \times \bar{H}^i) \times \bar{\nabla} \frac{e^{-jk|\bar{r}-\bar{r}_0|}}{|\bar{r}-\bar{r}_0|} dz dc$$

where \bar{H}^i is the incident magnetic field (see Fig. 9). The two dimensional far field scattering becomes from Eq. (36)

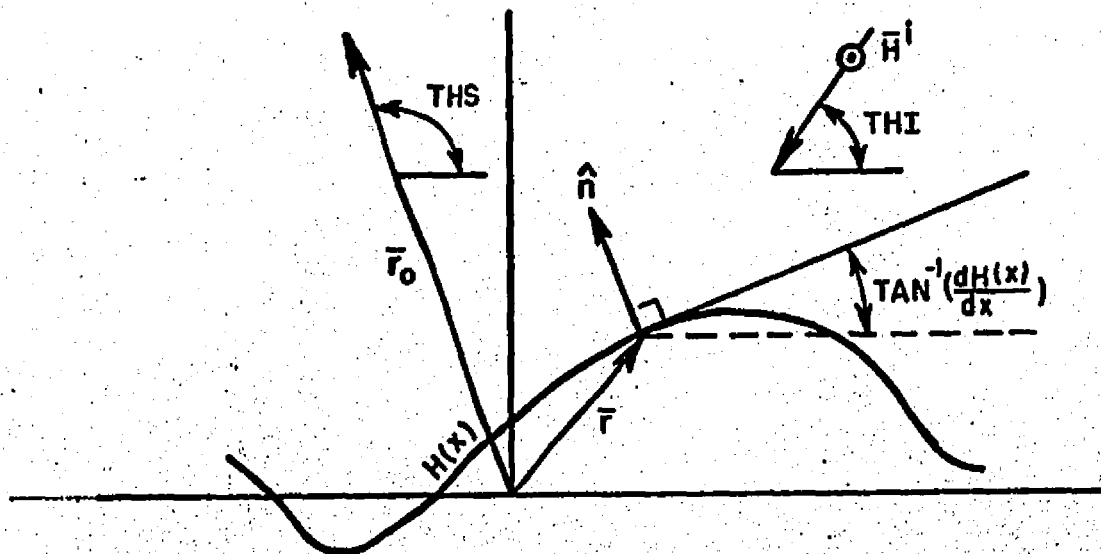


Fig. 9.--Geometry for T.E. physical optics.

$$(37) \quad H_z^S(\bar{\rho}_0) = \frac{e^{-jk|\bar{\rho}_0|}}{\sqrt{|\bar{\rho}_0|}} \frac{e^{j\frac{\pi}{4}}}{\sqrt{\lambda_e}} \int_{c_{111}} \sin(\tan^{-1}(\hat{H}) - THS) e^{jkQ(x)} \sqrt{1+\hat{H}^2} dx.$$

Again, the factor

$$\frac{e^{-jk|\bar{\rho}_0|}}{\sqrt{|\bar{\rho}_0|}}$$

is suppressed in the programs of Appendix A, so that the plotted or tabulated field strengths, H_z^S , are related to the true fields, $H_z^S(\bar{\rho}_0)$ by

$$(38) \quad H_z^S = H_z^S(\bar{\rho}_0) \sqrt{|\bar{\rho}_0|} e^{jk|\bar{\rho}_0|}.$$

There are two further considerations that may be discussed at this time. For bistatic scattering it may happen that not all of the currents set up on the surface by the incident field are optically visible to the observer (see Fig. 10). In the physical optics programs developed here no account was taken of this possibility. Obviously such considerations do not arise for backscattering.

So far, in this chapter a perfectly conducting surface has been assumed. Physical optics can be generalized to treat dielectric surfaces by using a pair of equivalent electric and magnetic surface

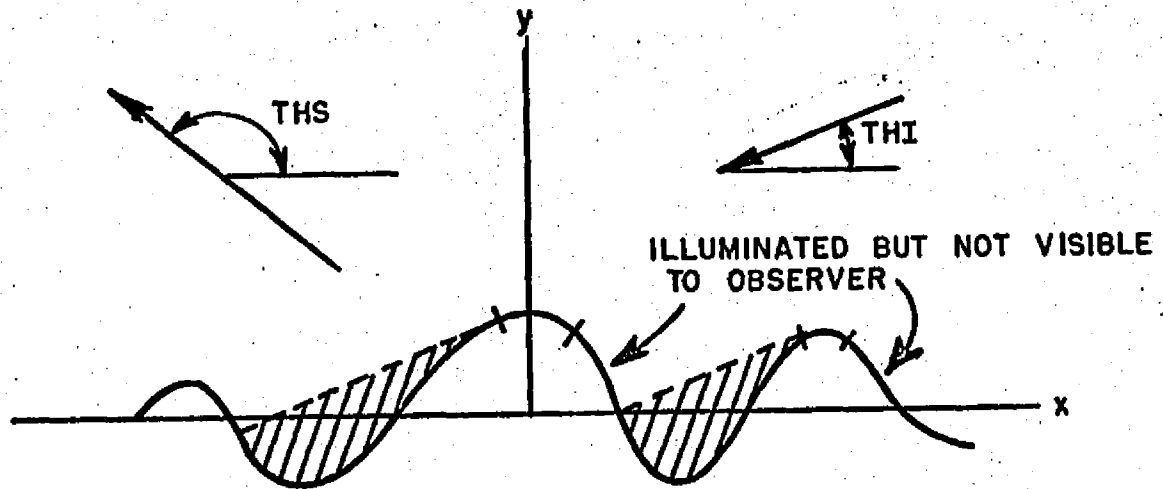


Fig. 10.--Optically invisible surface currents.

currents obtained from the fields of a plane wave incident on a dielectric half space (Ref. [21]). Since two integrations would be required to compute the scattered fields, it would seem that the running time should nearly double, but very little extra storage space would be required.

B. Discussion of the Physical Optics Computer Programs

For either polarization the physical optics program is divided into two parts. The first, and by far the most difficult, finds the shadow boundaries on the surface, since the integrations are to be performed only over the illuminated section of the contour. The second part performs the necessary integration to calculate the scattered far fields.

The program opens by considering the function $H(X)$ which describes the surface between the defined endpoints ALEP (Left End Point) and REP (Right End Point). The search for shadow boundaries begins at REP by determining whether or not the right endpoint casts a shadow on the surface and proceeds from right to left (see Fig. 11).

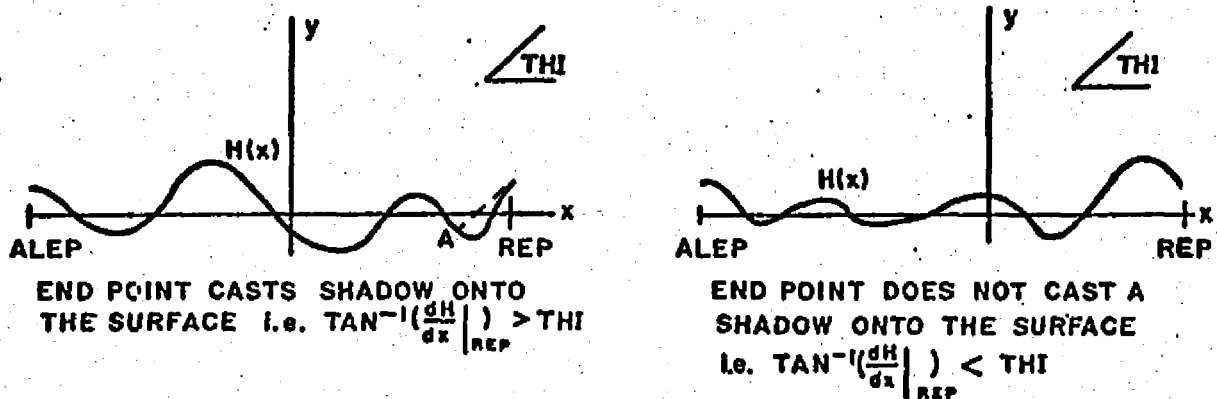


Fig. 11.--Shadowing at the right end point.

If THI (the incidence angle required to be less than 90°) is greater than 80° it is assumed that no shadowing occurs. The starting point of the illuminated zone (either REP or A of Fig. 11) is stored in the first position of an array called SX (Shadow boundaries X coordinate). The value of x is decremented until either a point on the surface is reached where the tangent-slope condition

$$(39) \quad \frac{dH}{dx} = \tan(\text{THI})$$

is satisfied, at which point a shadow zone begins, or x becomes less than ALEP, in which case the second entry in SX is ALEP. On the other hand if Eq. (39) is satisfied for some x between SX_1 and ALEP then this value of x is stored in SX_2 , a line with slope $\tan(\text{THI})$

is passed thru the point, and its intersection (if any) with $H(x)$ is found. If there are no such intersections, then all of the surface to the left of the point is shadowed. If an intersection does exist then the search for a point where the tangent-slope condition is satisfied begins again. This process continues until x is decremented past ALEP. The array SX thus stores the positions of points with an illuminated zone on their left in oddly subscripted locations and the points with an illuminated zone on their right in evenly subscripted locations (see Fig. 12). The size of the decrement used to locate the boundaries should be small enough to catch the surface features, and to locate the ends of the shadow zones within a fraction of a wavelength.

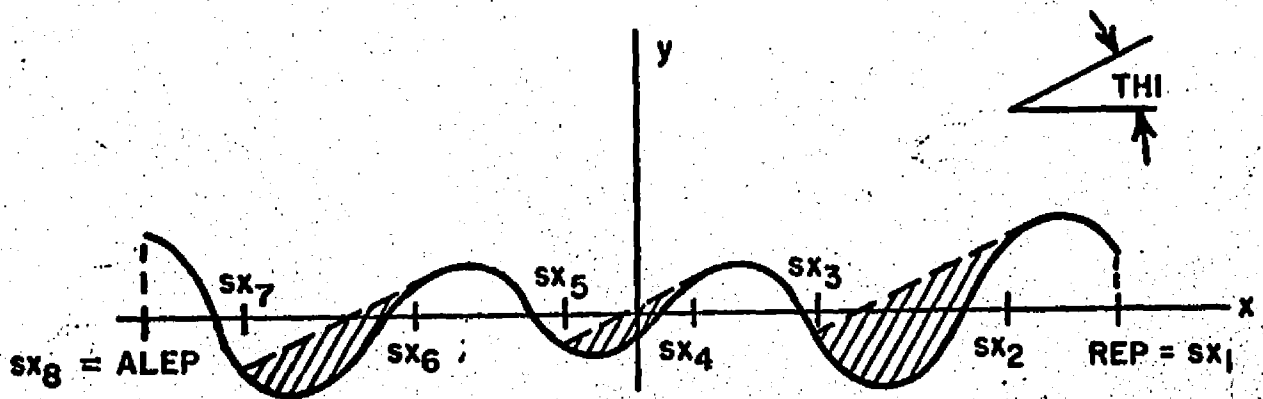


Fig. 12.--Illustration of shadowed and illuminated zones.

The integration over the illuminated sections of the surface to find the scattered fields is performed in a subroutine called BINT(XX,YY) (Bistatic radiation Integral) the arguments of which are the initial and final coordinates of one of the illuminated zones in

$sx(j)$. The integration is repeated for each zone until all illuminated zones have been considered. The total scattered field (called S) for a particular THI and TNS is the sum of the zone fields. Except for normalization, the programs for the two polarizations differ only in the subroutine called FTBI(X) (Function To Be Integrated); the factor $\sin(\text{THI} - \tan^{-1}(\dot{H}))$ for the T.M. polarization is replaced in the T.E. case by $\sin(\text{THS} - \tan^{-1}(\dot{H}))$. The actual integration over the physical optics surface currents is performed by a five point Gaussian integration. In choosing the interval on the x axis over which the five point Gaussian integration is to be applied, two conditions must be met. The first is that the number of sample points along the contour must exceed five per wavelength. Presuming surface slopes of less than 60° , this means that ten sample points should be taken per electrical wavelength on the x axis. The second condition is that, if the surface were to be represented by a Fourier series, there should be 8-10 sample points per minimum mechanical wavelength along the x axis. Presuming, for example, that the first of the above conditions is the most stringent, each section of illuminated surface (i.e., between $x = SX_{j+1}$ and $x = SX_j$, j odd) would be divided into half electrical wavelength intervals plus a fractional interval, and five point Gaussian integration would be applied to each of the half electrical wavelength intervals, and to the last, fractional, interval.

C. Comments on the Use of the Physical Optics Programs

As in the case of G.O., the storage requirements are minimal, while running time depends upon the length of the surface and number of incidence and scattering angles which are investigated. For each THI the search for illumination boundaries is performed only once, but the integration must be repeated for each scattering angle considered. For many of the scattered field computations considered here the angle of incidence was held fixed and the scattering angle was varied between 0 and 180°. For such cases the time required to find the illuminated zones on the surface is small compared to the time required to do the integrations for the scattered field.

As the surface length is increased the time required goes up rapidly since the integration for each scattering angle takes longer and THS must be incremented with a finer grain to get an accurate reproduction of the structure in the scattered field pattern. The size of the increment for THS has already been discussed in connection with the geometrical optics program. For example, the time required to run a surface 16 electrical wavelengths long, with THS incremented by 0.5° from 0 to 180°, was 1.8 min. By comparison, 21 min. were required for a surface 100 electrical wavelengths long with increments in THS of 0.25° from 30° to 170°, i.e., 560 values of THS. The value of the increment in the last case appears to have been just adequate to see the detail in the pattern.

Among the checks of the P.O. program is a computation for a flat strip with no tapering of the illumination, for which a closed form

physical optics result is easily obtained. The agreement was excellent for both polarizations. In Chapter V, P.O. will be compared with the other two methods of computing the scattered fields. Special attention will be given to the range of surface parameters over which the P.O. approximation is valid.

CHAPTER IV

THE INTEGRAL EQUATION METHOD

In this chapter the third and most accurate method for calculating the scattering will be examined. Here the scattered field is obtained from the exact surface current, which is found from a moment method solution of an integral equation. There are no restrictions on the curvature or form of the surface, but because of machine storage limitations only surfaces of rather short length ($30 \lambda_e$ to $60 \lambda_e$) can be handled.

A. Moment Methods

This section contains a brief introduction to the method of moments. For more information and other applications of this method refer to Ref. [22], on which the following is based.

The objective of the moment method is to determine, numerically, the function F which is a solution of the inhomogenous operator equation

$$(40) \quad C(F) = G$$

where $C()$ is a given linear operator and G is a given function. Suppose that F can be expanded in a set of basis functions b_n .

$$(41) \quad F = \sum_{n=1}^N F_n b_n$$

where F_n is the n -th unknown coefficient of the expansion of F in that basis. Note that if a computer is to be used, N will have to be finite. Using the linearity property of C

$$(42) \quad C(F) = C\left(\sum_{n=1}^N F_n b_n\right) = \sum_{n=1}^N F_n C(b_n) = G.$$

To convert the operator equation to a set of simultaneous equations an inner product, a scalar, $\langle h, g \rangle$ is defined for functions h, g and s such that

$$(43) \quad \langle h, g \rangle = \langle g, h \rangle$$

$$(44) \quad \langle \alpha h + \beta g, s \rangle = \alpha \langle h, s \rangle + \beta \langle g, s \rangle$$

$$(45) \quad \langle h, h^* \rangle = 0, \text{ if } h \equiv 0.$$

Let $\{W_i\}$ be a set of weighting functions and take the inner product of both sides of Eq. (42) with W_m . Using the properties of the inner product, the original operator equation is converted to

$$(46) \quad \sum_{n=1}^N \langle W_m, C(b_n) \rangle F_n = \langle W_m, G \rangle$$

which is exactly the familiar matrix equation

$$(47) \quad \sum_{n=1}^N C_{mn} f_n = G_m$$

where

$$(48) \quad C_{mn} = \langle W_m, C(b_n) \rangle$$

and

$$(49) \quad G_m = \langle W_m, G \rangle.$$

The solution, F_i , to this system of equations can be found by any one of several methods, two of which are discussed in Appendix B. The solution may be exact or approximate depending upon N , b_n , and W_n .

For the integral equations to be solved here, the current is expanded in a basis of non-overlapping pulses of unit amplitude, while the weighting functions are chosen to be delta functions whose singularities occur at the centers of the pulses. The inner product is chosen to be

$$(50) \quad \langle g, h \rangle = \int_c g h \, dc$$

where c is the contour of the scattering surface. This choice of basis and weight functions amounts to enforcing the integral equation at the centerpoints of the pulses, and is usually called "point-matching." For the operator equations considered in this work the system of simultaneous equations which result from point matching are well conditioned, i.e., suitable for computer solution (see Ref. [23]).

B. Integral Equation for Transverse Magnetic Polarization

In order to apply the point matching technique to the rough surface scattering problem, it is first necessary to find an appropriate linear operator. For this purpose the integral equation relating the unknown surface current to the known incident field has been chosen.

The incident electric field is \hat{z} directed, the incident magnetic field is transverse (T.M. polarization) to the generators of the surface with contour c as shown in Fig. 13. If the total electric

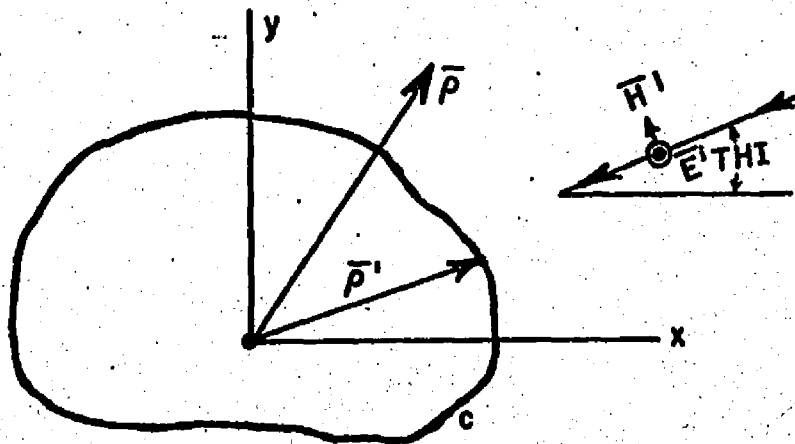


Fig. 13.--Geometry for T.M. scattering.

field is written as the sum of the incident field \vec{E}^i and the scattered field \vec{E}^s , the boundary condition

$$(51) \quad \vec{E}^i + \vec{E}^s = 0$$

must be satisfied on c . The scattered field is given in terms of the \hat{z} directed surface currents, $J_z(\vec{\rho}')$, by (see Ref. [24])

$$(52) \quad E_z^S(\bar{\rho}) = -\frac{k\eta}{4} \int_C J_z(\bar{\rho}') H_0^{(2)}(k|\bar{\rho}-\bar{\rho}'|) d\ell'$$

for the two dimensional case, where $H_0^{(2)}$ is the Hankel function of the second kind and order zero, η is the impedance of free space and k is the wave number, $2\pi/\lambda_e$. Combining this with the boundary condition (Eq. (51)) gives the integral equation for the unknown surface current

$$(53) \quad E_z^I(\bar{\rho}) = \frac{k\eta}{4} \int_C J_z(\bar{\rho}') H_0^{(2)}(k|\bar{\rho}-\bar{\rho}'|) d\ell'$$

where $\bar{\rho}$, $\bar{\rho}'$ are now both confined to the contour c . Equation (53) can now be identified with Eq. (42) as follows:

$E_z^I(\bar{\rho})$ corresponds to G ,

$J_z(\bar{\rho}')$ corresponds to F ,

and the operator

$$-\frac{k\eta}{4} \int_C () H_0^{(2)}(k|\bar{\rho}-\bar{\rho}'|) d\ell' \text{ corresponds to } C().$$

As it stands the integral equation requires the consideration of the current on the entire boundary c ; if the entire contour of a two dimensional earth were to be included, the storage requirements for a moment method solution would be astronomical. It seems reasonable to assume that for standard radar wavelengths and with directive antennas, the surface current is appreciable over only a very small

portion of this contour. Thus it will be presumed that the surface current outside a certain illuminated region, which extends from $-EP$ (End Point) to $+EP$, can be neglected (see Fig. 14). To simulate the

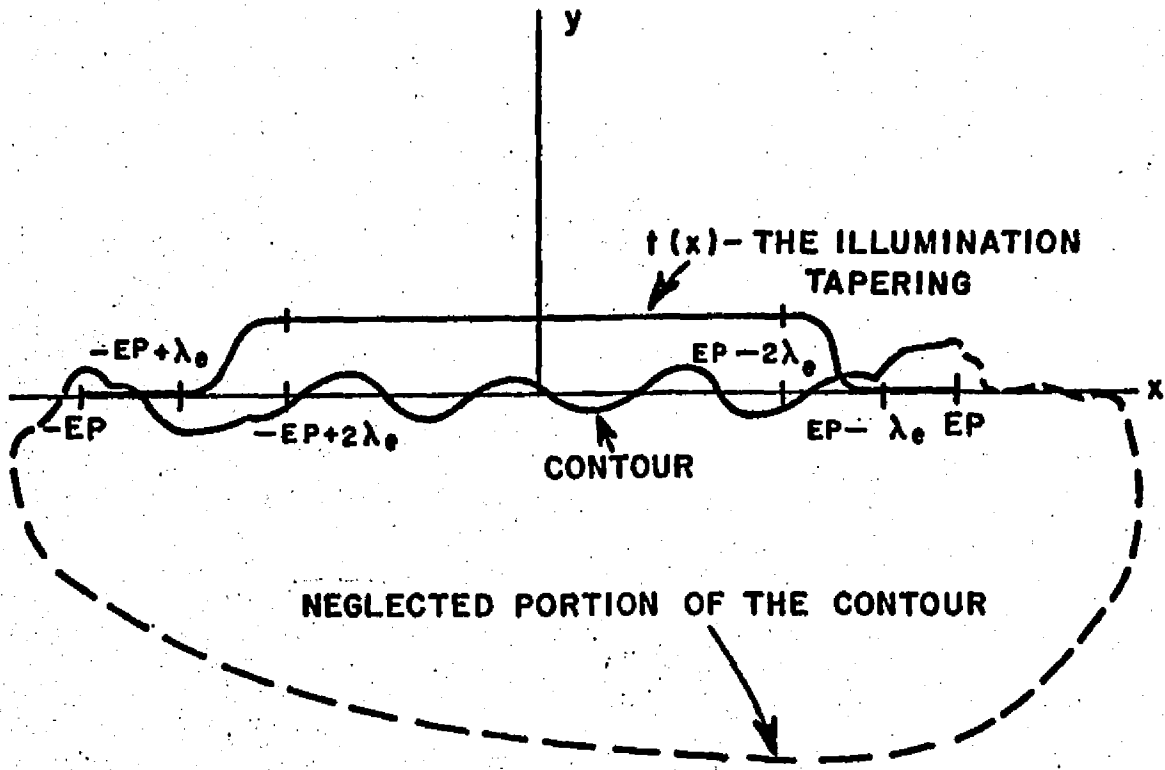


Fig. 14.--Modification of true contour to a shortened contour.

illumination of the surface by a directive antenna, tapering of the incident field strength is introduced via the function, $t(x)$, in the following way. The amplitude of the incident field is taken as unity to within two electrical wavelengths from each end point. Between one and two electrical wavelengths from each end the field is sinusoidally tapered to zero. Over the last wavelength the

incident field is taken to be zero. The incident field with tapering included, $E_z^i(\bar{\rho})$, is thus

$$(54) \quad E_z^i(\bar{\rho}) = t(x) e^{-j\bar{k} \cdot \bar{\rho}} = t(x) e^{+j\frac{2\pi}{\lambda}(\cos(\text{THI}) x + \sin(\text{THI}) H(x))}$$

The validity of this tapering approximation has been checked by lengthening the dead zone at each end of the region under consideration and noting the change in the surface currents and scattered fields. The results of this test are presented in Section D of this chapter and do indeed justify the assumption of negligible currents beyond the illuminated region.

Although tapering of the incident field is not needed in the P.O. or G.O. formulations, it has usually been included in the calculations so that the results of all the techniques can be fairly compared. The only cases in which tapering is not used are special tests of the individual methods.

The integral equation becomes

$$(55) \quad E_z^i(\bar{\rho}) = \frac{kn}{4} \int_{-EP}^{EP} J_z(\bar{\rho}') H_0^{(2)}(k|\bar{\rho}-\bar{\rho}'|) d\bar{\rho}'$$

with $\bar{\rho}, \bar{\rho}'$ both confined to the section of the contour for which $-EP < x < EP$.

The method of moments can now be applied. The surface is divided into segments of equal arclength DC , and the current, J_z , is expanded in a basis of non-overlapping pulse functions as

$$(56) \quad J_z(\bar{\rho}') = \sum_{n=1}^N F_n P_{\frac{DC}{\lambda_e}}(\bar{\rho}' - \bar{\rho}_n)$$

where $\bar{\rho}_n$ is the position vector of the midpoint of the n -th segment of the surface, F_n is a complex number representing the magnitude and phase of the current over the n -th segment of the contour, and the n -th basis function $P_{\frac{DC}{\lambda_e}}(\bar{\rho}' - \bar{\rho}_n)$ is a pulse of unit amplitude and width DC along the contour c . Thus the actual surface current is to be approximated as shown in Fig. 15. For a reasonable representation of the surface current, the pulse width, DC , must be a fraction

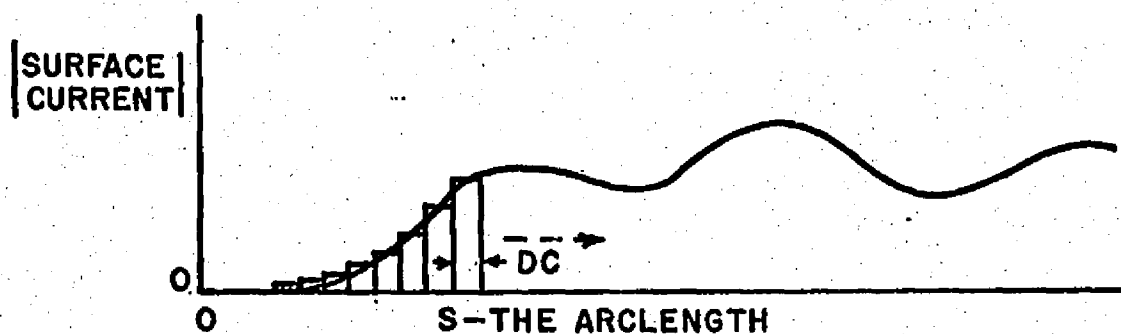


Fig. 15.--Approximation of the surface current.

of an electrical wavelength; $\lambda_e/10$ has been found to be satisfactory. The shape of the surface must also be considered in choosing DC , since the surface must be accurately modeled by strips of width DC . Hence, if λ_m is the shortest mechanical wavelength in the Fourier spectrum of the surface, then DC should also satisfy $DC \leq \lambda_m/10$. Of course the more restrictive of the two conditions should be met.

Applying the method of Section A of this chapter to Eq. (55)

$$\begin{aligned}
 (57) \quad E_Z^1(\bar{\rho}) &= \frac{k_n}{4} \int_{-EP}^{EP} \sum_{n=1}^N F_n P_{\frac{2\pi}{\lambda}}(\bar{\rho}' - \bar{\rho}_n) H_0^{(2)}(k|\bar{\rho} - \bar{\rho}'|) d\bar{\rho}' \\
 &= \frac{k_n}{4} \sum_{n=1}^N F_n \int_{-EP}^{EP} P_{\frac{2\pi}{\lambda}}(\bar{\rho}' - \bar{\rho}_n) H_0^{(2)}(k|\bar{\rho} - \bar{\rho}'|) d\bar{\rho}' \\
 &= \frac{k_n}{4} \sum_{n=1}^N F_n \int_{DC_n} H_0^{(2)}(k|\bar{\rho} - \bar{\rho}'|) d\bar{\rho}'
 \end{aligned}$$

where \int_{DC_n} means "integrate over the n-th segment of the contour".
 Taking the inner product of Eq. (57) with the weighting functions,

$$(58) \quad \langle \delta(\bar{\rho} - \bar{\rho}_m), E_Z^1(\bar{\rho}) \rangle = \frac{k_n}{4} \sum_{n=1}^N F_n \langle \delta(\bar{\rho} - \bar{\rho}_m), \int_{DC_n} H_0^{(2)}(k|\bar{\rho} - \bar{\rho}'|) d\bar{\rho}' \rangle$$

so

$$(59) \quad E_Z^1(\bar{\rho}_m) = \frac{k_n}{4} \sum_{n=1}^N F_n \int_{DC_n} H_0^{(2)}(k|\bar{\rho}_m - \bar{\rho}'|) d\bar{\rho}'$$

which is the same as the NXN matrix form

$$(60) \quad [C] [F] = [E]$$

where

$$(61) \quad C_{mm} = \frac{k_n}{4} \int_{DC_n} H_0^{(2)}(k|\bar{\rho}_m - \bar{\rho}'|) d\bar{\rho}'$$

$$(62) \quad E_m = E_z^i(\bar{\rho}_m)$$

and F_n is the unknown amplitude and phase of the current in the n -th contour segment. Once Eq. (60) is solved, the surface current is known.

The far field scattering from the surface is found from the surface currents and Eq. (52) to be

$$(63) \quad E_z^s(\bar{\rho}) = \frac{k\eta}{4} \sqrt{\frac{2}{\pi k}} e^{j\frac{5\pi}{4}} \frac{e^{-jk|\bar{\rho}|}}{\sqrt{|\bar{\rho}|}} \int_{-EP}^{EP} J_z(\bar{\rho}') e^{jk(\bar{\rho}' \cdot \hat{\rho})} d\ell'$$

$$\approx \frac{k\eta}{4} \sqrt{\frac{2}{\pi k}} e^{j\frac{5\pi}{4}} \frac{e^{-jk|\bar{\rho}|}}{\sqrt{|\bar{\rho}|}} \int_{-EP}^{EP} \sum_{n=1}^N F_n P_{\frac{DC}{2}}(\bar{\rho}' - \bar{\rho}_n) e^{jk(\bar{\rho}' \cdot \hat{\rho})} d\ell'$$

$$\approx \frac{k\eta}{4} \sqrt{\frac{2}{\pi k}} e^{j\frac{5\pi}{4}} \frac{e^{-jk|\bar{\rho}|}}{\sqrt{|\bar{\rho}|}} DC \sum_{n=1}^N F_n e^{jk(\bar{\rho}' \cdot \hat{\rho})}$$

The output of the computer programs is a normalized scattered field, E_z^s , which is related to the true scattered field, Eq. (63), by

$$(64) \quad E_z^s = E_z^s(\bar{\rho}) \sqrt{|\bar{\rho}|} e^{jk|\bar{\rho}|}$$

C. Discussion of the Computer Program for Transverse Magnetic Polarization

Several different programs were written using the above formulation of the problem. In the first part of this section the common

features of the programs will be discussed and later their differences and relative merits.

All of the T.M.I.E. (transverse magnetic integral equation) programs require that the surface have its arclength subdivided into segments of width DC , and have the endpoints and midpoints of these segments stored. The surface breakdown is shown in Fig. 16. The

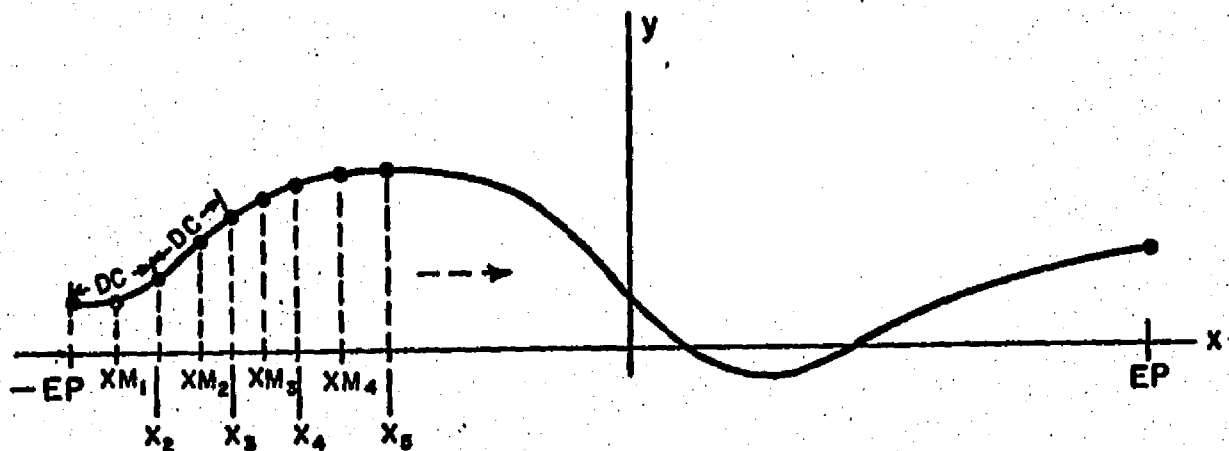


Fig. 16.--Breakdown of surface into segments of length DC .

j -th segment lies between x_j and x_{j+1} , while the j -th midpoint (XM_j) is such that $x_j < XM_j < x_{j+1}$. The surface is segmented by using the arclength formula and rectangular rule integration. After the surface subdivision is completed the programs differ somewhat depending on how the matrix elements are calculated.

Once the matrix elements have been calculated the first part of a two part solution of the system of equations begins. In all of the solution methods used the matrix is factored into an upper

and a lower triangular matrix, see Appendix B. The matrix elements depend only upon the surface profile $H(x)$, and are independent of the incident field, THI or THS so that the factorization need be done only once for a given profile. In the second part of the solution the array $[F]$ is loaded with the tapered incident electric field at each of the XM_j ; the back substitutions (described in Appendix B) are then carried out to find the current coefficients, F_n . The scattered fields are then calculated from Eqs. (63) and (64).

The differences in the several programs for the T.M.I.E. lie mainly in the calculation of the matrix elements (Eq. (61)). The simplest way to evaluate Eq. (61) for $m \neq n$ is to presume that $H_0^{(2)}(k|\bar{\rho}_m - \bar{\rho}'_n|)$ is constant over the n -th interval; then

$$(65) \quad C_{mn} \approx \frac{k_n}{4} H_0^{(2)}(k|\bar{\rho}_m - \bar{\rho}'_n|) DC$$

If $m=n$, a small argument approximation to $H_0^{(2)}(x)$ is made and integrated analytically, giving

$$(66) \quad C_{mm} \approx \frac{k_n}{4} DC H_0^{(2)}\left(\frac{k}{2} \frac{DC}{e}\right)$$

where e is the base of the natural logarithm. In practice the matrix elements are simply the Hankel function and the $\frac{k_n}{4} \cdot DC$ is accounted for when the fields are printed out. This approximation results in a symmetric matrix which, if efficiently stored, requires

only $N(N+1)/2$ storage locations. The length of surface which can be treated is increased by a factor of $\sqrt{2}$ over that which can be treated by methods requiring the storage of the full matrix. Appendix B gives the details of the storage and solution methods.

In another program, 5 point Gaussian integration, Ref. [25], is used to evaluate the C_{mn} for $m \neq n$, and when $m=n$ Eq. (66) is used. The matrix is no longer symmetric so all N^2 terms must be stored.

A third program was written which takes advantage of the fact that the currents are continuous on the surface except at sharp edges (Ref. [26]). Since the column vector $[F]$ of Eq. (60) represents the current, continuity requires that adjacent entries be similar. Hence it is possible to interpolate. The currents at the even numbered stations may be approximated in terms of the adjacent currents by

$$(67) \quad F_{2n} = (F_{2n-1} + F_{2n+1})/2.$$

For simplicity, the original matrix will be assumed to be of odd
or
order

$$(68) \quad N = 2kk + 1.$$

If, for example, $N=7$ then, using Eq. (67) in Eq. (60), one obtains the reduced system

$$\begin{aligned}
 E_1 &= C_{11}F_1 + \frac{C_{12}}{2}(F_1+F_3) + C_{13}F_3 + \frac{C_{14}}{2}(F_3+F_5) + C_{15}F_5 + \frac{C_{16}}{2}(F_5+F_7) + C_{17}F_7 \\
 E_3 &= C_{31}F_1 + \frac{C_{32}}{2}(F_1+F_3) + C_{33}F_3 + \frac{C_{34}}{2}(F_3+F_5) + C_{35}F_5 + \frac{C_{36}}{2}(F_5+F_7) + C_{37}F_7 \\
 E_5 &= C_{51}F_1 + \frac{C_{52}}{2}(F_1+F_3) + C_{53}F_3 + \frac{C_{54}}{2}(F_3+F_5) + C_{55}F_5 + \frac{C_{56}}{2}(F_5+F_7) + C_{57}F_7 \\
 E_7 &= C_{71}F_1 + \frac{C_{72}}{2}(F_1+F_3) + C_{73}F_3 + \frac{C_{74}}{2}(F_3+F_5) + C_{75}F_5 + \frac{C_{76}}{2}(F_5+F_7) + C_{77}F_7
 \end{aligned}
 \tag{69}$$

where only odd rows have been retained, i.e., F_2, F_4, F_6 are considered known. Collecting terms,

$$\begin{aligned}
 (70) \quad E_k &= (C_{k1} + \frac{C_{k2}}{2}) F_1 + (\frac{C_{k2}}{2} + C_{k3} + \frac{C_{k4}}{2}) F_3 + (\frac{C_{k4}}{2} + C_{k5} + \frac{C_{k6}}{2}) F_5 \\
 &\quad + (\frac{C_{k6}}{2} + C_{k7}) F_7
 \end{aligned}$$

for $k = 1, 3, 5, 7,$

and the number of unknowns has been reduced to kk . Since matrix manipulations are made using regular subscripts in the machine, it is very desirable to relabel the coefficients in the reduced system as follows

$$(71) \quad C'_{mi} = \frac{C_{(2m-1), (2i-2)}}{2} + C_{(2m-1), (2i-1)} + \frac{C_{(2m-1), (2i)}}{2}$$

for the "interior" columns where $m=1, 2, 3, \dots, kk$ and $i=2, 3, \dots, kk-1$.

The first and last columns of the reduced matrix are

$$(72) \quad C'_{m2} = C_{(2m-1), 1} + \frac{C_{(2m-1), 2}}{2} \quad m=1, 2, 3, \dots, kk$$

$$(73) \quad C'_{m,kk} = \frac{C_{(2m-1), (2kk-2)}}{2} + C_{(2m-1), (2kk-1)}.$$

The C_{ij} are the elements of the original $N \times N$ matrix while C'_{ij} are elements of the $kk \times kk$ reduced matrix. In the computer program the C'_{ij} are called C_{ij} while the original matrix elements C_{ij} are labeled CO_{ij} .

When using the interpolation technique the surface is subdivided as usual except that, if an even number of segments is produced, then the last segment is dropped to make N odd. The system of equations is now

$$(74) \quad [C][FP] = [E]$$

where $[E]$ is filled with the incident electric field at the midpoints of the segments with odd subscripts and the matrix $[C]$ is loaded according to Eqs. (71), (72) and (73). After the solution has been found the column vector $FP(j)$ contains the currents on the segments with odd subscripts. The complete set of surface currents $[F]$ is obtained by interpolation with

$$(75) \quad \begin{aligned} F_{2j-1} &= FP_j & \text{for } j = 1, 2, \dots, kk \\ F_{2j} &= (FP_j + FP_{j+1})/2 & \text{for } j = 1, 2, \dots, kk-1. \end{aligned}$$

Once the column vector $[F]$ has been filled in, the calculation of the scattered field proceeds as in Eqs. (63) and (64). The interpolation technique has been applied to the program which uses Gaussian integration to calculate the matrix elements.

The big advantage of interpolation is the dramatic increase in the size of the surface which can be handled for a given storage capacity. If the machine can handle an arclength of L using the non-symmetric, non-interpolation program then the symmetric matrix program can handle an arclength of $\sqrt{2} L$ while the interpolation technique will do an arclength of $2 L$ with the same amount of storage. The interpolation program still requires that all of the original matrix elements be evaluated to fill in the reduced matrix (Eqs. (71), (72) and (73)).

The integral equation programs require large amounts of storage and fairly long running times compared to either the G.O. or P.O. programs. The IBM 360-75 used here can hold a 275×275 complex matrix in high speed storage so that surfaces of length $27 \lambda_e$, or $54 \lambda_e$ if interpolation is used, can be handled with $DC = \lambda_e/10$. As for the running time, consider the $16 \lambda_e$ long surface mentioned in Chapter III Section C, which took 1.8 minutes using the P.O. program. The scattering from the same surface was computed by the three T.M. integral equation methods. The symmetric formulation required 2.8 minutes and storage for 14,000 complex numbers. The program which uses Gaussian integration to evaluate the matrix coefficients required 5.0 minutes and twice as much storage, while the interpolation program required 3.3 minutes and storage for 7,000 complex numbers. Where speed is important the use of the symmetric I.E. program is indicated, while long surfaces are best handled by the two point interpolation program.

D. Tests of the Transverse Magnetic Integral Equation Programs

The shortened contour assumption is one of the most crucial in the construction of the integral equation programs (Fig. 14). The obvious way to test it is to extend the non-illuminated portion of the surface, which amounts to lengthening the contour without changing the non-zero portion of the illumination (see Fig. 17). If the approximation is indeed valid, then the current in the non-illuminated sections should fall off rapidly and the scattered fields should be the same in both cases. The assumption was tested on a sinusoidal surface, using the program with Gaussian integration. When regular tapering was used, the current at the outer ends of the dead zones was down by a factor of 30 from that in the central part of the contour. When the extended taper was used, the current at the new outer ends was down by a factor of 100. The scattered fields for the two cases are displayed in Fig. 18 and show clearly that the differences are insignificant. Thus it may be concluded that tapering of the incident field does permit the replacement of the true contour by the shortened contour.

The wedge, Fig. 19, for which asymptotic solutions are available, provides a test case for the integral equation programs. The angle of incidence, θ_{HI} , was chosen to be 90° . In order to emphasize the corner contribution, a Gaussian tapering of the incident field was used, i.e.,

$$(76) \quad t(x) = e^{-(x/2\lambda_e)^2}$$

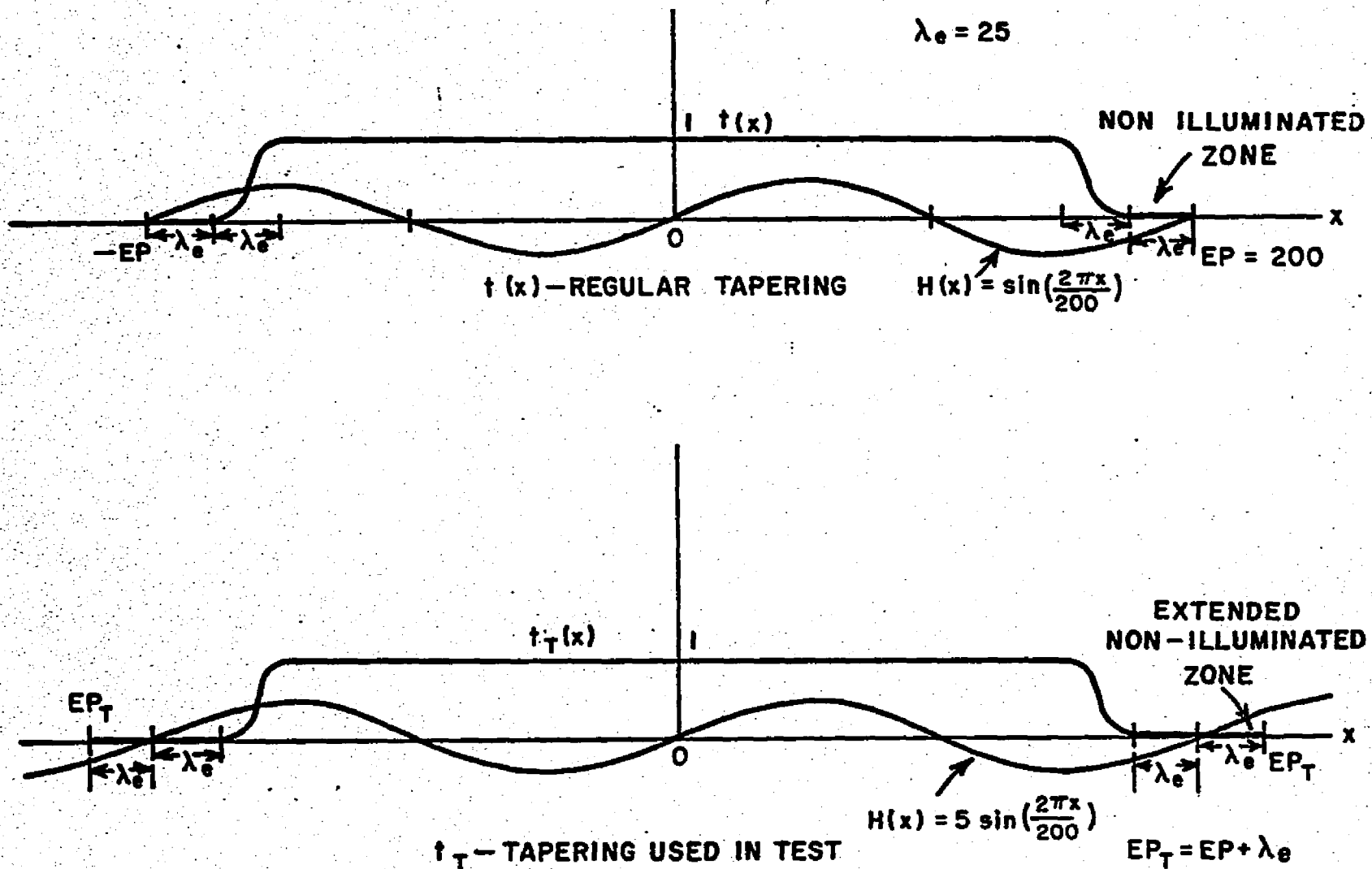


Fig.17.--Contour and tapering function used to test the shortened contour assumption.

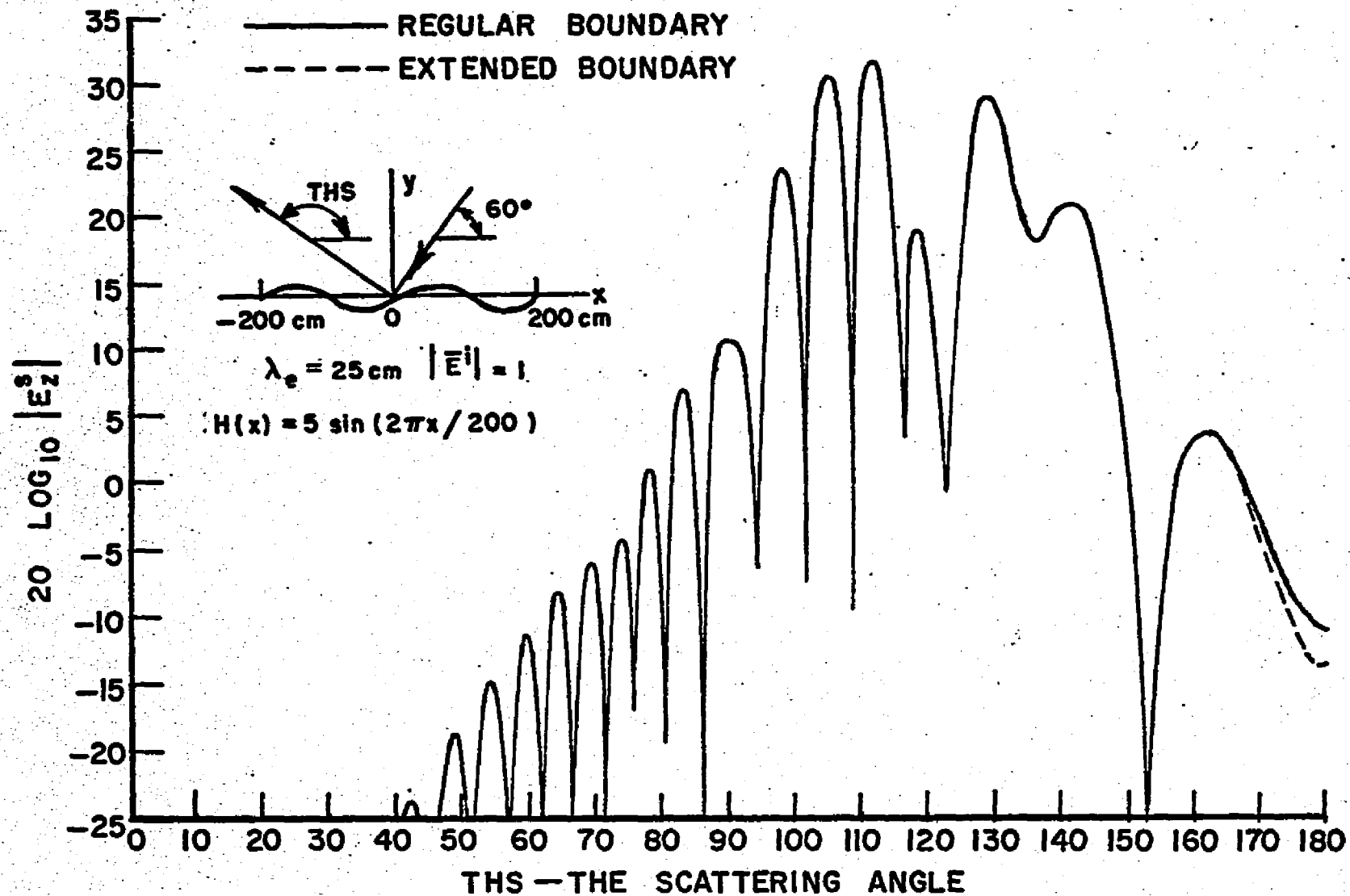


Fig. 18.--Scattered fields with and without extended boundaries, T.M. case.

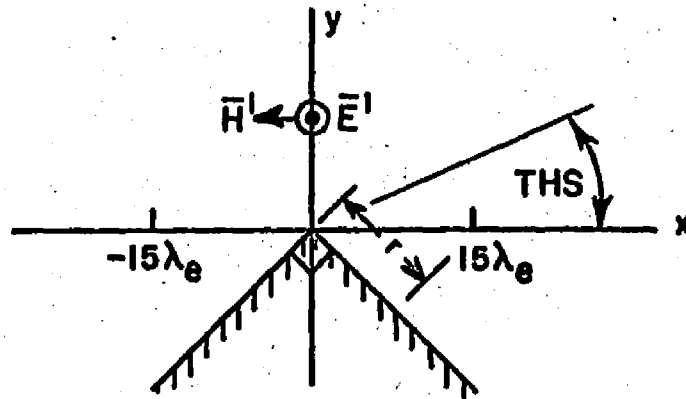


Fig. 19.--Geometry for wedge test.

The surface current, Fig. 20, shows the expected singularity at the corner. The computed scattered field is plotted in Fig. 21 along with the scattered field calculated independently using the geometrical theory of diffraction, Ref. [27]. Again, the agreement is seen to be excellent. All three T.M. integral equation programs produced essentially identical scattered fields. In a test of the self consistency of the three programs the scattering from the surface $H(x) = 5 \sin \frac{2\pi}{200} x$ was computed. The differences in the scattered fields are very minor and would not be perceptible on the scale of, e.g., Fig. 18.

In the light of the above tests, there seems to be no reason to prefer one T.M. integral equation program over the other two if numerical accuracy is the only criterion. If the running time or storage requirements must be considered then the preferred formulation can be determined by the comments at the end of Section C of this Chapter.

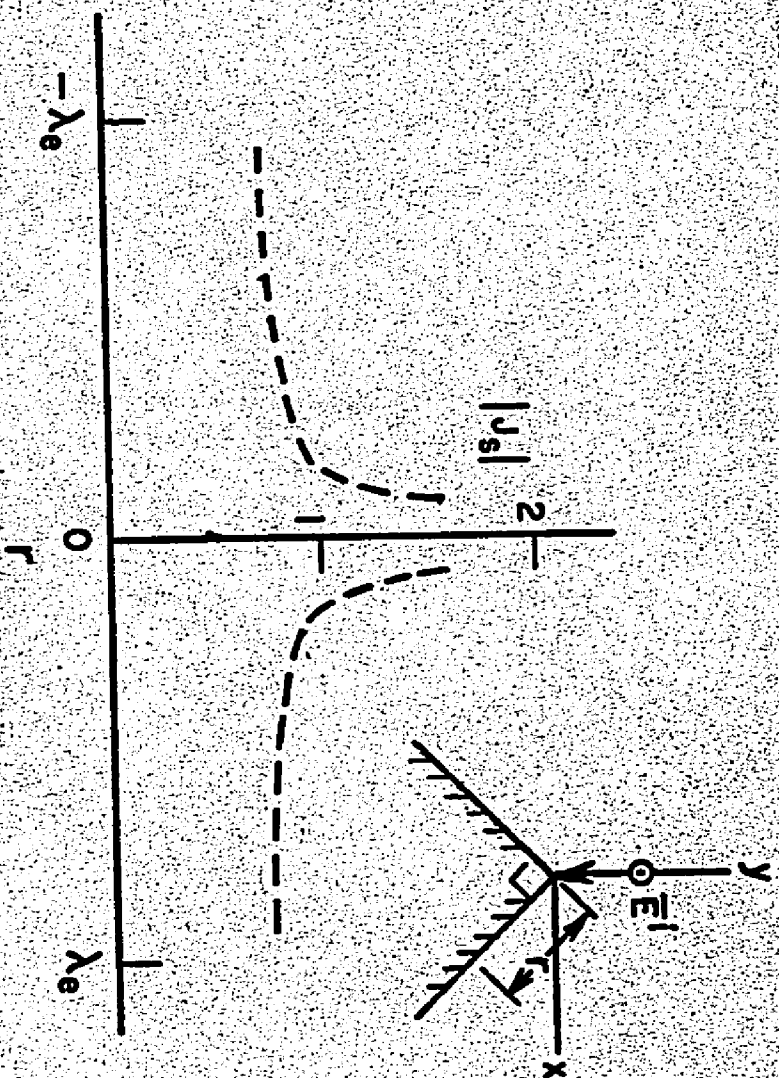


Fig. 20.--Computed $|J_s|$ on a wedge, T.M. case.

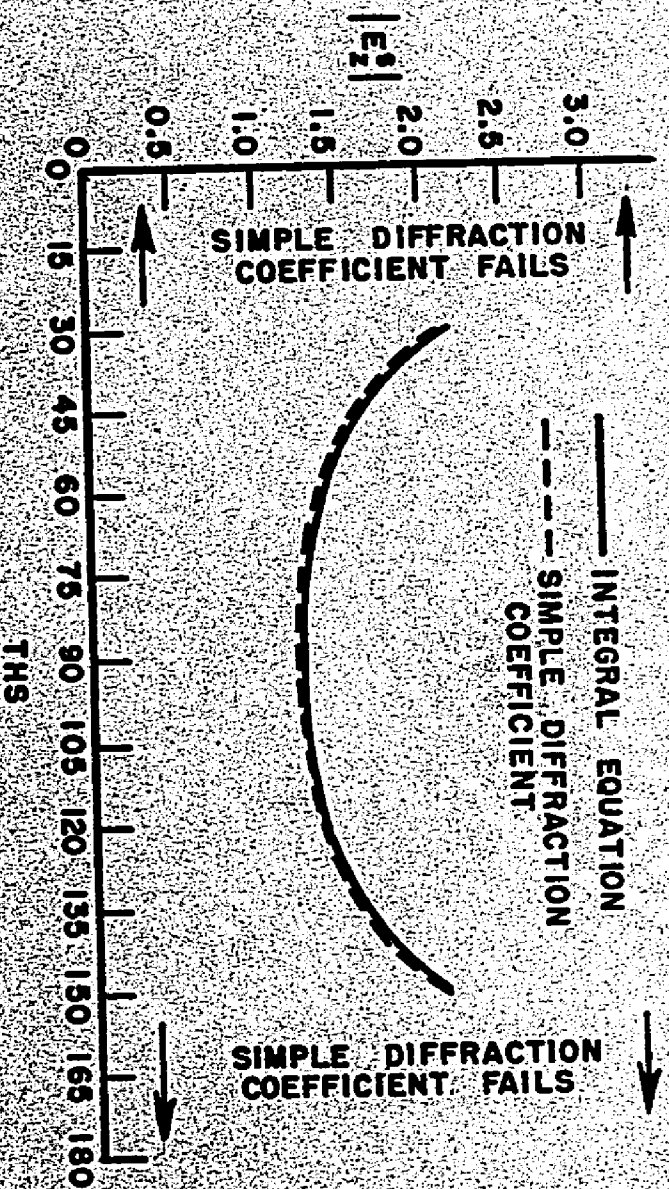


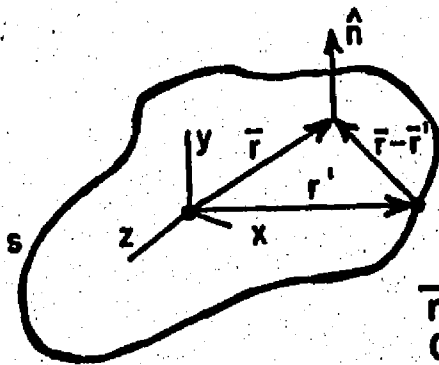
Fig. 21.--Wedge scattered fields, T.M. case

E. Integral Equation for Transverse Electric Polarization

For the T.E. polarization, the incident magnetic field \vec{H}^i is \hat{z} directed and it will be convenient to work with the integral equation for the magnetic field given (Ref. [28]) by

$$(77) \quad \vec{J}_s(\vec{r}) = 2 \hat{n} \times \vec{H}^i(\vec{r}) + \frac{1}{2\pi} \hat{n}(\vec{r}) \times \int_s \vec{J}_s(\vec{r}') \times \vec{\nabla}' \frac{e^{-jk|\vec{r}-\vec{r}'|}}{|\vec{r}-\vec{r}'|} ds$$

where \vec{r} , \vec{r}' are both position vectors of points on the surface, $\vec{H}^i(\vec{r})$ is the incident magnetic field, $\vec{J}_s(\vec{r})$ is the surface current, \hat{n} is the outward normal to the surface and \int_s indicates that the region about $\vec{r}' = \vec{r}$ is to be deleted from the integration. See Fig. 22.



\vec{r}, \vec{r}' BOTH ARE POSITION VECTORS OF POINTS ON THE SURFACE s

Fig. 22.--Three dimensional geometry for T.E. integral equation.

The two dimensional integral equation can be obtained by considering an infinitely long cylinder as shown in Fig. 23. When the incidence direction lies in the x,y plane the fields and surface current have no z dependence so that Eq. (77) can be reduced to

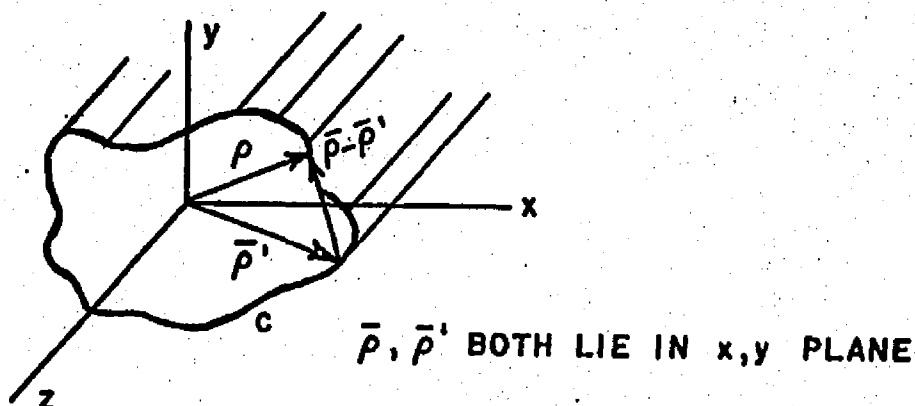


Fig. 23.--Two dimensional geometry for T.E. integral equation.

$$(78) \quad \mathbf{J}_s(\bar{\rho}') = 2 \hat{n}(\bar{\rho}) \times \mathbf{H}^1(\bar{\rho}) + \frac{k}{2j} n(\bar{\rho}) \times \int_C \mathbf{J}_s(\bar{\rho}') \times \hat{(\bar{\rho}-\bar{\rho}')} H_1^{(2)}(k|\bar{\rho}-\bar{\rho}'|) dc'$$

where $\hat{(\bar{\rho}-\bar{\rho}')}$ is the unit vector in the $\bar{\rho}-\bar{\rho}'$ direction and $H_1^{(2)}(x)$ is the Hankel function of the second kind and order 1.

Just as in the T.M. case, tapering is introduced to account for the directional properties of radar antennas, and to limit the size of the system of linear equations which will result from Eq. (78). One may now assume that the surface currents are zero except near the illuminated region and the closed contour can then

be replaced by the open contour of Fig. 24. For this polarization the current flows transverse to \hat{z} along the surface so

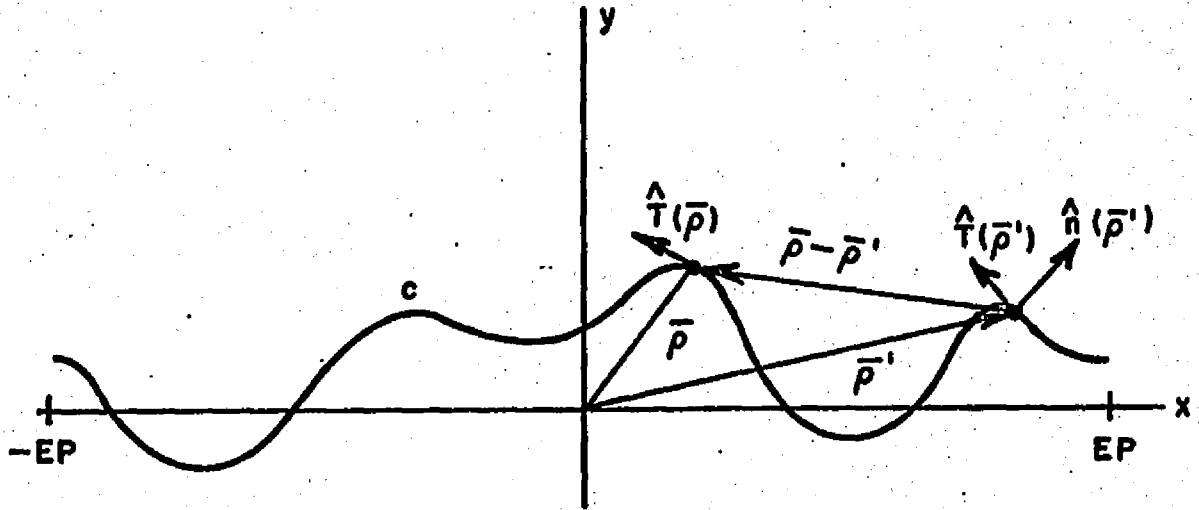


Fig. 24.--Open contour.

$$(79) \quad \bar{J}_s(\bar{\rho}') = (\hat{z} \times \hat{n}(\bar{\rho}')) J_s(\bar{\rho}') = \hat{T}(\bar{\rho}') J_s(\bar{\rho}')$$

where $\hat{T}(\bar{\rho}')$ and $\hat{n}(\bar{\rho}')$ are the unit tangent vector and the unit normal vector to the surface, as shown in Fig. 24. $\hat{T}(\bar{\rho}')$ is given in terms of the profile, $H(x)$, by

$$(80) \quad \hat{T}(\bar{\rho}') = - \frac{[\hat{x} + \hat{H}(x')\hat{y}]}{\sqrt{1 + (\hat{H}(x'))^2}}$$

where \hat{H} has the meaning assigned by Eq. (34). Using

$$(81) \quad dC' = (1 + (\hat{H}(x'))^2)^{1/2} dx'$$

and Eqs. (78) and (79) with the tapered incident field

$$(82) \quad H_2^i(\bar{\rho}) = t(x) e^{-j\bar{k}_i \cdot \bar{\rho}}$$

the integral equation becomes

$$(83) \quad -t(x) e^{j\bar{k}_i \cdot \bar{\rho}} = \frac{J_s(\bar{\rho})}{2} + \frac{jk}{4} \int_{-EP}^{EP} \frac{J_s(\bar{\rho}') H_1^{(2)}(k|\bar{\rho}-\bar{\rho}'|)}{\sqrt{(x-x')^2 + (H(x)-H(x'))^2}} \cdot [(H(x)-H(x')) - \hat{n}(x)(x-x')] dx'$$

where the integration over x' excludes a small region in the contour about the point described by $\bar{\rho}$.

The method of moments is applied to Eqs. (83) just as in the T.M. case. the current is expanded in a basis of non-overlapping pulse functions of width DC , delta functions are used as weighting functions and the scalar product is the same as in the T.M. case. The current is thus represented by

$$(84) \quad J_s(\bar{\rho}') = \sum_{n=1}^N F_n P_{DC}(\bar{\rho}' - \bar{\rho}_n)$$

where, $\bar{\rho}'$, $\bar{\rho}_n$ lie on the contour c and $\bar{\rho}_n$ is the position vector of the midpoint of the n -th segment, the F_n 's are the unknown expansion coefficients and the pulse functions $P_{DC}(\bar{\rho}' - \bar{\rho}_n)$ have been described in connection with the T.M. case. Placing this current in Eq. (83), taking the scalar product of both sides with the weighting functions and using the non-overlapping property of the basis functions results in

$$(85) \quad -t(x_m) e^{-jk_i \cdot \bar{\rho}_m} = \frac{F_m}{2} + \frac{jk}{4} \sum_{n=1}^N F_n \int_{-EP}^{EP} P_{\frac{z}{2}}(\bar{\rho}' - \bar{\rho}_n) H_1^{(2)}(k|\bar{\rho}_m - \bar{\rho}'|) \frac{[(H(x_m) - H(x')) - \dot{H}(x_m)(x_m - x')]}{\sqrt{(x_m - x')^2 + (H(x_m) - H(x'))^2}} dx'$$

Since it is necessary to avoid $\bar{\rho}' = \bar{\rho}_m$ in the integration of Eq. (85), the summation will be forced to skip $n=m$ giving as a system of equations

$$(86) \quad -t(x_m) e^{-jk_i \cdot \bar{\rho}_m} = \sum_{n=1}^N C_{mn} F_n$$

where

$$(87) \quad C_{mn} = \begin{cases} \frac{1}{2} & \text{if } m=n \\ \frac{jk}{4} \int_{x_n}^{x_{n+1}} H_1^{(2)}(k|\bar{\rho}_m - \bar{\rho}'|) \frac{[(H(x_m) - H(x')) - \dot{H}(x_m)(x_m - x')]}{\sqrt{(x_m - x')^2 + (H(x_m) - H(x'))^2}} dx' & \text{if } m \neq n \end{cases}$$

and x_{n+1} , x_n are the upper and lower x coordinates of the endpoints of the n -th surface segment respectively.

Once Eq. (86) is solved for the coefficients of the surface current, F_m , the scattered field may be found from Ref. [29]

$$(88) \quad H^s(\vec{r}) = \frac{1}{4\pi} \int_s \vec{J}_s(\vec{r}') \times \vec{v}' \frac{e^{-jk|\vec{\rho}-\vec{\rho}'|}}{|\vec{r}-\vec{r}'|} ds'$$

Specializing this to the far field scattering from an infinite cylinder and using the fact that $\vec{J}_s(\vec{r}')$ is independent of z and non zero only over a portion of the cylinder (see Fig. 25).

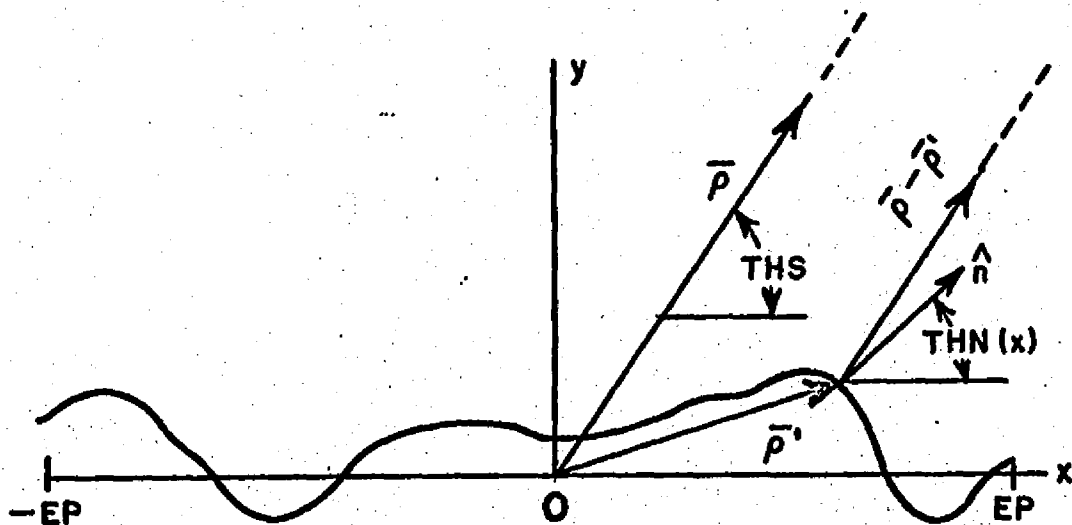


Fig. 25.--Geometry for calculation of far field scattering, T.E. case.

$$(89) \quad H_z^s(\vec{\rho}) = \frac{e^{-jk|\vec{\rho}|}}{\sqrt{|\vec{\rho}|}} \frac{j}{2} e^{j\frac{3\pi}{4}} \int_{-EP}^{EP} J_s(\vec{\rho}') \frac{[\sin(\text{THS}) - \dot{H}(x') \cos(\text{THS})]}{\sqrt{1+(\dot{H}(x'))^2}} e^{jk(x' \cos(\text{THS}) + H(x') \sin(\text{THS}))} dx'$$

Substituting Eq. (84) whose coefficients are now known into Eq. (89) and assuming that the integrand is nearly constant over a surface segment of length DC,

$$(90) \quad H_z^S(\rho) = \frac{e^{-j\frac{3\pi}{4}}}{2\sqrt{\lambda}} \text{DC} \frac{e^{-jk|\bar{\rho}|}}{\sqrt{|\bar{\rho}|}} \sum_{n=1}^N F_n \cos(\text{THS} - \text{THN}(X_{M_n})) \cdot e^{jk(X_{M_n} \cos(\text{THS}) + H(X_{M_n}) \sin(\text{THS}))}$$

where $\text{THN}(x)$ (THETA NORMAL) is given by

$$(91) \quad \text{THN}(x) = (\pi/2) + \tan^{-1} (\dot{H}(x))$$

as shown in Fig. 25. The computed and plotted value of the scattered field, H_z^S , is given by

$$(92) \quad H_z^S = H_z^S(\rho) \sqrt{|\bar{\rho}|} e^{+jk|\bar{\rho}|}$$

F. Discussion of the Computer Program for the Transverse Electric Polarization

The programs for the T.E. polarization are very similar to those for the T.M. polarization. As in the T.M. case the contour is broken up into segments of equal length DC. The same notation is used for the endpoints (x) and midpoints (XM) of the segments (Fig. 16). The T.E. and T.M. programs differ mainly in the values of the elements of the matrix [C], and in the driving side of the system of equations.

Also, for the integral equation used, the matrix is non-symmetric no matter how the coefficients are evaluated. Once again the system of equations, (Eq. (86)), is solved in such a way that different scattering and incidence angles do not require a completely new solution. Only the back substitution portion need be repeated (see Appendix B).

Several different programs have been written for the T.E. case, the major difference between them being the method used to evaluate the coefficients (Eq. (87)). The simplest way is to assume that the integrand is constant over the strip width so that

$$(93) \quad C_{mn} = \begin{cases} \frac{1}{2} & \text{if } m=n \\ \frac{jk}{4} \text{ (DC)} \frac{H_1^{(2)}(k|\bar{\rho}_m - \bar{\rho}_n|)}{|\bar{\rho}_m - \bar{\rho}_n|} [(H(XM_m) - H(XM_n)) - \dot{H}(XM_m) \\ & (XM_m - XM_n)] \text{ if } m \neq n. \end{cases}$$

In practice, only the five point Gaussian integration was used to evaluate the off diagonal elements of $[C]$, since it did not require much more running time than the simpler method. However, the interpolation technique retains all of its advantages and goes exactly as in the T.M. case with the C_{ij}^1 given by Eqs. (71), (72), and (73). Thus surface lengths of $27\lambda_e$ (or $54\lambda_e$ with interpolation) can be handled. As an example of the running times required, consider again the surface of length $16\lambda_e$ mentioned in Chapter 3 Section C. The T.E. physical optics program required 1.8 minutes while an equivalent run using the T.E. integral equation program required 5.0 minutes.

The interpolation program for this polarization took 3.5 minutes. Thus the interpolation program is superior to the non-interpolation program both with respect to storage requirement and running time.

G. Tests of the Transverse Electric Integral Equation Programmes

The shortened contour assumption plays the same role and is tested in the same way in the T.E. integral equation programs as in the T.M. case. The contour is extended as shown in Fig. 17. When the regular tapering was used, the current at the outer ends of the dead zones was down by a factor of 70 from that in the central portion of the contour. When the extended surface was considered the current at the new outer ends was down by slightly more. The nearly identical scattered fields for the two cases are shown in Fig. 26.

The wedge provides a test case for which an independent result is available. The test geometry is as shown in Fig. 19 except that here the incident magnetic field is parallel to the corner of the wedge. Gaussian tapering of the incident field, Eq. (76), is used. In contrast to the current singularity in the T.M. case, the surface current in the T.E. case, Fig. 27, shows the expected $r^{2/3}$ behavior at the corner. The excellent agreement between the scattered fields calculated by the integral equation method and the fields obtained from the geometrical theory of diffraction, Ref. [30], is illustrated in Fig. 28. Both the non-interpolation and the interpolation T.E. integral equation programs gave the same result in this test.

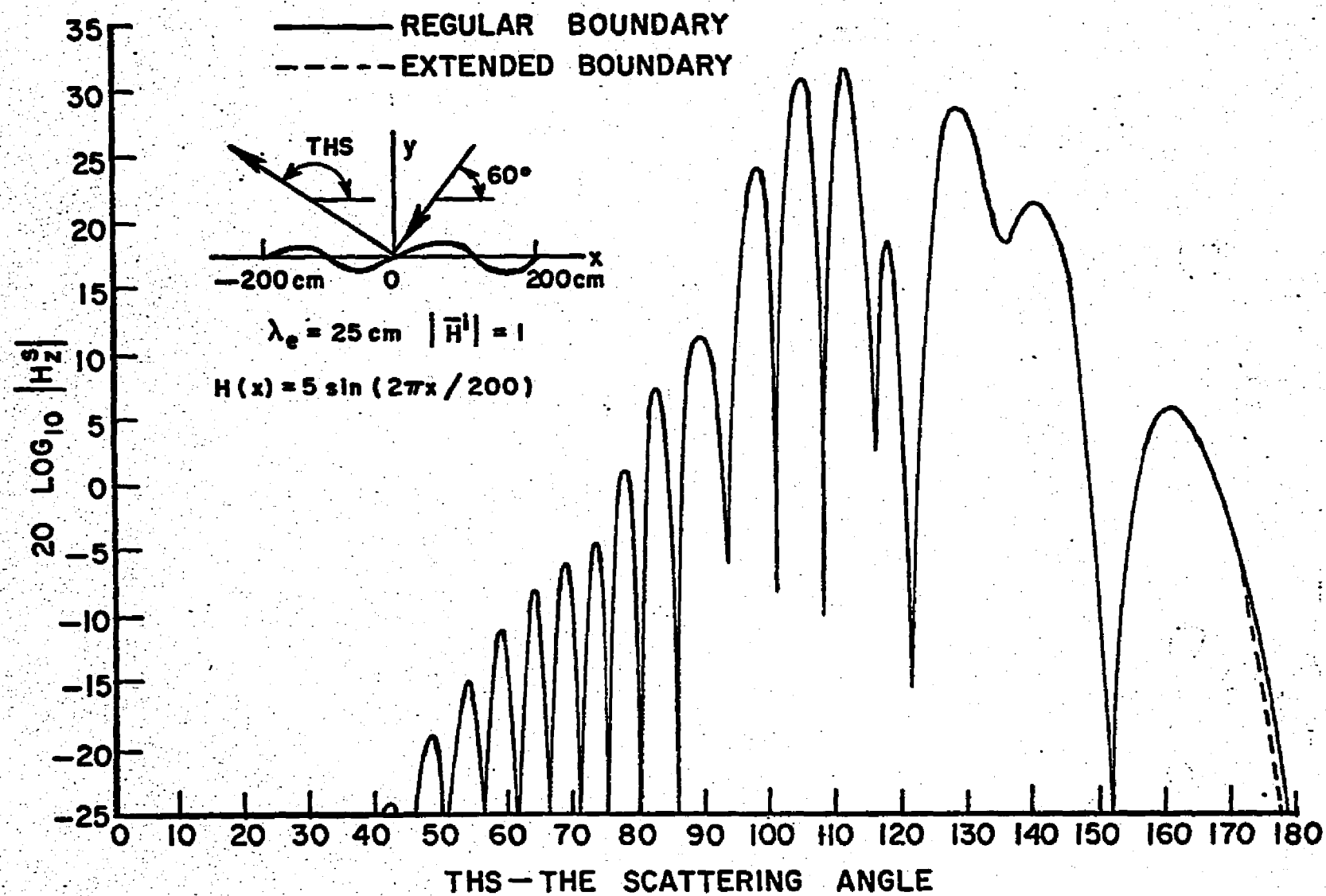


Fig. 26.--Scattered field with and without extended boundaries, T.E. case.

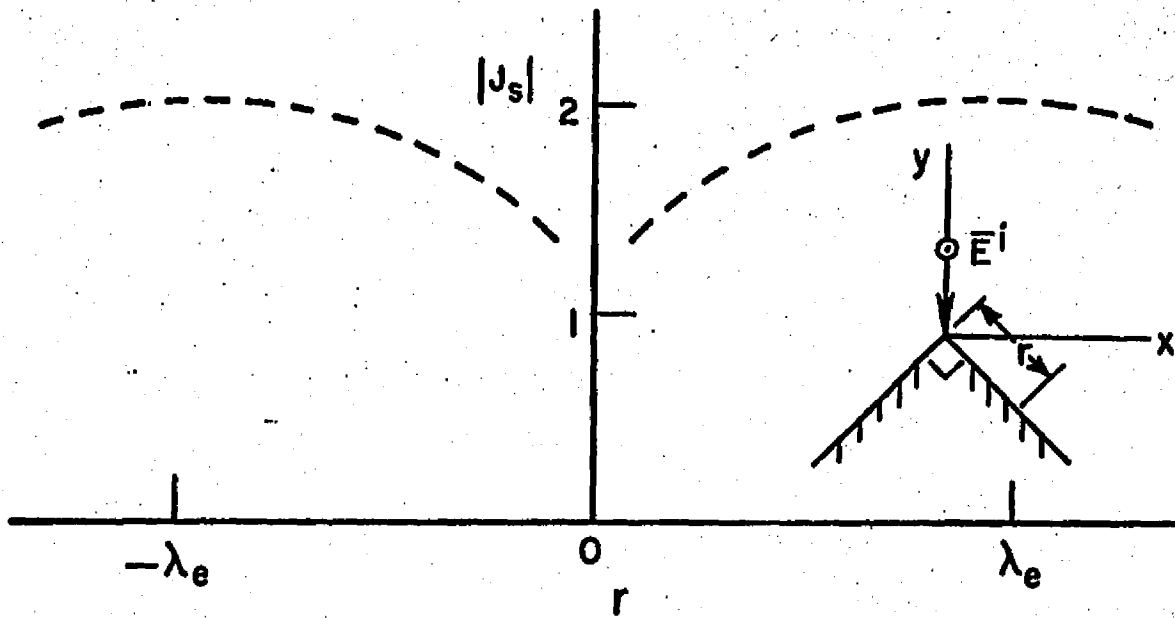


Fig. 27.--Computed $|J_s|$ near corner of wedge, T.E. case.

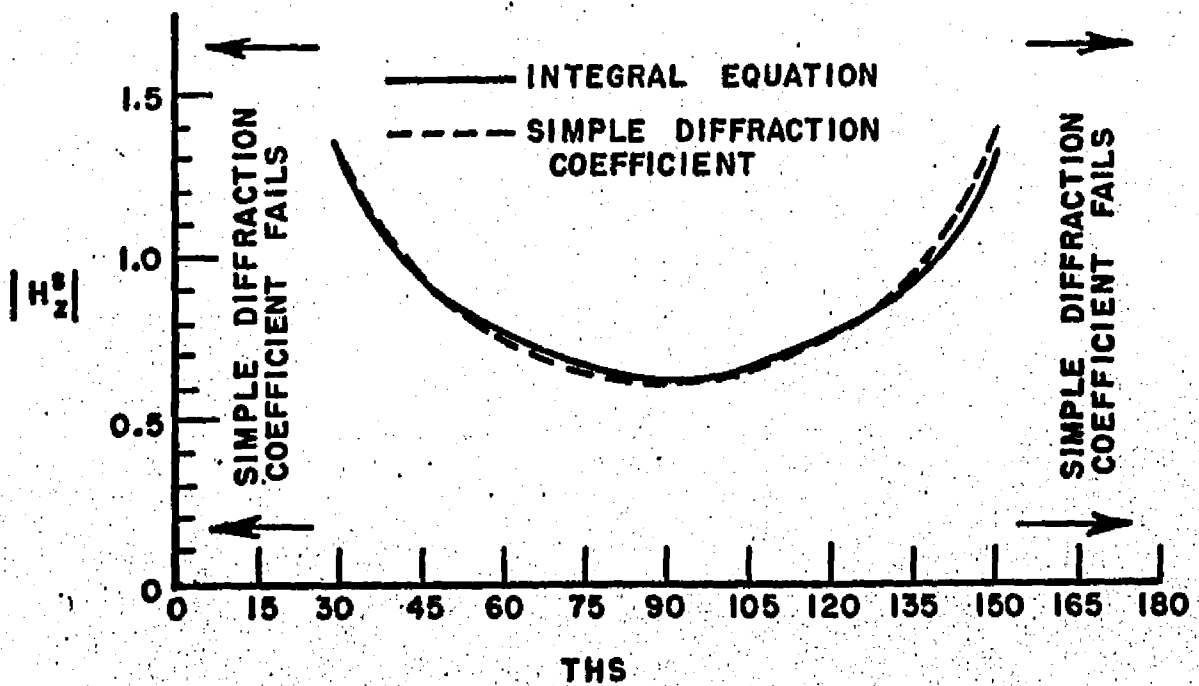


Fig. 28.--Wedge scattered fields, T.E. case.

The consistency of the two T.E. integral equation programs was checked on a surface with a height profile $H(x) = 5 \sin(2\pi x/200)$. The results were nearly identical.

The above tests indicate that so far as numerical accuracy is concerned the non-interpolation and interpolation T.E. integral equation programs do not differ. The interpolation program is preferred however because of the savings in storage.

CHAPTER V

APPLICATIONS

In this chapter the previously developed computer programs will be used to check the applicability of the geometrical optics, physical optics and perturbation approximations to the calculation of the scattering from non-uniform surfaces. The integral equation programs, which are believed to be exact, are used as standards.

The first surface to be considered has been especially chosen so that it fulfills the requirements necessary in order that physical and geometrical optics both give a valid approximation to the true scattered fields. The surface, a single half-cycle of a sine wave, has a profile $H(X) = 50 \cos(2\pi X/800)$ with x between 200.0 cm. and -200.0 cm, and clearly has but one specular point for scattering in the forward direction. The incident field is tapered, and has an electrical wavelength of 25 cm. Unless otherwise noted, these conventions have been used throughout. The criteria for the successful application of G.O. and P.O. are met by this profile since the minimum radius of curvature is $12.8 \lambda_e$ and, having a maximum height of two λ_e , there are several Fresnel zones on the surface. The scattered fields predicted by the G.O., P.O. and I.E. programs are shown in Figs. 29 and 30 for the T.M. and T.E. polarizations respectively.

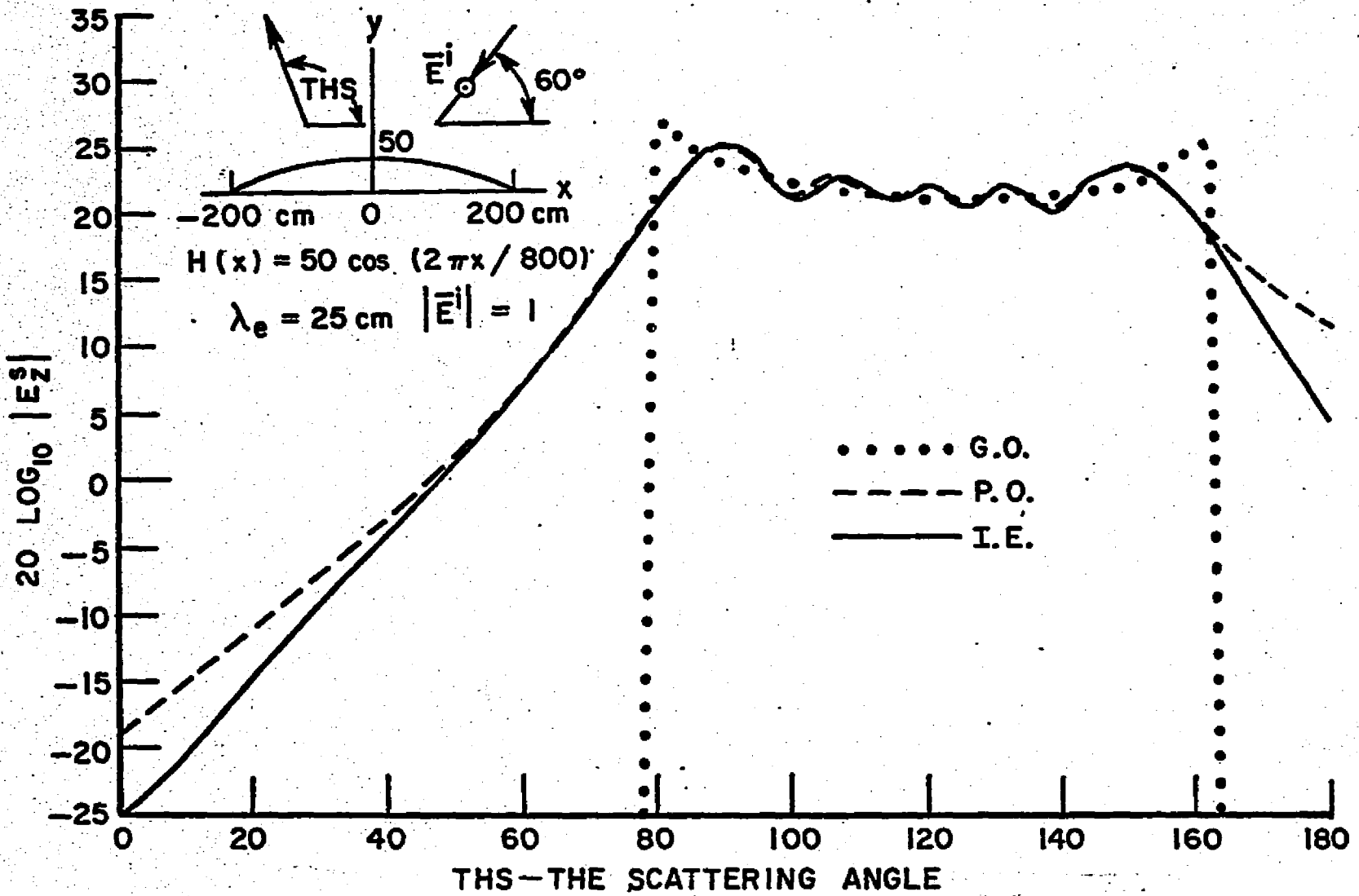


Fig. 29.--Scattering from $50 \cos(2\pi x/800)$ as calculated by I.E., P.O., and G.O.; T.M. polarization.

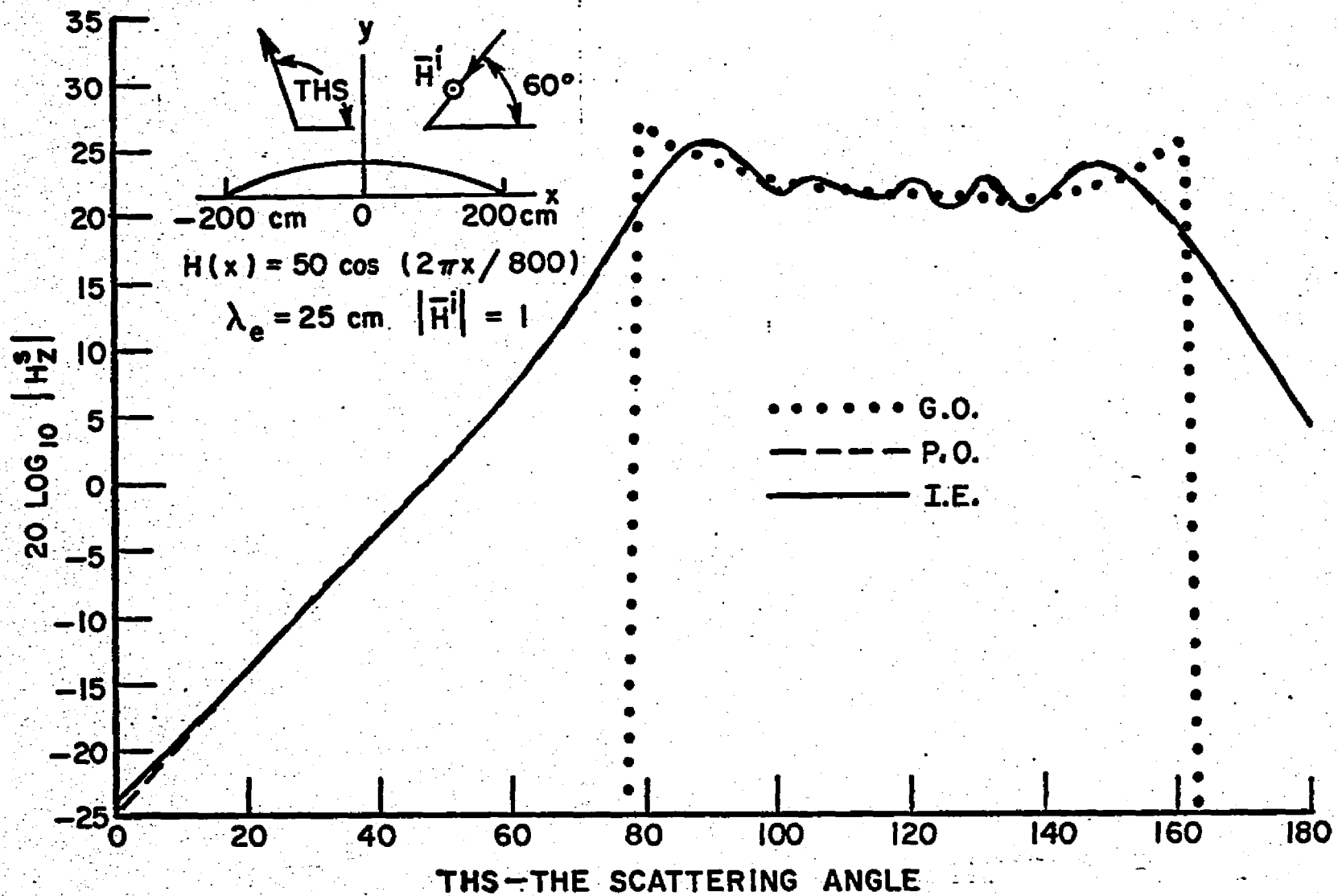


Fig. 30.--Scattering from $50 \cos 2\pi x/800$ as calculated by I.E., P.O., and G.O.; T.E. polarization.

It is apparent that all methods give nearly the same result for THS between 87° and 155° . No scattered fields are predicted by G.O. for THS outside the range 78° and 163° since the normals to the surface have a limited range of directions as illustrated in Fig. 31. The

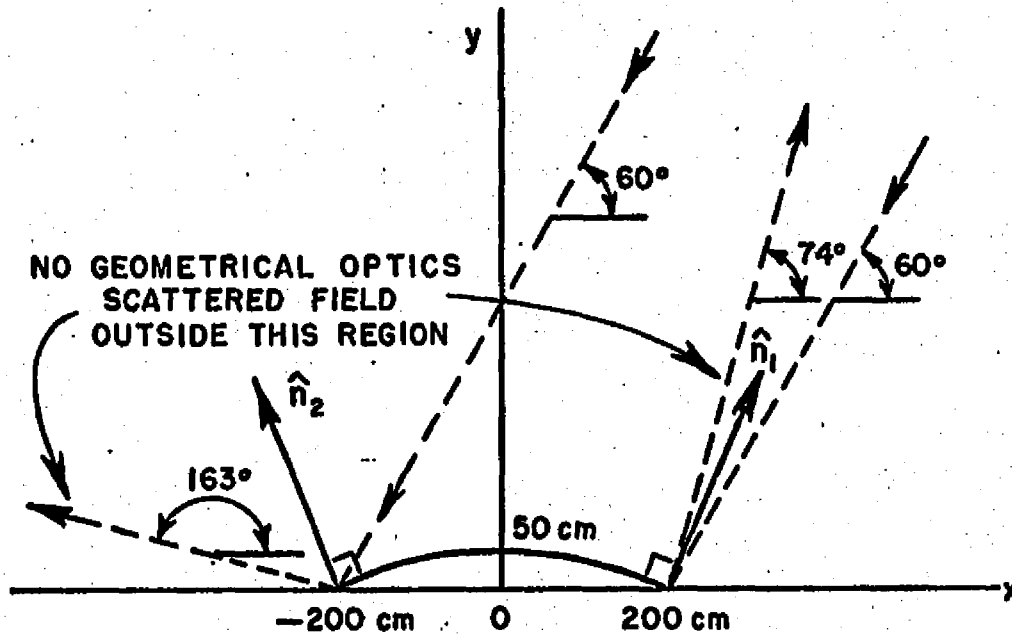


Fig. 31.--Limitation of scattering directions predicted by geometrical optics.

rise in the value of scattered field predicted by G.O. near 78° and 163° is due to the movement of the specular point into a region of the surface of increasing radius of curvature. However, as the specular point gets within two wavelengths of either endpoint the tapering of the incident field suppresses the expected singularity in the scattered field.

It should also be noted that for the P.O. results, the T.M. fields differ slightly from the correct fields for THS near grazing.

For either polarization the ripple observed in the scattered field and correctly predicted by P.O. is probably a consequence of the finite length of the surface. G.O., being a purely local theory, will not predict effects of this nature.

As a further check of the programs, the above profile was multiplied by minus one, i.e., instead of being concave down the surface was concave up. The amplitudes of the scattered fields remained unchanged but they all showed a phase shift of 90° due to what in G.O. theory is termed the caustic correction factor.

In order to establish more quantitatively the limitations on the G.O. and P.O. approximations, the scattered fields have been computed for a set of surfaces with height profile.

$$(94) \quad H(x) = A \sin(2\pi x/200) \quad -200 \text{ cm.} \leq x \leq 200 \text{ cm.},$$

i.e., the surfaces are two complete mechanical wavelengths long. With THI fixed at 60° , the amplitude, A , was varied over a range of 5.0 cm. to 50.0 cm. so that the minimum radius of curvature, r_{cm} , varied from $8.0 \lambda_e$ to $0.8 \lambda_e$. The important features of the scattered fields over this range of r_{cm} for each polarization are shown in Figs. 32-37 in order of decreasing r_{cm} . Some general trends are worthy of mention.

In the first place, as r_{cm}/λ_e decreases from 8 to 0.8, the agreement between the P.O. results and the exact fields goes from excellent to poor. It would appear that as long as the surface always has r_{cm}/λ_e greater than, say, 2.5, the P.O. approximation will

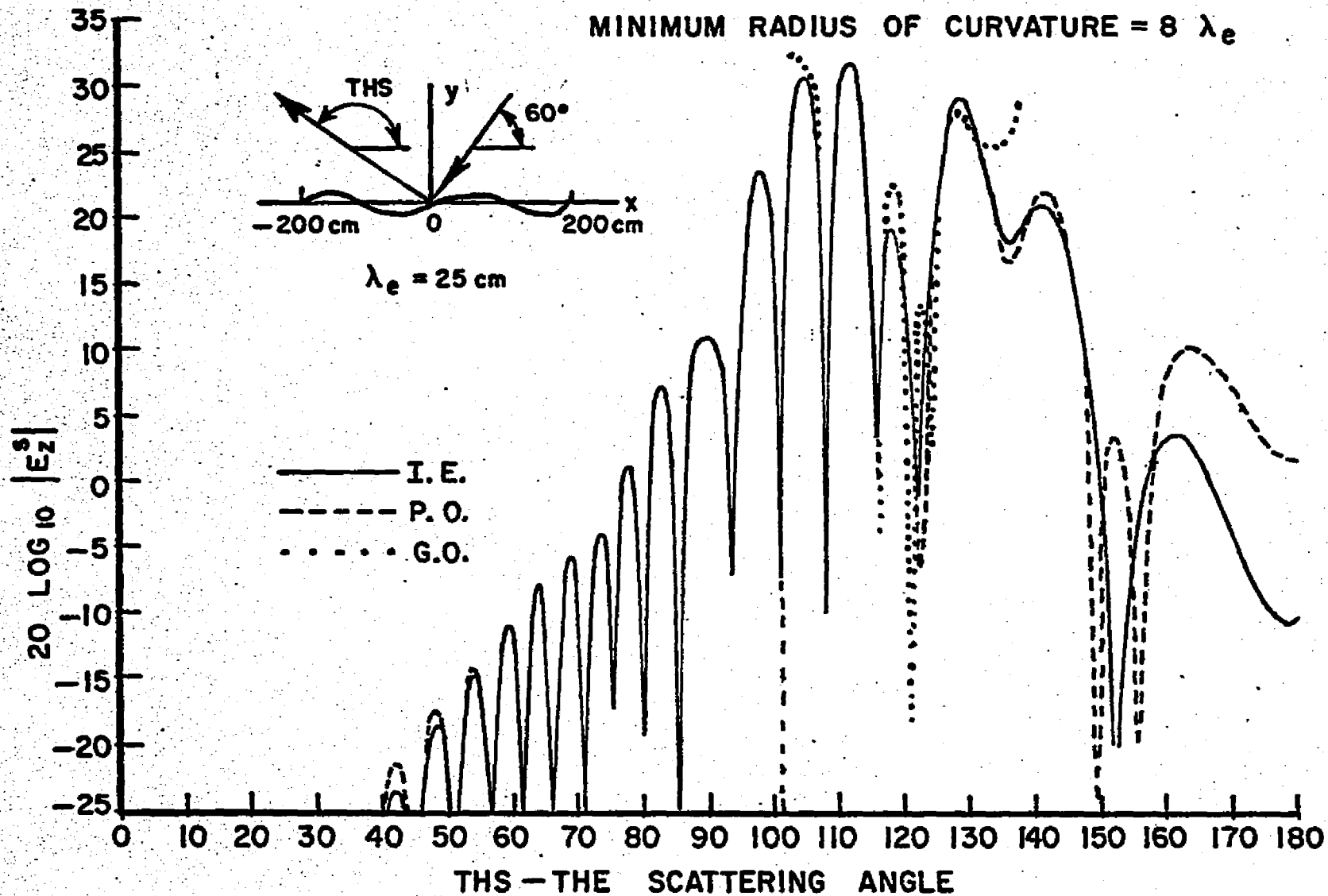


Fig. 32.—Scattered fields predicted by P.O., G.O., and I.E. methods for $H(x) = 5 \sin(2\pi x/200)$, T.M. polarization

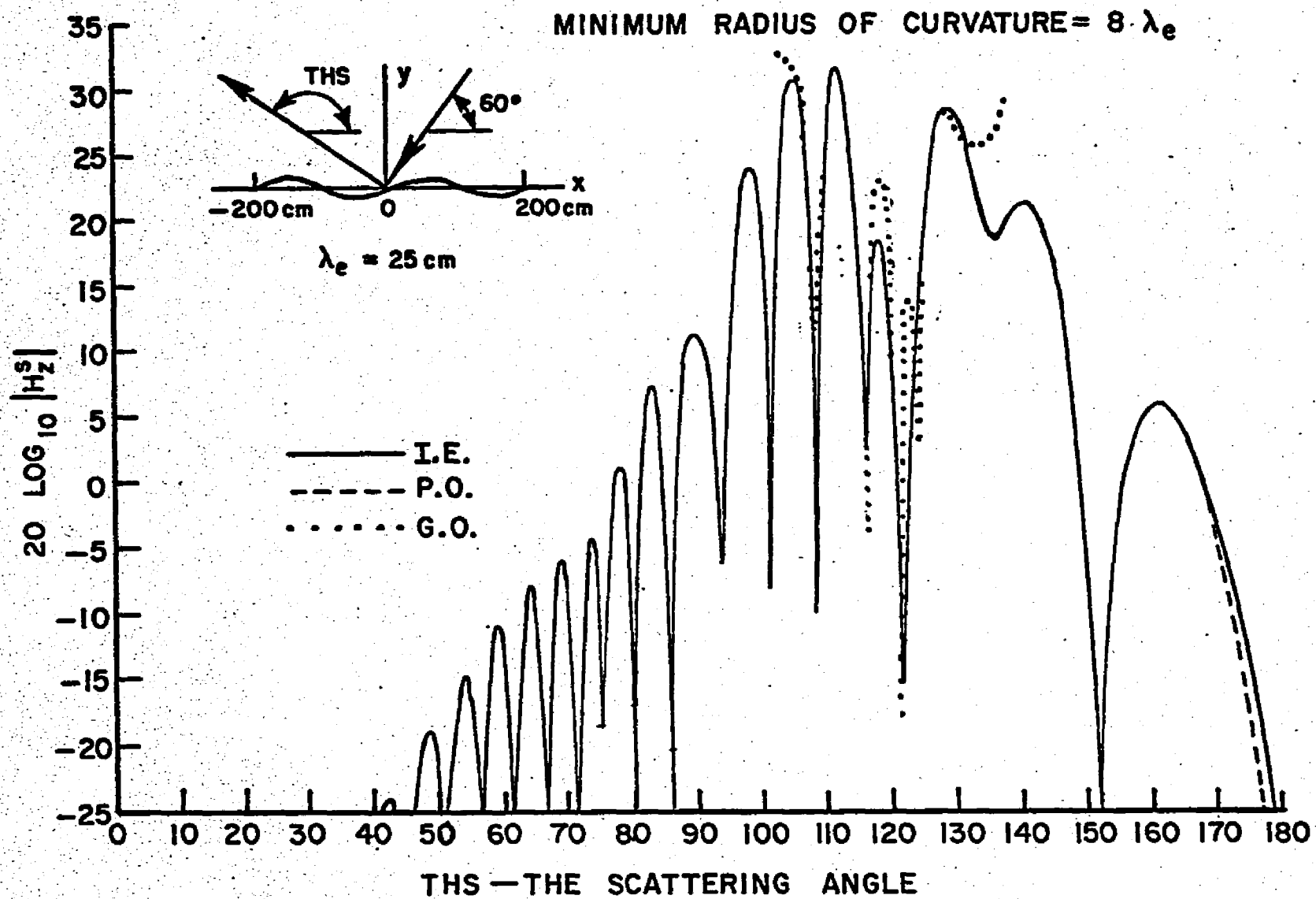


Fig. 33.—Scattered fields predicted by P.O., G.O., and I.E. methods for $H(x) = 5 \sin(2\pi x/200)$, T.E. polarization

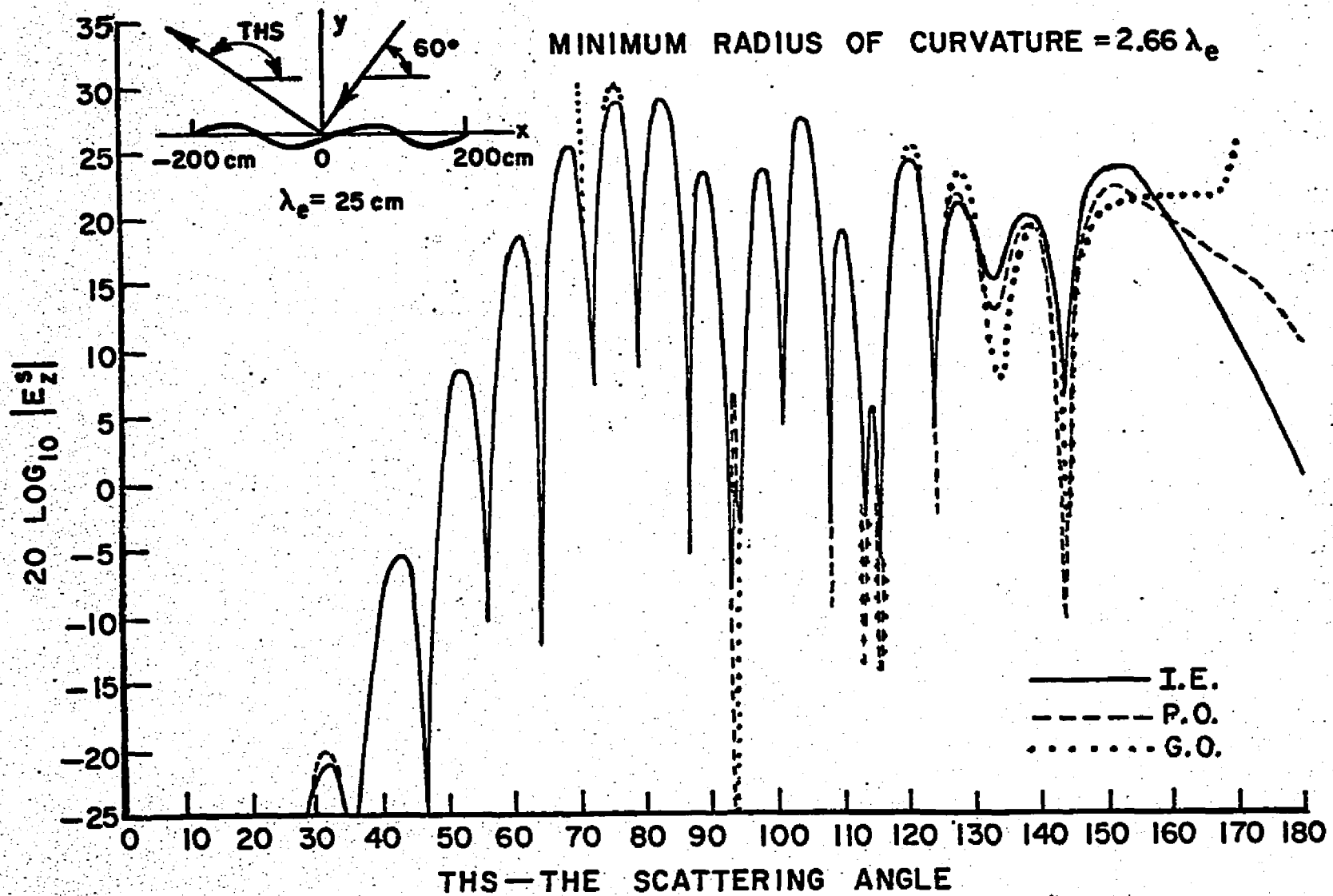


Fig. 34.—Scattered fields predicted by P.O., G.O., and I.E. methods for $H(x) = 15 \sin(2\pi x/200)$, T.M. polarization

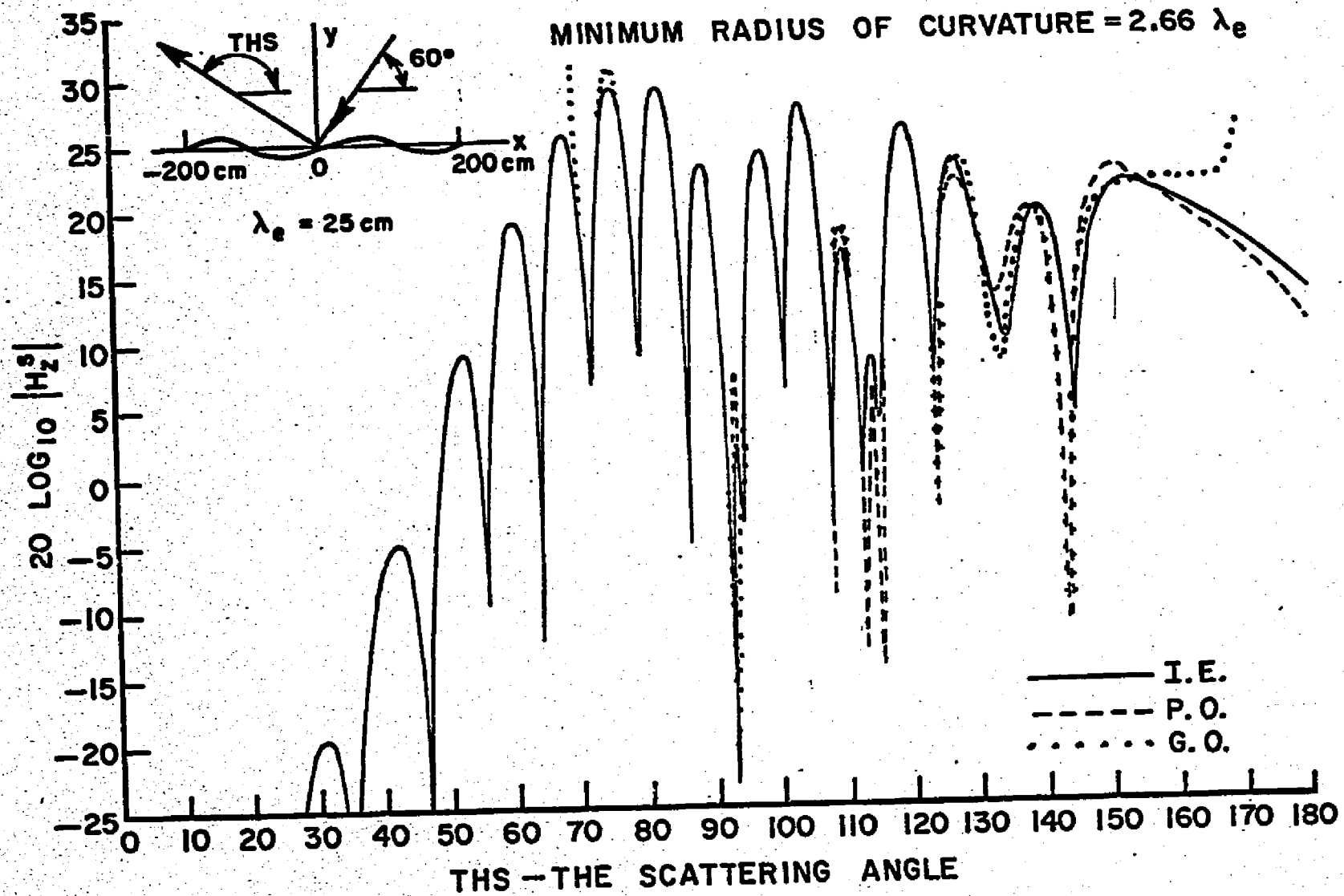


Fig. 35.—Scattered fields predicted by P.O., G.O., and I.E. methods for $H(x) = 15 \sin(2\pi x/200)$, T.E. polarization

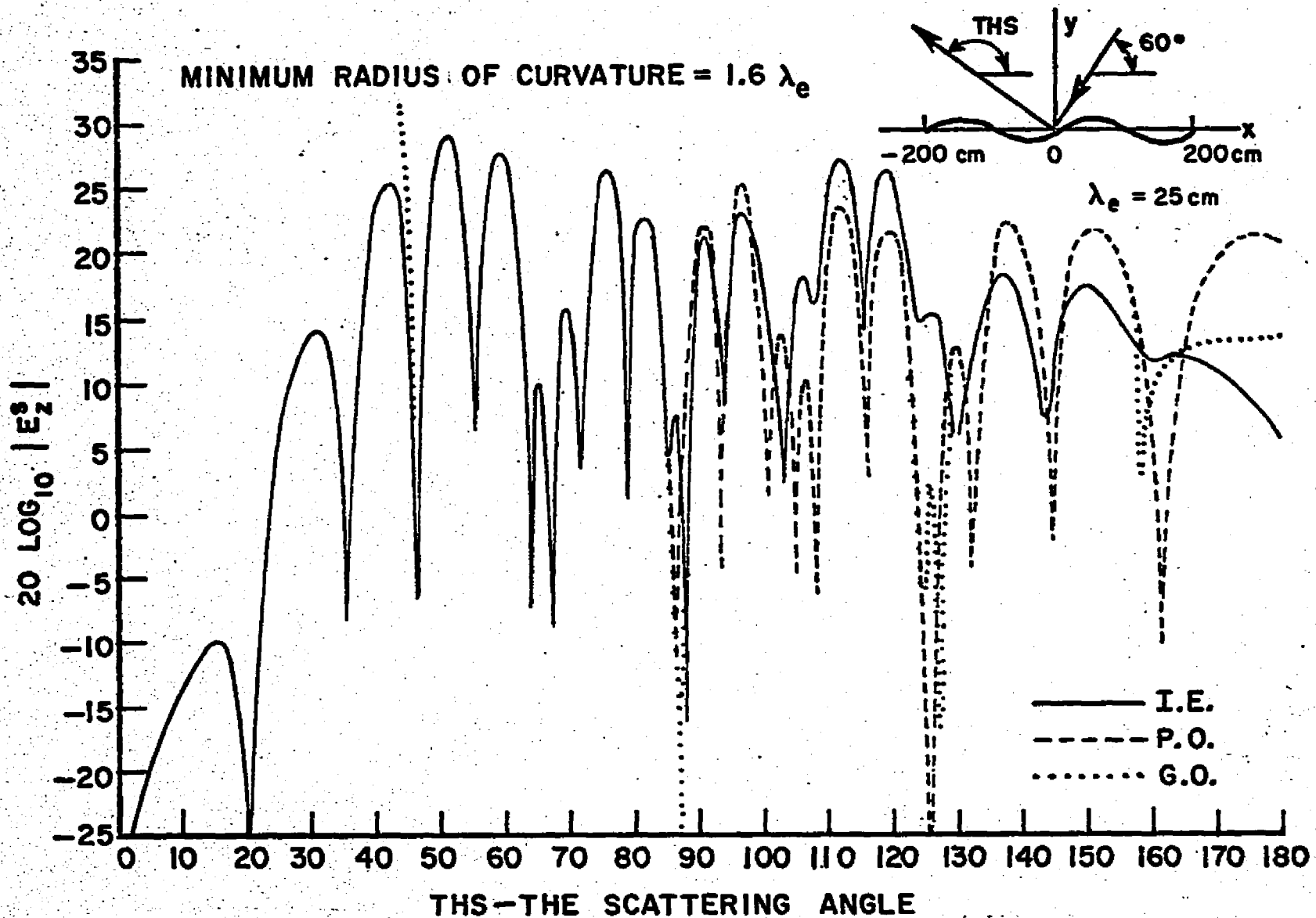


Fig. 36.—Scattered fields predicted by P.O., G.O., and I.E. methods for $H(x) = 25 \sin(2\pi x/200)$, T.M. polarization

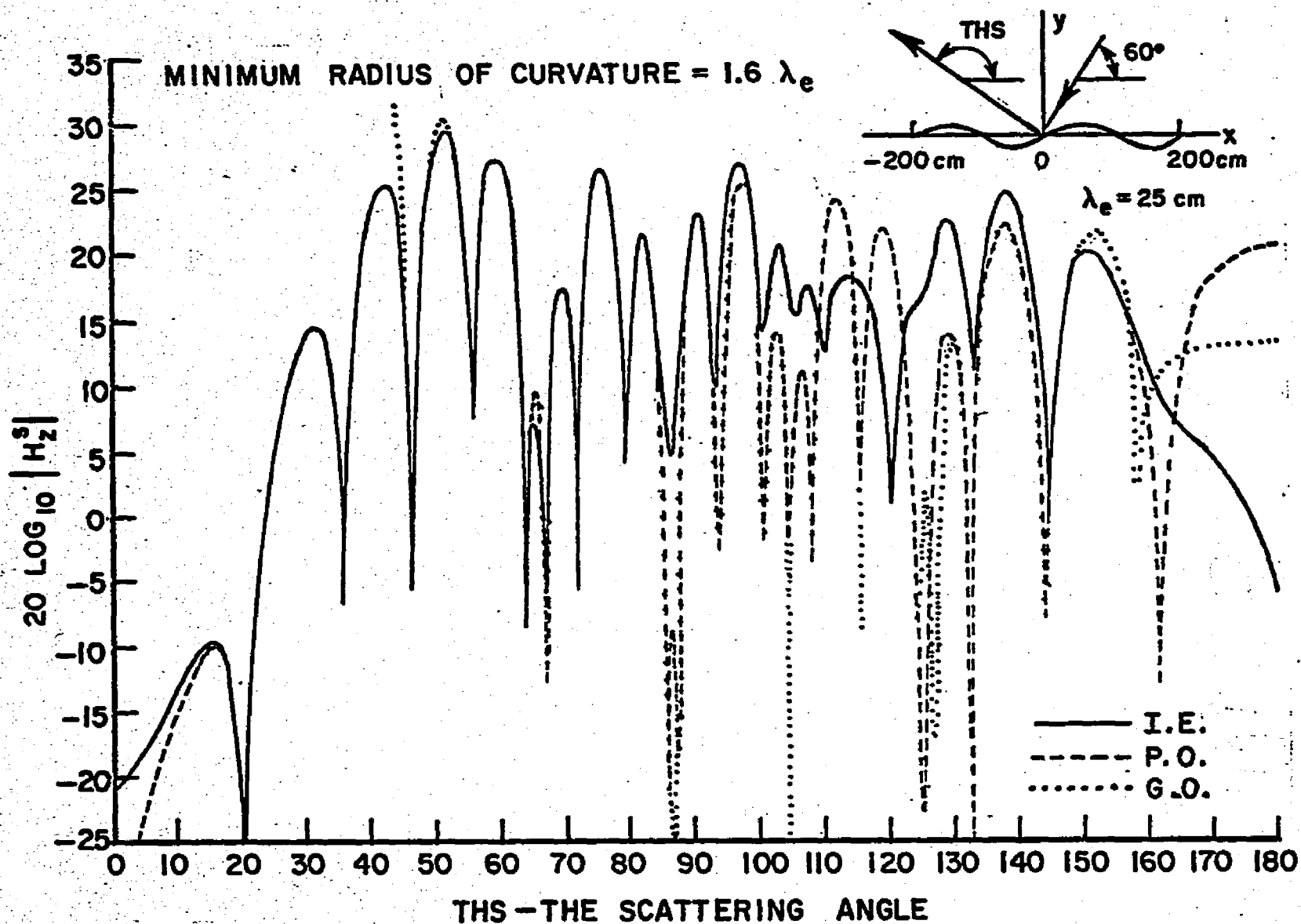


Fig. 37.—Scattered fields predicted by P.O., G.O., and I.E. methods for $H(x) = 25 \sin(2\pi x/200)$, T.E. polarization

give reliable values for the scattered field. Even for values of $r_{cm}/\lambda_e = 1$, P.O. may still be considered usable, that is, it will reproduce the general structure of the scattered fields although with significantly lower accuracy. This limitation on the radius of curvature necessary for the successful application of the P.O. approximation is in agreement with the results of Ref. [31] in which the current on a sinusoidal surface of infinite extent is found. Except for scattering and incidence angles for which no specular points occur or for which a specular point coincides with a point of infinite radius of curvature, the G.O. and P.O. approximations give scattered fields very similar to each other even when they are not correct, e.g., Fig. 38. It is interesting to note that where the I.E. and P.O. (and hence the G.O.) fields agree the T.E. and T.M. fields are nearly identical but as the radius of curvature decreases the exact fields, T.E. and T.M., not only differ from the respective P.O. fields but from each other. This behavior is not entirely unexpected since for bodies with large radius of curvature in terms of wavelength the polarization independent G.O. is known to be a good approximation. As the radius of curvature goes to zero, e.g. a wedge, G.O. and P.O. both fail and the scattering is polarization dependent (see the wedge tests in Chapter IV).

The failure of G.O. when no specular point occurs on the surface or when a specular point coincides with a point of infinite radius of curvature makes it far less attractive than P.O., especially when numerical methods are involved. For example, when $A=5$, (see Fig. 32)

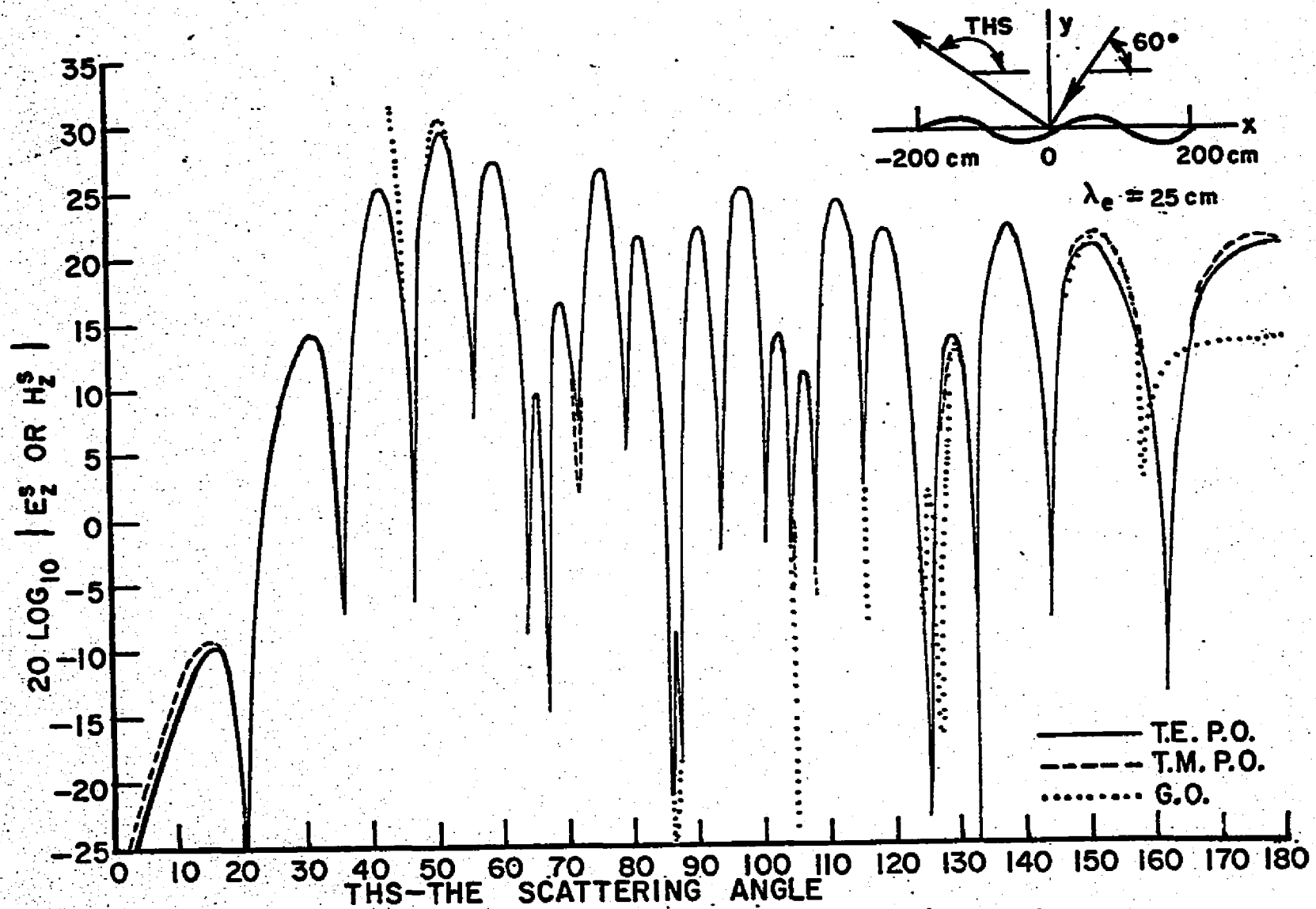


Fig. 38.--Agreement of G.O. and P.O. when they are incorrect.

G.O. predicts no scattered field outside the range $102^\circ < \text{THS} < 138^\circ$, and gives fields which are singular at either end of the range. On the other hand, the P.O. approximation correctly predicts the scattered fields for a far wider range of THS, including backscatter, and the fields are always bounded.

It is also of interest to note that what might be called the "fine structure" of the scattering, particularly for $\text{THS} < 80^\circ$, (see Fig. 32) is not due entirely to the finite length of the illuminated region as in Figs. 29 and 30 but is strongly controlled by the height profile.

Another approximate theory whose validity can be checked by the numerical methods developed here is the perturbation theory for the scattering from "slightly rough" surfaces as formulated in Refs. [32] and [33]. Perturbation theory predicts that if the amplitude of the surface profile is much less than the electrical wavelength of the incident fields, then the amplitude of the scattered field due to the perturbation of the surface is proportional to the surface height amplitude. This was checked by calculating, using the T.M. integral equation program, the scattering from a surface profile described by

$$(95) \quad H(x) = c (\sin(2\pi x/50) + 1/2 \sin(2\pi x/19.71))$$

for various values of c . The field scattered by slightly rough surfaces is dominated by the scattered field from the unperturbed surface ($c=0$) which is quite complex for the finite strips considered

here. Thus the behavior of the perturbed fields can best be illustrated by considering the difference between the actual field and the flat plate field. The perturbation in the scattered field, E_p , due to the perturbation in the height profile of the originally flat strip is then given by

$$(96) \quad E_p = E_Z^S - E_{Z_0}^S$$

where E_Z^S is the total scattered field as predicted by the computer program, and $E_{Z_0}^S$ is the field scattered when c is zero (i.e., a flat strip). In order to test the prediction that $|E_p| \propto c$, a low value of c ($c=0.01$ cm.), was chosen as a reference surface amplitude with reference scattered field $|E_{p1}|$, so that for a fixed scattering angle

$$(97) \quad \frac{|E_p|}{|E_{p1}|} = \frac{c}{c_1}$$

expresses the perturbation theory result. The exact fields are compared with perturbation theory in Fig. 39 for several values of c . The theory appears to fail at about $c/c_1 = 200$ which corresponds to a root mean square surface amplitude of approximately $\lambda_e/10$.

In addition to permitting the examination of the applicability of various electromagnetic approximations to the ocean surface scattering problem, the programs permit direct calculation of the scattered fields from any appropriate surface. One such application is to the calculation of the expected value of the backscattered power from an ensemble of ocean-like surfaces. Such an ensemble may be constructed from the known height spectrum, Ref. [34]. For a sea surface, the

$$H(x) = \frac{C}{C_1} (C_1 \sin(2\pi x/50) + \frac{C_1}{2} \sin(2\pi x/19.71))$$

THI = 60°
THS = 90°

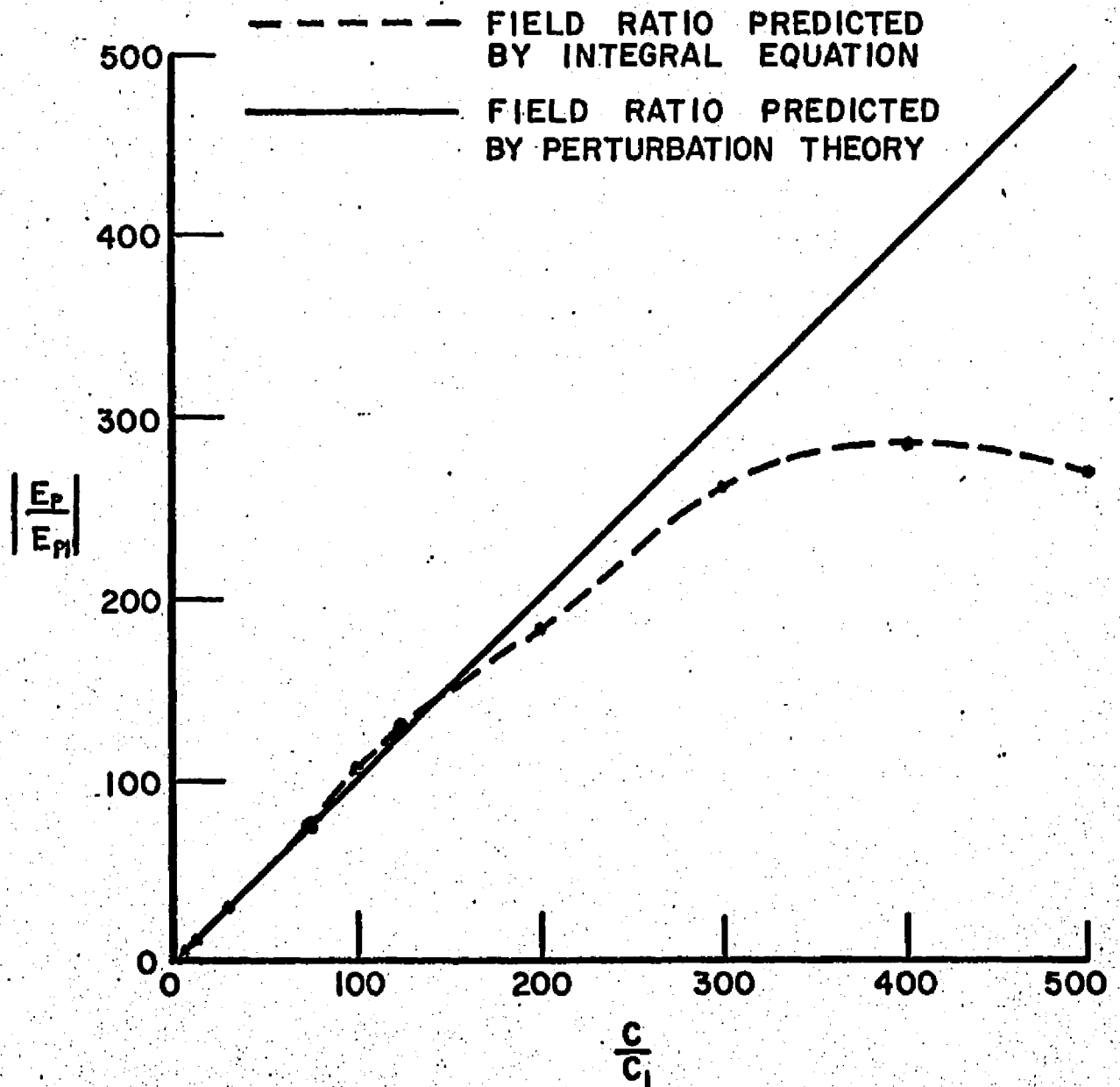


Fig. 39.--Perturbation theory test.

height spectrum, Fig. 40, decays as k_m^{-4} where k_m is the mechanical

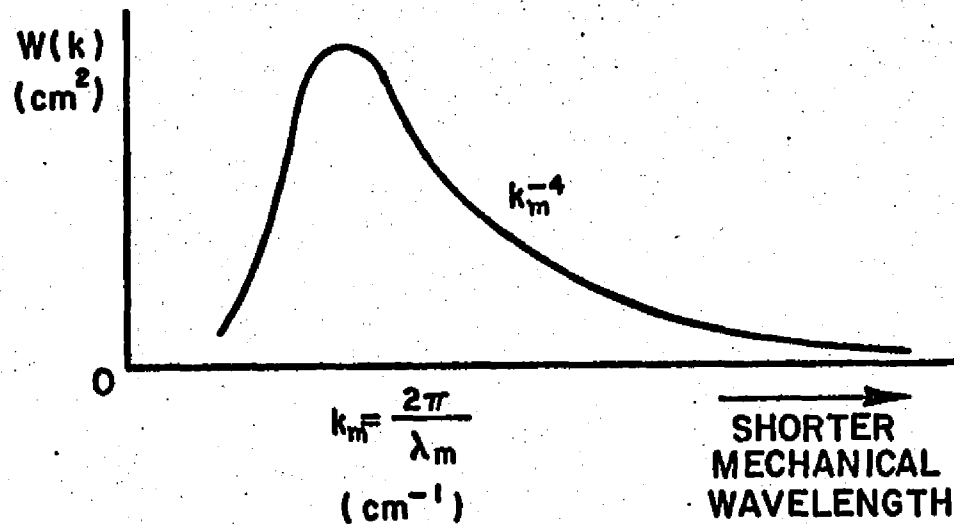


Fig. 40.--Sea surface height spectrum.

wavenumber. A particular member of the ensemble is chosen to be a finite sum of sinusoids with random phases whose amplitudes vary as k_m^{-2} . The k_m 's are not harmonically related so that the surface, like the ocean, will be aperiodic. A surface of this type given by

$$(98) \quad H(x) = 2.5(0.4 \sin(2\pi x/200.0 + 0.78) \\ + 0.8(10.0/20.0)^2 \sin(2\pi x/10.954 + 1.6) \\ + 0.8(6.66/20.0)^2 \sin(2\pi x/6.28318 + 2.4) \\ + 0.8(5.0/20.0)^2 \sin(2\pi x/4.795 + 0.4))$$

can be used to generate an ensemble whose elements are different sections of this surface.

Physical optics was used to calculate the expected value of the backscattered power and field strength from a 75 member ensemble made from the surface described by Eq. (98). Each member of the ensemble was 75 electrical wavelengths long. On a CDC 6600 computer,

the time required for the run was about 40 minutes. The expected values $\langle |E_z^S|^2 \rangle$ are shown in Fig. 41; the expected value of E_z^S was found to be extremely small compared to the root mean square field.

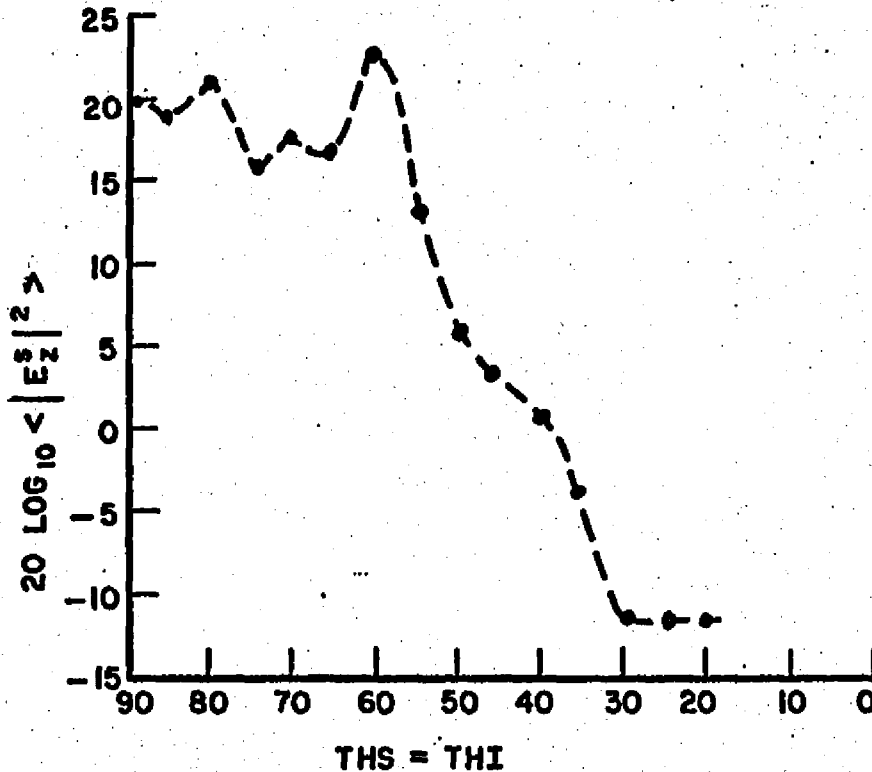


Fig. 41.--Expected value of backscattered $|E_z^S|^2$ from ensemble.

Notice that no special form of the slope distribution or other statistical properties of the surface have to be assumed. It is also possible to use a point by point, i.e. discrete, representation of the surface, such as might be generated by the prescribed statistical properties of the surface.

CHAPTER VI

SUMMARY AND CONCLUSIONS

In this work the scattering properties of cylindrical rough surfaces have been investigated by several numerical techniques in order to test the validity of previous theoretical work. The results, using as checks the integral equation solutions, show that geometrical optics is not usable for surfaces with radius of curvature smaller than $2.5 \lambda_e$ and may give poor results even when this condition is satisfied should the scattering geometry be such that no specular point exists or a specular point coincides with a point of infinite radius of curvature. With the exception of these two cases, geometrical optics and physical optics give nearly the same scattered fields.

It was found that the numerical evaluation of the scattered fields from the physical optics currents gives good results for almost any geometry (except perhaps deeply shadowed configurations) as long as the radius of curvature condition, $r_{cm} > 2.5 \lambda_e$, is satisfied. Physical optics, although not always so accurate, has an advantage over the integral equation formulation in that the length of surface which can be treated is not limited by machine storage capacity.

The integral equation program has been used to check the perturbation theory prediction that the amplitude of the scattered field increases in proportion to the increase in the amplitude of the surface height profile. The numerical results confirm in a quantitative way the fact that the theory fails when the root mean square height is about one tenth of an electrical wavelength.

The physical optics program, because of its ability to handle long surfaces and its superiority to geometrical optics, has been applied to the direct calculation of the expected value of the scattered power from an ensemble of ocean-like surfaces which were constructed from a height spectrum similar to that of the sea. The computer time required, while lengthy, was not found to be prohibitive.

The extension of the programs to very long surfaces or to non-cylindrical surfaces appears feasible only for the G.O. and P.O. methods; the storage requirements for an I.E. solution in either case would be prohibitive. P.O. would probably be the easiest to modify to non-cylindrical surfaces, especially if shadowing were neglected. Since location of the specular points becomes much more complicated in the non-cylindrical case, the G.O. method would be more difficult to implement.

APPENDIX A
COMPUTER PROGRAMS

A listing of all the programs discussed in the text is presented here. To facilitate understanding of the programs, the symbols used in the programs have been used in the text whenever possible.

All programs require the plot subroutine listed at the end. The function subprograms AHAN20(x) and AHAN21(x) are required in the T.M. and T.E. integral equation programs respectively.

```

C THIS PROGRAM IS FOR BISTATIC BACKSCATTERING
C ESCNS IS THE RETURNED E FIELD WITH SHADOWING NOT ACCOUNTED FOR
C ESCNS IS E SCATTERED WITH SHADOWING ACCOUNTED FOR
C
C GEOMETRICAL OPTICS FOR THE OCEAN SURFACE
C
C SPECULAR POINT SEARCH IS DONE IN TWO STEPS
C #1 IS MECHANICAL WAVELENGTH DEPENDENT, #2 IS REFINED MECHANICAL OR
C ELECTRICAL WHICHEVER IS MORE STRINGENT
C DLTAX IS THE SEARCH SIZE#1, DLTAX00 IS SEARCH SIZE#2
C DELSHA IS SHADOW TEST STEP SIZE
C THIS PROGRAM CAN HANDLE 200 SPECULAR POINTS /PASS IE. ONE THIRDS
C DIMENSION XN(200), ANGLE(200)
C DIMENSION ACDNS(720), AWS(720), AACS(720), ASNS(720), ADS(720)
C DIMENSION ECDNS(720), EWS(720), EWCS(720), Y(10), ESNS(720)
C REAL PI, PI2
C REAL MTWO
C COMPLEX ESCNS, ESCWS, ENS
C COMMON CA, CB, CKA, CKB, PHA, PHB, CC, CKC, PHC
C COMPLEX ESCNS, ESCD
C NAMELIST/CAT/CA, CB, CKA, CKB, PHA, PHB, CC, CKC, PHC, WAVE, THID
C NAMELIST/CUT/ESNS, ASNS, ECDNS, ACDNS, EWS, AWS, EWCS, AACS, ADS
C
C THE FUNCTION WHICH DESCRIBES THE SURFACE IS
C  $H(X) = CA * SIN((CKA * X) + PHA) + CB * SIN((CKB * X) + PHB) + CC * SIN((CKC * X) + PHC)$ 
C CA=10.0
C CKA=6.28318/200.0
C PHA=0.0
C CB=0.0
C CKB=0.0
C PHB=0.0
C CC=0.0
C CKC=0.0
C PHC=0.0
C HMAX=ABS(CA)+ABS(CB)+ABS(CC)
C PI=3.14159
C PI2=1.5707963
C TPI=6.283185
C WMMIN IS THE MINIMUM MECHANICAL WAVELENGTH
C WMMIN=TPI/AMAX1(CKA, CKB, CKC)
C DLX=0.01000
C TWDLX=20.0*DLX
C NANI IS THE NUMBER OF ANGLES TO BE INVESTIGATED
C NANI=360
C XSTRT=-200.0
C XSTOP=-XSTRT
C THS IS THE ANGLE BETWEEN THE POS. X AXIS AND THE SCATTERING DIREC.
C TH1 IS THE ANGLE BETWEEN THE POS. X AXIS AND THE INC. DIRECTION
C
C TH1=60.0*3.1415927/180.0
C WAVE IS THE ELECTRICAL WAVELENGTH
C WAVE=25.0
C DLTAX=WMMIN/10.0
C DLTAX00=AMIN1((DLTAX/5.0), (WAVE/20.0))
C DELSHA=WMMIN/10.0
C XSKIP=XSTOP+(10**9)
C TANTH1=TAN(TH1)
C THID=TH1*180.0/3.14159
C CSTH1=COS(TH1)
C SNTH1=SIN(TH1)
C NAMELIST/TOM/DLTAX, DLTAX00, DELSHA
C WRITE(6, TOM)
C DO 93 IRE=1, NANI
C ASNS(IRE)=0.0
C ACDNS(IRE)=0.0
C AWS(IRE)=0.0
C AACS(IRE)=0.0
C ESNS(IRE)=0.0
C ECDNS(IRE)=0.0

```



```

EMS(IRE)=0.0
EMCS(IRE)=0.0
93 CONTINUE
DO 17 IJ=1,NANI
THS=FLOAT(IJ)*0.8726646 E-02
THSD=THS*57.29578
ADS(IJ)=THSD
WRITE(6,356) THID,THSD
356 FORMAT(11H INC ANGLE=,E15.8,13H SCATT ANGLE=,E15.8)
SUCOS=CSTHI+COS(THS)
SUSIN=SNTHI+SIN(THS)
N=0
C FIRST FIND POSITIONNS CF SPECULAR RETURN AND STORE THEM
C THE FIRST POSITION CAN NOT BE A SPECULAR POINT
XP=XSTRT
SUMD2=(THI+THS)/2.0
E=SUMD2-(TH(XP)+PI2)
102 KP=XP+DLTAX
EQ=E
E=SUMD2-(TH(XP)+PI2)
IF(E.EQ.0.0) GO TO 100
IF(((EQ.GT.0.0).AND.(E.LT.0.0)).OR.((EQ.LT.0.0).AND.(E.GT.0.0)))
2 GO TO 100
GO TO 101
100 N=N+1
XN(N)=XP
ANGLE(N)=THS-(TH(XP)+PI2)
101 IF (XP.LE. XSTOP) GO TO 102
IF(N.EQ.0) GO TO 372
C THIS IS TO REFINE THE POSITION OF THE SPECULAR POINT
DO 25 K=1,N
XSO=XN(K) -DLTAX
E=SUMD2-(TH(XSO)+PI2)
222 XSO=XSO+DLTXOO
EQ=E
E=SUMD2-(TH(XSO)+PI2)
IF(E.EQ.0.0) GO TO 252
IF(((EQ.GT.0.0).AND.(E.LT.0.0)).OR.((EQ.LT.0.0).AND.(E.GT.0.0)))
2 GO TO 252
GO TO 253
252 XN(K)=XSO
ANGLE(K)=THS-(TH(XSO)+PI2)
253 CONTINUE
IF (XSO.LT.XN(K)) GO TO 222
25 CONTINUE
ESCNS=CMPLX(0.0,0.0)
ESCDNS=CMPLX(0.0,0.0)
DO 10 K=1,N
PHASE=(TP/WAVE)*((SUCOS*XN(K))+SUSIN*H(XN(K)))
RC=RS(XN(K))*COS(ANGLE(K))
IF(RC.LT.0.0) PHASE=PHASE+(PI/2.0)
ENS=-((SQRT(ABS(RC/2.0)))*CEXP(CMPLX(0.0,PHASE)))
C TAPPING INCLUDED
XG=XN(K)
IF(XG.GT.(XSTOP-WAVE)) ENS=CMPLX(0.0,0.0)
IF(XG.LT.(XSTRT+WAVE)) ENS=CMPLX(0.0,0.0)
IF(((XG.GT.(XSTOP-(2.0*WAVE))).AND.(XG.LE.(XSTOP-WAVE)))
2ENS=ENS*(0.5+(0.5*SIN((3.14159/WAVE)*(XG-(XSTOP-(1.5*WAVE))))))
IF(((XG.GE.(XSTRT+WAVE)).AND.(XG.LE.(XSTRT+(2.0*WAVE))))
2ENS=ENS*(0.5+(0.5*SIN((3.14159/WAVE)*(XG-(XSTRT+(1.5*WAVE))))))
ESCNS=ESCNS+ENS
IF(RS(XN(K)).LE.0.0) GO TO 10
ESCDNS=ESCDNS+ENS
10 CONTINUE
ACD=CABS(ESCDNS)
IF(ACD.LT.1.0 E-05) GO TO 59
ANACD=57.29578*ATAN2(ATMAG(ESCDNS),REAL(ESCDNS))
59 CONTINUE
IF(ACD.LT. 1.0 E-05) ANACD=0.0

```

```

ESMAG=CABS(ESCNS)
ESANG=ATAN2(AIMAG(ESCNS),REAL(ESCNS))*180.0/3.1415927
WRITE(6,726) ESMAG,ESANG
726 FORMAT(' ', 'MAG. OF SCATT. E FIELD=',E15.8, 'PHASOR ANGLE=',E15.8,
23X, 'WITHOUT SHADOWING' )
WRITE (6,121) ACD,ANACC
121 FORMAT(' ', 'SCATT. FIELD NO SHADOW CONCAVE DOWN TIPS ONLY=',E15.8,
2'PHASOR ANGLE=',E15.8)
ESNS(IJ)=ESMAG
ECDNS(IJ)=ACD
ASNS(IJ)=ESANG
ACONS(IJ)=ANACC
C NOW FIND THE SHADOWING EFFECT
C INBOUND SHADOWING
IF (ABS(THI-PI/2).LT.0.05) GO TO 500
DO 327 K=1,N
BI=H(XN(K))-(TANTHI*XN(K))
STEPI=DELSHA
IF (TANTHI.LT.0.0) STEPI=-DELSHA
XI=XN(K)+STEPI
GO TO 471
470 XI=XI+STEPI
471 YI=(TANTHI*XI)+BI
IF (YI.LE.H(XI)) XN(K)=XSKIP
IF (ABS(XN(K)).GT.XSTOP) GO TO 499
IF (ABS(XI).GT.XSTOP) GO TO 499
IF (YI.LE.HMAX) GO TO 470
499 CONTINUE
327 CONTINUE
500 CONTINUE
C OUT BOUND SHADOWING
IF (ABS(THS-PI/2).LT.0.05) GO TO 639
TANTHS=TAN(THS)
DO 633 KK=1,N
IF (XN(KK).GT.XSTOP) GO TO 633
C THE ABOVE CARD MAKES SURE THAT TIME IS NOT SPENT ON A PT, ALREADY
C KNOWN TO BE SHADOWED
BO=H(XN(KK))-(TANTHS*XN(KK))
STEPO=DELSHA
IF (TANTHS.LT.0.0) STEPO=-DELSHA
XO=XN(KK)+STEPO
GO TO 671
670 XO=XO+STEPO
671 YO=(TANTHS*XO)+BO
IF (YO.LE.H(XO)) XN(KK)=XSKIP
IF (ABS(XN(KK)).GT.XSTOP) GO TO 699
IF (ABS(XO).GE.XSTOP) GO TO 699
IF (YO.LE.HMAX) GO TO 670
699 CONTINUE
633 CONTINUE
639 CONTINUE
C END OF SHADOWING EFFECT
ININ=0
ESCHS=CMPLX(0.0,0.0)

```

```

ESCDC=CMPLX(0.0,0.0)
DO 19 K=1,N
C   NEXT CARD SKIPS THE SHADOWED SPECULAR POINTS
   IF (XN(K).GT.XSTOP ) GO TO 19
   INININ=K
   PHASE=(PI/hAVE)*((SUCOS*XN(K))+(SUSIN*H(XN(K))))
   RC=RS(XN(K))*COS(ANGLE(K))
   IF(RC.LT.0.0) PHASE=PHASE+(PI/2.0)
   ENS=-((SQRT(ABS(RC/2.0)))*CEXP(CMPLX(0.0,PHASE)))
C   TAPERING INCLUDED
   XG=XN(K)
   IF(XG.GT.(XSTOP-WAVE)) ENS=CMPLX(0.0,0.0)
   IF(XG.LT.(XSTRT+WAVE)) ENS=CMPLX(0.0,0.0)
   IF((XG.GT.(XSTOP-(2.0*WAVE))) .AND. (XG.LE.(XSTOP-WAVE)))
2ENS=ENS*(0.5-(0.5*SIN((3.14159/WAVE)*(XG-(XSTOP-(1.5*WAVE))))))
   IF((XG.GE.(XSTRT+WAVE)) .AND. (XG.LE.(XSTRT+(2.0*WAVE))))
2ENS=ENS*(0.5+(0.5*SIN((3.14159/WAVE)*(XG-(XSTRT+(1.5*WAVE))))))
   ESCWS=ESCWS+ENS
   IF(RS(XN(K)).LE.0.0) GO TO 19
   ESCDC=ESCDC+ENS
19  CONTINUE
   IF( INININ.EQ.0) WRITE(6,3149)
   IF(INININ.EQ.0) GO TO 23
   ABESCD=CABS(ESCDC)
   IF(ABESCD.LT. 1.0 E-05) GO TO 58
   ANESCD=57.29578*ATAN2(AIMAG(ESCDC),REAL(ESCDC))
58  CONTINUE
   IF(ABESCD .LT. 1.0E-05) ANESCD=0.0
   ESMAGS=CABS(ESCWS)
   ESANGS=ATAN2(AIMAG(ESCWS),REAL(ESCWS))*180.0/3.1415927
3149 FORMAT(' ','NO SCATTERED E FIELD WITH SHADUWING')
   IF(INININ.NE.0) WRITE(6,776) ESMAGS,ESANGS
776  FORMAT(' ','MAG OF SCATT. E FIELD WITH SHADUWING=',E15.8,'PHASOR
      2 ANGLE=',E15.8)
   IF(INININ.NE.0) WRITE(6,2118) ABESCD,ANESCD
2118 FORMAT(' ','SCAT FIELD WITH SHAD. CCNCAVE DOWN ONLY=',E15.8,
      2' PHASOR ANGLE=',E15.8)
   EWS(IJ)=ESMAGS
   EWCS(IJ)=ABESCD
   AWS(IJ)=ESANGS
   AWCS(IJ)=ANESCD
   GO TO 23
372  WRITE (6,3152) THID,THSD
3152 FORMAT(' NO SPECULAR POINTS FOR THID=',E15.8,' AND THSD=',E15.8)
23  WRITE(6,779)
     WRITE(6,779)
779  FORMAT(1H )
17  CONTINUE

C   FOR THE PLOTS
DO 536 IKO=1,NANI
   IND=IKO-1
   THSD=AOS( IKO)
   Y(1)=ESNS( IKO)
536  CALL PLOT(THSD,Y,1,IND,50.0,0.0)
     DO 537 IKO=1,NANI
       IND=IKO-1
       THSD=AOS( IKO)
       Y(1)=EWS( IKO)
537  CALL PLCT(THSD,Y,1,IND,50.0,0.0)
     DO 538 IKO=1,NANI
       IND=IKO-1
       THSD=AOS( IKO)
       Y(1)=ECDNS( IKO)
538  CALL PLOT(THSD,Y,1,IND,50.0,0.0)
     DO 539 IKO=1,NANI
       IND=IKO-1
       THSD=AOS( IKO)
       Y(1)=ENCNS( IKO)

```

```

539 CALL PLOT(THSD,Y,1,IND,50.0,0.0)
      DO 936 KKRL=1,NANI
      ANGOS=FLOAT(KKRL)/2.0
      IF(ESNS(KKRL).LE.0.0001) GO TO 936
      DBNS=20.0*ALOG10(ESNS(KKRL))
      WRITE(6,937) DBNS,ANGOS
937  FORMAT('  DBNS=',E15.8,'  ANGOS=',E15.8)
936  CONTINUE
      DO736 KKRL=1,NANI
      ANGOS=FLOAT(KKRL)/2.0
      IF( EWS(KKRL).LE.0.0001) GO TO 736
      DBS=20.0*ALOG10(EWS(KKRL))
      WRITE(6,737) DBS,ANGOS
737  FORMAT('  DBS=',E15.8,'  ANGOS=',E15.8)
736  CONTINUE
      STOP
      END

```

```

      FUNCTION RS(X)
      COMMON CA,CB,CKA,CKB,PHA,PHB,CC,CKC,PHC
C     THIS GIVES THE RADIUS OF CURVATURE AT X
      HP=(CA*CKA*COS((CKA*X)+PHA))+(CB*CKB*COS((CKB*X)+PHB))
      2+(CC*CKC*COS((CKC*X)+PHC))
      HPP=-((CA*CKA*CKA*SIN((CKA*X)+PHA))+(CB*CKB*CKB*SIN((CKB*X)+PHB))
      2+(CC*CKC*CKC*SIN((CKC*X)+PHC)))
      RS=((1.0+(HP*HP))**1.5)/(-HPP)
      RETURN
      END

```

```

      FUNCTION TH(X)
      COMMON CA,CB,CKA,CKB,PHA,PHB,CC,CKC,PHC
      TH=ATAN2((CA*CKA*COS((CKA*X)+PHA))+(CB*CKB*COS((CKB*X)+PHB))
      2+(CC*CKC*COS((CKC*X)+PHC)),1.0)
C     THIS FUNCTION GIVES THE ANGLE BET. THE TANGENT TO H(X) AND THE
C     HORIZONTAL
      RETURN
      END

```

```

      FUNCTION H(X)
      COMMON CA,CB,CKA,CKB,PHA,PHB,CC,CKC,PHC
      H=(CA*SIN((CKA*X)+PHA))+(CB*SIN((CKB*X)+PHB))+CC*SIN((CKC*X)+PHC)
      RETURN
      END

```

```

DIMENSION Y(10),ESSS(360)
C THIS IS THE TM CASE
C THIS PROGRAM USES PHYSICAL OPTICS TO CALCULATE THE BACKSCATTERING
C FROM A SEA SURFACE BY DIVIDING SURFACE INTO LIT AND UNLIT REGIONS
C IN THE LIT REGIONS THE SURFACE CURRENT IN 2NXH
C GAUSSIAN INTEGRATION USED
C FOR THIS PROGRAM TO GIVE USEFUL RESULTS THE SURFACE MUST HAVE
C RADII OF CURVATURE NO LESS THAN 1*WE
C NSP IS THE NUMBER OF SHADOW POINTS
C SURFACE IS DESCRIBED BY AONE*SIN(CONE*X+PONE) +ATWO*SIN(CTWO*X
C +PTWO)+ATRE*SIN(CTRE*X+PTRE)
C SURFACE UNDER CONSIDERATION LIES BETWEEN ALEP AND REP
C SN IS THE STEP SIZE TAKEN TO DETERMINE SHADOWING
C IT MUST BE SMALLER THAN ANY SURFACE FEATURES AND MUST ALSO
C ALLCW THE LOCATION OF THE END POINTS OF INTEGRATION WITHIN
C A SMALL FRACTION OF A WAVELENGTH
C NANI IS THE NUMBER OF ANGLES (SCATTERING) TO BE EXAMINED
C MAKE DIMENSIONS OF ESSS , SCANG,EPA SMALL AS POSSIBLE TO AVOID
C LAGE # OF CARDS RETURNED
C NANI SHOULD BE THE DIMENSION OF ESSS,SCANG,EPA
NAMELIST/ROD/AB,ANG,DTHS
DIMENSION SCANG(360),EPA(360)
COMPLEX S,BINT
C SCATTER SHADOWING HAS NOT BEEN ACCOUNTED FOR
COMMON /DOG/AONE,CONE,PONE,ATWO,CTWO,PTWO,ATRE,CTRE,PTRE
COMMON /HOG/ G,THI,THS,WE
COMMON/PIG/ SECTOR,DX,REP,SECD10
COMMON/GSNN/GW1,GW2,GW3,GW4,GW5,GU1,GU2,GU3,GU4,GU5
WE=25.0
C WE IS THE ELECTRICAL WAVELENGTH
G=2.0*3.1415927/WE
SRTWE=SQRT(WE)
CX=WE/15.0
ADNE=50.0
CONE=2.0*3.1415927/800.0
PONE=3.14159/2.0
ATWO=0.0
CTWO=0.0
PTWO=0.0
ATRE=0.0
CTRE=0.0
PTRE=0.0
NANI=360
SECTOR=WE/2.0
SECD10=SECTOR/10.0
C CONSTANTS FOR GAUSSIAN INTEGRATION
GW1=0.2369268
GW2=0.47862867
GW3=0.568889
GW4=GW2
GW5=GW1
GU1=-0.9061798
GU2=-0.53846931
GU3=0.0
GU4=-GU2
GU5=-GU1
C THE ANGLE OF INCIDENCE SHOULD NOT BE GREATER THAN 90 DEG
THI=60.0*3.1415927/180.0
C IF THE INCIDENCE ANGLE IS WITHIN TEN DEGREES OF 90 NO SHADOWING
C TAKEN INTO ACCBUNT
IF(ABS(THI-1.5707).LT.0.175) GO TO 563
TANTHI=TAN(THI)
DTHI=180.0*THI/3.1415927
WRITE(6,1071) DTHI
1071 FORMAT(' ',ANG OF INC FROM POS X AXIS =',E15.0)

```

```

REP=200.0
ALEP=-REP
SN=WE/10.0
NSP=1
DIMENSION SX(1000)
IF(DH(REP).GT.TANTHI) GO TO 106
SX(NSP)=REP
GO TO 105
106 SLOPE=TANTHI
B=H(REP)-(SLOPE*REP)
X=REP
109 X=X-SN
IF((SLOPE*X)+B.GT.H(X)) GO TO 109
IF(X.LE.ALEP) GO TO 1000
SX(NSP)=X-(SN/2.0)
105 CONTINUE
C THIS ABOVE TAKES CARE OF THE FIRST RIGHTENDPOINT
15 X=SX(NSP)
22 X=X-SN
XN=X-SN
IF((DH(X).LT.TANTHI).AND.(DH(XN).GT.TANTHI)) GO TO 53
IF(X.GT.ALEP) GO TO 22
GO TO 92
53 NSP=NSP+1
SX(NSP)=XN
SLOPE=TANTHI
B=H(SX(NSP))-(SLOPE*SX(NSP))
X=SX(NSP)-SN
29 X=X-SN
IF((SLOPE*X)+B.LT.H(X)) GO TO 39
IF(X.GT.ALEP) GO TO 29
GO TO 92
39 NSP=NSP+1
SX(NSP)=X-(SN/2.0)
GO TO 15
92 NSP=NSP+1
SX(NSP)=ALEP
GO TO 564
563 SX(1)=REP
SX(2)=ALEP
NSP=2
564 CONTINUE
C LAST VALUE IN SX(J) IS ALEP
WRITE (6,101) (K,SX(K),K=1,NSP)
101 FORMAT(' ',SX(' ',14,' ')=' ',E15.8)
DO 317 JNX=1,NANI
THS=FLOAT(JNX)*(0.8726646 E-02)
DTHS=180.0*THS/3.1415927
SCANG(JNX)=DTHS
S=CMPLX(0.0,0.0)
KKN=1.
10 CONTINUE
ALOW=SX(KKN+1)
AUPP=SX(KKN)
S=S+BINT(ALOW,AUPP)
KKN=KKN+2
IF ((KKN.LT.NSPI).AND.((KKN+1).LT.NSPI)) GO TO 10
C TO CONVERT TO TRUE SCATTERED E FIELD FOR EINC OF UNITY MAG.
S=CMPLX(-0.70711,-0.70711)*S/SRTWE
AB=CABS(S)
ESSS(JNX)=AB
ANG=180.0*ATAN2(AIMAG(S),REAL(S))/3.1415927
EFPA(JNX)=ANG
317 CONTINUE
DO 531 JK=1,NANI

```

```

E=ESSS(JK)
DB=20.0*ALOG10(E)
A=FFPA(JK)
AS=SCANG(JK)
531 WRITE (6,532) AS,E,A,DB
532 FORMAT(' ', ' SCAT ANG FROM HORIZ=' ,E15.8, ' MAG OF E FIELD=' ,
2 E15.8, ' PHASE ANG=' ,E15.8, ' DB=' ,E15.8)
DO 535 IKE=1,NANI
IND=IKE-1
THSD=FLOAT(IKE)/2.00
Y(I)=ESSS(IKE)
535 CALL PLOT (THSD,Y,1,IND,50.0,0.0)
GO TO 1002
1000 WRITE(6,1592)
1592 FORMAT(' SURFACE IS NOT ILLUMINATED')
1002 CONTINUE
STOP
END

FUNCTION H(X)
COMMON /DCG/AONE,CONE,PONE,ATWO,CTWO,PTWO,ATRE,CTRE,PTRE
H=AONE*SIN(CONE*X+PONE)+ATWO*SIN(CTWO*X+PTWO)+ATRE*SIN(CTRE*X+PTRE)
2)
RETURN
END

FUNCTION DH(X)
COMMON /DCG/AONE,CONE,PONE,ATWO,CTWO,PTWO,ATRE,CTRE,PTRE
DH=AONE*CONE*COS(CONE*X+PONE)+ATWO*CTWO*COS(CTWO*X+PTWO)
2 +ATRE*CTRE*COS(CTRE*X+PTRE)
RETURN
END

FUNCTION BINT(XX,YY)
C XX IS LOWER LIMIT OF INTEGRATION,YY IS UPPER LIMIT
C PHYSICAL OPTICS RADIATION INTEGRAL WITH PLANE WAVE INCIDENT
C TM CASE
C COMPLEX S,BINT
C COMPLEX GASS5
COMMON /HOG/ G,TH1,THS,WE
COMMON/PIG/ SECTOR,DX,REP,SECD10
C BREAK INTEGRAL FROM XX TO YY INTO SMALLER SEGMENTS OF LENGTH
C SECTOR AND INTEGRATE OVER EACH SEGMENT USING GAUSSIAN INTEGRATION
S=CMPLX(0.0,0.0)
LDS=INT((YY-XX)/SECTOR)
IF(LDS.EQ.0) GO TO 10
DO 100 INJ=1,LDS
UL=XX+(FLOAT(INJ)*SECTOR)
ALL=XX+(FLOAT(INJ-1)*SECTOR)
100 S=S+GASS5(ALL,UL)
C NOW TO GET LAST FRACTION OF SEGMENT LEFT OVER FROM SURFACE SEGMENTATION
S=S+GASS5(XX+(FLOAT(LDS)*SECTOR),YY)
GO TO 50
10 S=GASS5(XX,YY)
50 CONTINUE
BINT=S
RETURN
END

```

```

.....
FUNCTION GASS5 (XL,XU)
COMPLEX GASS5,FTBI
C ..... FIFTH ORDER GAUSSIN INTEGRATION
C ..... XL IS LOWER LIMIT,XU IS UPPER LIMIT
C ..... XU-XL IS LESS THAN OR EQUAL TO SECTOR
COMMON/GSNN/GW1,GW2,GW3,GW4,GW5,GU1,GU2,GU3,GU4,GU5
DVPFEP=(XU-XL)/2.0
DVSMEP=(XU+XL)/2.0
XU5=GU5*DVPFEP+DVSMEP
XU4=GU4*DVPFEP+DVSMEP
XU3=GU3*DVPFEP+DVSMEP
XU2=GU2*DVPFEP+DVSMEP
XU1=GU1*DVPFEP+DVSMEP
GASS5=DVPFEP*(GW1*FTBI(XU1)+GW2*FTBI(XU2)+GW3*FTBI(XU3)
2 +GW4*FTBI(XU4)+GW5*FTBI(XU5))
RETURN
END

```

```

.....
FUNCTION FTBI(X)
COMPLEX FTBI
C ..... THIS IS THE FUNCTION TO BE INTEGRATED
C ..... THIS IS FOR THE TM CASE
COMMON/HOG/G,THI,THS,WE
COMMON/PIG/ SECTOR,DX,REP,SECD10
GCC=G*(COS(THI)+COS(THS))
GSS=G*(SIN(THI)+SIN(THS))
RCK=REP-(2.0*WE)
FTBI=SIN(THI-ATAN(DH(X)))*SQRT(1.0+(DH(X)**2))*
2 CEXP(CMPLX(0.0,((X*GCC)+(H(X)*GSS))))
C ..... THE FOLLOWING ACCOUNTS FOR TAPERING
ABSX=ABS(X)
IF(ABSX-RCK) 1500,1500,2000
2000 IF(X.LE.(WE-REP)) FTBI=CMPLX(0.0,0.0)
IF(X.GE.(REP-WE)) FTBI=CMPLX(0.0,0.0)
IF((X.GT.(WE-REP)).AND.(X.LE.((2.0*WE)-REP)))
2 FTBI=FTBI*(0.5+(0.5*SIN((G/2.0)*(X-((1.5*WE)-REP))))))
IF((X.LT.(REP-WE)).AND.(X.GT.(REP-(2.0*WE))))
2 FTBI=FTBI*(0.5-(0.5*SIN((G/2.0)*(X-(REP-(1.5*WE))))))
1500 CONTINUE
RETURN
END

```



```

C THIS IS THE TE CASE
C THIS PROGRAM USES PHYSICAL OPTICS TO CALCULATE THE BACKSCATTERING
C FROM A SEA SURFACE BY DIVIDING SURFACE INTO LIT AND UNLIT REGIONS
C IN THE LIT REGIONS THE SURFACE CURRENT IN 2NXH
C GAUSSIAN INTEGRATION USED
C FOR THIS PROGRAM TO GIVE USEFUL RESULTS THE SURFACE MUST HAVE
C RADI[1] OF CURVATURE NO LESS THAN 1*WE
C NSP IS THE NUMBER OF SHADOW POINTS
C SURFACE IS DESCRIBED BY AONE*SIN(CONE*X+PONE) +ATWO*SIN(CTWO*X
C +PTWO)+ATRE*SIN(CTRE*X+PTRE)
C SURFACE UNDER CONSIDERATION LIES BETWEEN ALEP AND REP
C SN IS THE STEP SIZE TAKEN TO DETERMINE SHADOWING
C IT MUST BE SMALLER THAN ANY SURFACE FEATURES AND MUST ALSO
C ALLOW THE LOCATION OF THE END POINTS OF INTEGRATION WITHIN
C A SMALL FRACTION OF A WAVELENGTH
C NANI IS THE NUMBER OF ANGLES (SCATTERING) TO BE EXAMINED
C MAKE DIMENSIONS OF ESSS , SCANG,EFPA SMALL AS POSSIBLE TO AVOID
C LAGE # OF CARDS RETURNED
C NANI SHOULD BE THE DIMENSION OF ESSS,SCANG,EFPA
C DIMENSION Y(10),ESSS(360)
C NAMELIST/ROK/AB,ANG,DTHS
C DIMENSION SCANG(360),EFPA(360)
C COMPLEX S,BINT
C SCATTER SHADOWING HAS NOT BEEN ACCOUNTED FOR
C COMMON /DOG/AONE,CONE,PDNE,ATWO,CTWO,PTWO,ATRE,CTRE,PTRE
C COMMON /HDC/ G,THI,THS,WE
C COMMON/PIG/ SECTOR,DX,REP,SECD10
C COMMON/GSNN/GW1,GH2,GH3,GH4,GW5,GU1,GU2,GU3,GU4,GU5
C WE=25.0
C WE IS THE ELECTRICAL WAVELENGTH
C G=2.0*3.1415927/WE
C SRTHE=SQRT(WE)
C DX=WE/15.0
C AONE=40.0
C CONE=2.0*3.1415927/200.0
C PDNE=0.0
C ATWO=0.0
C CTWO=0.0
C PTWO=0.0
C ATRE=0.0
C CTRE=0.0
C PTRE=0.0
C NANI=360
C SECTOR=WE/2.0
C SECD10=SECTOR/10.0
C CONSTANTS FOR GAUSSIAN INTEGRATION
C GW1=0.2369268
C GH2=0.47862867
C GH3=0.568889
C GH4=GH2
C GH5=GH1
C GU1=-0.9061798
C GU2=-0.53846931
C GU3=0.0
C GU4=-GU2
C GU5=-GU1
C THE ANGLE OF INCIDENCE SHOULD NOT BE GREATER THAN 90 DEG
C THI=60.0*3.1415927/180.0
C IF THE INCIDENCE ANGLE IS WITHIN TEN DEGREES OF 90 NO SHADOWING
C TAKEN INTO ACCOUNT
C IF(ABS(THI-1.5707).LT.0.175) GO TO 563
C TANTHI=TAN(THI)
C DTHI=180.0*THI/3.1415927
C WRITE(6,1071) DTHI
1071 FORMAT(' ',' ' ANG OF INC FROM POS X AXIS =',E15.8)

```

```

REP=200.0
ALEP=-REP
SN=WE/10.0
NSP=1
DIMENSION SX(1000)
IF(DH(REP).GT.TANTHI) GO TO 106
SX(NSP)=REP
GO TO 105
106 SLOPE=TANTHI
B=H(REP)-(SLOPE*REP)
X=REP
109 X=X-SN
IF((SLOPE*X)+B.GT.H(X)) GO TO 109
IF(X.LE.ALEP) GO TO 1000
SX(NSP)=X-(SN/2.0)
105 CONTINUE
C THIS ABOVE TAKES CARE OF THE FIRST RIGHTENDPOINT
15 X=SX(NSP)
22 X=X-SN
XN=X-SN
IF((DH(X).LT.TANTHI).AND.(DH(XN).GT.TANTHI)) GO TO 53
IF(X.GT.ALEP) GO TO 22
GO TO 92
53 NSP=NSP+1
SX(NSP)=XN
SLOPE=TANTHI
B=H(SX(NSP))-(SLOPE*SX(NSP))
X=SX(NSP)-SN
29 X=X-SN
IF((SLOPE*X)+B.LT.H(X)) GO TO 39
IF(X.GT.ALEP) GO TO 29
GO TO 92
39 NSP=NSP+1
SX(NSP)=X-(SN/2.0)
GO TO 15
92 NSP=NSP+1
SX(NSP)=ALEP
GO TO 564
563 SX(1)=REP
SX(2)=ALEP
NSP=2
564 CONTINUE
C SURFACE IS NOW SEPERATED INTO LIT AND UNLIT ZONES
C LAST VALUE IN SX(J) IS ALEP
WRITE(6,101) (K,SX(K),K=1,NSP)
101 FORMAT(' ',SX(' ',14,' '),'E15.8)
C THE FOLLOWING FINDS THE SCATTERED FIELDS DUE TO THE LIT ZONES
DO 317 JNX=1,NANI
THS=FLOAT(JNX)*(0.8726646 E-02)
DTHS=180.0*THS/3.1415927
SCANG(JNX)=DTHS
S=CMPLX(0.0,0.0)
KKN=1
10 CONTINUE
ALOW=SX(KKN+1)
AUPP=SX(KKN)
S=S+B*INT(ALOW,AUPP)
KKN=KKN+2
IF((KKN.LT.NSP).AND.((KKN+1).LT.NSP)) GO TO 10
C TO CONVERT TO TRUE SCATTERED H FIELD FOR HINC OF UNITY MAG
S=S*CMPLX(0.70711,0.70711)/SRTWE
AB=CABS(S)
DB=20.0*ALDGI0(AB)
ESSS(JNX)=AB
ANG=180.0*ATAN2(AIMAG(S),REAL(S))/3.1415927
EPPA(JNX)=ANG
C WRITE(6,143) DTHS,AB,ANG,DB

```

```

143 FORMAT(' SCATTERING ANG',E15.8,' MAG=',E15.8,' PHASE ANGLE=',
2E15.8,' DB=',E15.8)
317 CONTINUE
DO 531 JK=1,NANI
E=ESSS(JK)
A=EFPA(JK)
AS=SCANG(JK)
531 WRITE (6,532) AS,E,A
532 FORMAT(' ', ' SCAT ANG FROM HORIZ=' ,E15.8,' MAG OF H FIELD=',
2 E15.8,' PHASE ANG=',E15.8)
DO 535 IKE=1,NANI
IND=IKE-1
THSD=FLOAT(IKE)/2.00
Y(I)=ESSS(IKE)
535 CALL PLOT (THSD,Y,1,IND,50.0,0.0)
GO TO 1002
1000 WRITE(6,1592)
1592 FORMAT(' SURFACE IS NOT ILLUMINATED')
1002 CONTINUE
STOP
END

```

```

FUNCTION H(X)
COMMON /DOG/AONE, CONE, PONE, ATWO, CTWO, PTHO, ATRE, CTRE, PTRE
H=AONE*SIN(CONE*X+PONE)+ATWO*SIN(CTWO*X+PTHO)+ATRE*SIN(CTRE*X+PTRE)
2)
RETURN
END

```

```

FUNCTION DH(X)
COMMON /DOG/AONE, CONE, PONE, ATWO, CTWO, PTHO, ATRE, CTRE, PTRE
DH=AONE*CDNE*CDN(CONE*X+PONE)+ATWO*CTWO*CDN(CTWO*X+PTHO)
2 +ATRE*CTRE*CDN(CTRE*X+PTRE)
RETURN
END

```

```

FUNCTION BINT(XX,YY)
C XX IS LOWER LIMIT OF INTEGRATION, YY IS UPPER LIMIT
C PHYSICAL OPTICS RADIATION INTEGRAL WITH PLANE WAVE INCIDENT
C TH CASE
COMPLEX S, BINT
COMPLEX GASS5
COMMON /HOG/ G, THI, THS, WE
COMMON/PIG/ SECTOR, DX, REP, SECD10
C BREAK INTEGRAL FROM XX TO YY INTO SMALLER SEGMENTS OF LENGTH
C SECTOR AND INTEGRATE OVER EACH SEGMENT USING GAUSSIAN INTEGRATION
S=CHPLX(0.0,0.0)
LDS=INT((YY-XX)/SECTOR)
IF(LDS.EQ.0) GO TO 10
DO 100 INJ=1,LDS
UL=XX+(FLOAT(INJ)*SECTOR)
ALL=XX+(FLOAT(INJ-1)*SECTOR)
100 S=S+GASS5(ALL,UL)
S=S+GASS5(XX+(FLOAT(LDS)*SECTOR),YY)
GO TO 50
10 S=GASS5(XX,YY)
50 CONTINUE
BINT=S
RETURN
END

```

```

FUNCTION GASS5 (XL,XU)
COMPLEX GASS5,FTBI
C FIFTH ORDER GAUSSIN INTEGRATION
C XL IS LOWER LIMIT,XU IS UPPER LIMIT
C XU-XL IS LESS THAN OR EQUAL TO SECTOR
COMMON/GSNN/GW1,GW2,GW3,GW4,GW5,GU1,GU2,GU3,GU4,GU5
DVPFEP=(XU-XL)/2.0
DVSMEP=(XU+XL)/2.0
XU5=GU5*DVPFEP+DVSMEP
XU4=GU4*DVPFEP+DVSMEP
XU3=GU3*DVPFEP+DVSMEP
XU2=GU2*DVPFEP+DVSMEP
XU1=GU1*DVPFEP+DVSMEP
GASS5=DVPFEP*(GW1*FTBI(XU1)+GW2*FTBI(XU2)+GW3*FTBI(XU3)
2 +GW4*FTBI(XU4)+GW5*FTBI(XU5))
RETURN
END

```

```

FUNCTION FTBI(X)
COMPLEX FTBI
C THIS IS THE FUNCTION TO BE INTEGRATED
C THIS IS FOR THE TM CASE
COMMON/HOG/G,THI,THS,HE
COMMON/PIG/SECTOR,DX,REP,SECD10
GCC=G*(COS(THI)+COS(THS))
GSS=G*(SIN(THI)+SIN(THS))
RCK=REP-(2.0*WE)
FTBI=SIN(THS-ATAN(DH(X)))*SQRT(1.0+(DH(X)**2))*
2 CEXP(CMPLX(0.0,((X*GCC)+(H(X)*GSS)))
C THE FOLLOWING ACCOUNTS FOR TAPERING
ABSX=ABS(X)
IF(ABSX-RCK) 1500,1500,2000
2000 IF(X.LE.(WE-REP)) FTBI=CMPLX(0.0,0.0)
IF(X.GE.(REP-WE)) FTBI=CMPLX(0.0,0.0)
IF((X.GT.(WE-REP)).AND.(X.LE.((2.0*WE)-REP)))
2 FTBI=FTBI*(0.5+(0.5*SIN((G/2.0)*(X-((1.5*WE)-REP))))
IF((X.LT.(REP-WE)).AND.(X.GT.(REP-(2.0*WE))))
2 FTBI=FTBI*(0.5-(0.5*SIN((G/2.0)*(X-(REP-(1.5*WE))))))
1500 CONTINUE
RETURN
END

```

```

C   THIS IS A METHOD OF MOMENTS SOLUTION
C   TH POLARIZATION SYMMETRIC MATRIX
C   NSUB SEGMENTS HAVE N MIDPOINTS
C   NSUB IS THE SUBSCRIPT WHICH COUNTS THE END POINTS
C   N IS THE SUBSCRIPT WHICH COUNTS THE MIDPOINTS
C   WATCH MAX SLOPE SO THAT THE X INCREMENTS ARE SMALL ENOUGH
C   THE REGION UNDER CONSIDERATION LIES BETWEEN -EP AND EP
C   DIMENSION Y(10),CMC(360)
C   COMPLEX SNN,SST
C   COMPLEX FSS
C   DOUBLE PRECISION DAL,DDX,DDC2,DDC,DALC,DR
C   COMPLEX FINC(30),STS
C   COMMON /PIG/ AONE,CONE,PCNE,ATWO,CTWO,PTWO,N
C   COMPLEX AHAN20
C   COMPLEX F(300),S(45150),SS,T
C   COMPLEX FIN
C   DIMENSION X(300)
C   DIMENSION XMID(300)
C   COMPLEX STO
C   WE IS THE ELECTRICAL WAVELENGTH
C   WE=25.0
C   G=6.2831853 /WE
C   STS=SQRT(WE)*CMLX(1.0,1.0)*(+0.707107)/3.1415927
C   DC=WE/10.0
C   DX=DC/100.0
C   DC2=DC/2.0
C   EP=200.0
C   API=3.1415927
C   THE FOLLOWING CONSTANTS DEFINE THE SURFACE
C   AONE=25.0
C   CCNE=2.0*3.1415927/200.0
C   PCNE=C.0
C   ATWO=C.0
C   CTWO=C.0
C   PTWO=0.0
C   CALL SCLOK1
C   THE FOLLOWING BREAKS THE SURFACE INTO SEGMENTS DC CENTIMETERS LONG
C   BY LINE INTEGRATION USING STEPS OF LENGTH DX FOR THE INTEGRATION
C   NSUB=1
C   X(NSUB)=-EP
C   DDC=DBLE(DC)
C   DDX=DBLE(DX)
C   DDC2=DBLE(DC2)
1002 DAL=0.00D 00
C   DR=CPLX(X(NSUB))
1001 DR=DR+DDX
C   R=SNGL(DR)
C   DAL=DAL
C   CAL=CAL+(CDX*DSQRT(1.0D 00 +((DBLE(DH(R)))**2)))
C   IF(((DDC2-DAL).LE.C.0D 00).AND.((DDC2-CALO).GE.0.0D 00))
2   XMID(NSUB)=R
C   IF(DAL.LT.CDC)GO TO 1001
C   NSUB=NSUB+1
C   X(NSUB)=R
C   AL=SNGL(CAL)
C   WRITE(6,352) AL,NSUB
352 FORMAT(' ',AL=' ',E15.8,' NSUB=',I4)
C   IF(R.LT.EP) GO TO 1002
C   TIME=RCLCK1(1.0)
C   WRITE(6,3276) TIME
3276 FORMAT(' ',TIME=' ',F10.6,'SECCNDS')
C   N=NSUB-1
C   DO 1004 J=1,NSUB
C   IF (J.EQ.NSUB) XMID(NSUB)=0.0
C   XXX=X(J)
C   XMD=XMID(J)

```

```

1004 WRITE (6,1003) XXX,XMD,J
1003 FORMAT (6H X(J)=,E15.8,9H XMD(J)=,E15.8,3H J=,I3)
C THIS ENDS THE SURFACE SUBDIVISION
NM0=N-1
NM3=N-3
C DIMENSION OF S IS N(N+1)/2
C DIMENSION OF FINC,F IS N
DPIF=0.7853982
EE=2.71828
GA=G*DC/(2.0*EE)
C SNN IS THE DIAGONAL ELEMENT OF THE INPUT MATRIX
SNN=AHANZO(GA)
WRITE (6,400) SNN
400 FORMAT (5H SNN=,2E15.8)
DO 100 NJ=1,N
NJPD=NJ+1
S(ISUB(NJ,NJ))=SNN
C THIS FINDS ELEMENTS ON THE DIAGONAL
IF (NJPD.GT.N) GO TO 100
DO 100 NA=NJPD,N
C THIS FINDS OFF DIAGONAL ELEMENTS
XM=XMD(NJ)
XN=XMD(NA)
RHO=SQRT(((XN-XM)**2)+((H(XN)-H(XM))**2))
RHG=RHO*G
S(ISUB(NJ,NA))=AHANZO(RHG)
100 CONTINUE
C THIS COMPLETES THE FILLIN OF THE MATRIX
C THIS BEGINS THE CONVERSION TO UPPER TRIANGULAR MATRIX
S(1)=CSQRT(S(1))
DO 1 K=2,N
1 S(K)=S(K)/S(1)
DO 2 I=2,N
IM0=I-1
IPO=I+1
T=CMPLX(0.0,0.0)
DO 3 L=1,IM0
LI=(L*N)-(((L-1)*L)/2)+N-1
3 T=T+(S(LI)**2)
II=(I*N)-(((I-1)*I)/2)+N-1
S(II)=CSQRT(S(II)-T)
IF (IPO.GT.N) GOTO 2
DO 5 J=IPO,N
T=CMPLX(0.0,0.0)
DO 6 M=1,IM0
MI=(M*N)-(((M-1)*M)/2)+N-1
MJ=(M*N)-(((M*(M-1))/2)+N-J)
6 T=T+(S(MJ)*S(MI))
IJ=(I*N)-(((I-1)*I)/2)+N-J
5 S(IJ)=(S(IJ)-T)/S(II)
2 CONTINUE
C THIS ENDS THE CONVERSION TO UPPER TRIANGULAR MATRIX
WRITE (6,1222) N,WE
1222 FORMAT(3H N=,I3,4H WE=,E15.8)
TH=60.0*3.1415927/180.0
THXD=180.0*TH/3.1415927
WRITE (6,9333) THXD
9333 FORMAT(9H INC ANG=,E15.8)
C TH IS THE ANGLE OF INCIDENCE FROM THE HORIZONTAL
STH=SIN(TH)
CTH=COS(TH)
C THIS FINDS THE INCIDENT FIELD ION THE NJTH SEGMENT
DO 455 NJ=1,N
ENJ=FLOAT(NJ)
XM=XMD(NJ)
F(NJ)=CEXP(CMPLX(0.0,G*(XM*CTH)+(H(X)*STH)))

```

C
C
C
C
C

TAPERED ILLUMINATION *****

```

IF(XM.LE.((WE*1.0)-EP)) F(NJ)=CMPLX(0.0,0.0)
IF(XM.GE.(EP-(1.0*WE))) F(NJ)=CMPLX(0.0,0.0)
IF((XM.GT.((1.0*WE)-EP)).AND.(XM.LE.((2.0*WE)-EP)))
2 F(NJ)=F(NJ)*(0.5+(0.5*SIN((G/2.0)*(XM -((1.5*WE)-EP))))))
IF((XM .GE.(EP-(2.0*WE))).AND.(XM .LT.(EP-(1.0*WE))))
2 F(NJ)=F(NJ)*(0.5-(0.5*SIN((G/2.0)*(XM -(EP-(1.5*WE))))))
455 CONTINUE
WRITE(6,2948) (NJ,F(NJ),NJ=1,N)
2948 FORMAT(' ', ' INC FIELD F(',14,')=' ,2E15.8)
C THIS BEGINS THE BACK SUBSTITUTION
F(1)=F(1)/S(1)
DO 10 I=2,N
IMD=I-1
T=CMPLX(0.0,0.0)
DO 11 L=1,IMG
LI=(L*N)-(((L-1)*L)/2)+N-1
11 T=T+(S(LI)*F(L))
II=(I*N)-(((I-1)*I)/2)+N-1
10 F(I)=(F(I)-T)/S(II)
NN=(N*(N+1))/2
F(N)=F(N)/S(NN)
NMC=N-1
DO 25 I=1,NMD
K=N-I
KPD=K+1
T=CMPLX(0.0,0.0)
DO 26 L=KPD,N
KL=(K*N)-(((K-1)*K)/2)+N-L
26 T=T+(S(KL)*F(L))
KK=(K*N)-(((K-1)*K)/2)+N-K
F(K)=(F(K)-T)/S(KK)
25 CONTINUE
C THIS ENDS THE BACK SUBSTITUTIONS
DO 491 K=1,N
STT=CABS(F(K))
STO=F(K)
ANNN=ATAN2(AIMAG(F(K)),REAL(F(K)))*180.0/3.1415927
491 WRITE(6,492) K,STO,STT,ANNN
492 FORMAT(' ', 'F(',14,')=' ,2E15.8, ' OR ', 'AMP=' ,E15.8, ' AT ANGLE=' ,
2 E15.8)
DO 317 JNX=1,360
TH=0.872664625E-02 *FLOAT(JNX)
T=CMPLX(0.0,0.0)
DO 310 I=1,N
XN=XMID(I)
310 T=T+ ((F(I)*CEXP(CMPLX(0.0,G*(XN*COS(TH))+H(XN)*SIN(TH))))))
C THIS CORRECTS T TO TRUE SCATTERED FIELD
T=STS*T
CM=CARS(T)
CMC(JNX)=CM
CANG=57.296*ATAN2(AIMAG(T),REAL(T))
THD=TH*57.296
DB=20.0*ALOG10(CM)
317 WRITE (6,312) CM,CANG,THD,DB
312 FORMAT (18H RELATIVE E FIELD=,E15.8,7H ANGLE=,E15.8,
2 23H ANGLE FROM HOPIZONTAL=,E15.8,7H DB=,E15.8)

```

```

DO 576 IKE=1,360
THSD=FLOAT(IKE)/2.0
IND=IKE-1
Y(I)=CMC(IKE)
576 CALL PLOT(THSD,Y,1,IND,50.0,0.0)
STOP
END

FUNCTION H(X)
C THIS DEFINES THE SURFACE
COMMON /PIG/ AONE,CONE,PONE,ATWO,CTWO,PTWO,N
H=AONE*SIN(CONE*X+PONE)+ATWO*SIN(CTWO*X+PTWO)
RETURN
END

FUNCTION DH(X)
C DH(X) IS THE DERIV. OF H(X)
COMMON /PIG/ ACNE,CONE,PONE,ATWO,CTWO,PTWO,N
DH=ACNE*CONE*COS(CONE*X+PONE)+ATWO*CTWO*COS(CTWO*X+PTWO)
RETURN
END

FUNCTION ISUB(J,K)
COMMON /PIG/ AONE,CONE,PONE,ATWO,CTWO,PTWO,N
C THIS CONVERTS ELEMENTS OF UPPER TRIANGULAR MATRIX TO A LINEAR
ISUB=(N*J)-((((J-1)*J)/2)+N-K)
C ARRAY COUNTING LEFT TO RIGHT STARTING WITH FIRST ROW
RETURN
END

```



```

C THIS IS A METHOD OF MOMENTS SOLUTION FOR BISTATIC SCATT TM CASE
C GAUSSIAN INTEGRATION IS USED TO CALCULATE THE MATRIX ELEMENTS
C UNIT INCIDENT ELECTRIC FIELD IS ASSUMED, OF COURSE THIS IS MODIFIED
C NEAR THE ENDPOINTS OF THE SURFACE BY ILLUMINATION TAPERING
C NSUB SEGMENTS HAVE N MIDPOINTS
C NSUB IS THE SUBSCRIPT WHICH COUNTS THE END POINTS
C N IS THE SUBSCRIPT WHICH COUNTS THE MIDPOINTS
C WATCH MAX SLOPE SO THAT THE X INCREMENTS ARE SMALL ENOUGH
C THE SURFACE UNDER CONSIDERATION LIES BETWEEN -EP AND +EP
C THE ARRAY XM(J) CONTAINS THE X COORDINATES OF THE MIDPOINTS OF THE
C SEGMENTS, XM(1) IS THE MIDPOINT OF THE 1' TH SEGMENT
C THE ARRAY X(J) CONTAINS THE X COORDINATES OF THE ENDPOINTS OF THE
C SURFACE SEGMENTS, X(I), X(I+1) ARE THE LOWER AND UPPER X COORDINATES
C OF THE ENDPOINTS OF THE I' TH SEGMENT
C PHASE REFERENCE IS AT THE ORIGIN OF THE COORDINATE SYSTEM
C
C COMPLEX SNN, SST
C COMPLEX S
C DIMENSION Y(10), CNC(360)
C NAMELIST /D/ WE, EP, THXXD, AONE, CONE, PONE, ATWO, CTWO, PTWO, N
C NAMELIST /E/F, XMID
C COMPLEX FSS
C COMPLEX STS
C COMMON /PIG/ AONE, CONE, PONE, ATWO, CTWO, PTWO, N
C COMPLEX C(236,236)
C COMPLEX F(236), SS, T, CTEST
C THE DIMENSIONS OF C AND F MUST BE COMMENSURATE
C THAT IS C(L,L) ---- F(L)
C COMPLEX FIN
C COMPLEX HAN2
C DIMENSION X(500)
C DIMENSION XM(500)
C THE FOLLOWING CONSTANTS DESCRIBE THE SURFACE
C ACNE=-50.0
C CONE=6.28318/800.0
C PONE=3.1415927/2.0
C ATWO=0.0
C CTWO=0.0
C PTWO=0.0
C WE IS THE ELECTRICAL WAVELENGTH
C WE=25.0
C G=6.2831853 /WE
C DC=WE/10.0
C DX=DC/1000.0
C DC2=DC/2.0
C EP=200.0
C THE FOLLOWING BREAKS THE SURFACE INTO SEGMENTS DC CENTIMETERS LONG
C BY LIVE INTEGRATION USING STEPS OF LENGTH DX FOR THE INTEGRATION
C NSUB=1
C X(NSUB)=-EP
1002 AL=0.000
C R=X(NSUB)
1001 R=R+DX
C ALU=AL
C AL=AL+(DX*SQRT(1.0+(DH(R)**2)))
C IF(((DC2-AL).LE.0.0).AND.((DC2-ALD).GT.0.0)) XM(NSUB)=R
C IF(AL.LT.DC) GO TO 1001
C WRITE (6,352) AL, NSUB
352 FORMAT(' ', 'AL=', E15.8, ' NSUB=', I4)
C NSUB=NSUB+1
C X(NSUB)=R
C IF (R.LT.EP) GO TO 1002
C N=NSUB-1
C DO 1004 J=1, NSUB
C IF (J.EQ.NSUB) XM(NSUB)=0.0
C XXX=X(J)
C XND= XM(J)

```

```

1004 WRITE (6,1003) XXX,XMD,J
1003 FORMAT (6H X(J)=,E15.8,9H XM(J)=,E15.8,3H J=,I3)
C THIS ENDS THE SURFACE SUBDIVISION
NM0=N-1
NM3=N-3
C DIMENSION OF FINC,F IS N
DP1F=0.7853982
EE=2.71828
GA=G*DC/(2.0*EE)
C SNN IS THE DIAGONAL ELEMENT OF THE INPUT MATRIX
SNN=HAN2(GA)*DC
WRITE (6,400) SNN
400 FORHAT (5H SNN=,2E15.8)
DO 100 NJ=1,N
C(NJ,NJ)=SNN
100 CONTINUE
C CONSTANTS FOR GAUSSIAN INTEGRATION 5 TH. ORDER
GU1=-0.9061798
GU2=-0.53846931
GU3=0.0
GU4=-GU2
GU5=-GU1
GM1=0.2369268
GM5=0.2369268
GM4=0.47862867
GM2=0.47862867
GM3=0.5688888
DO 3361 MR=1,N
XMM=XM(MR)
HXMM=H(XMM)
DO 3361 MC=1,N
IF (MC.EQ.MR) GO TO 3361
EPL=X(MC)
EPU=X(MC+1)
DVDFEP=(EPU-EPL)/2.0
DVSMEP=(EPU+EPL)/2.0
XU5=GU5*DVSMEP+DVSMEP
XU1=GU1*DVSMEP+DVSMEP
XU2=GU2*DVSMEP+DVSMEP
XU3=GU3*DVSMEP+DVSMEP
XU4=GU4*DVSMEP+DVSMEP
C(MR,MC)=DVSMEP*(
2+GM1*HAN2(G*SQRT(((XU1-XMM)**2)+(H(XU1)-HXMM)**2)))*SQRT(1.0+(DH(
2 XU1)**2))
2+GM2*HAN2(G*SQRT(((XU2-XMM)**2)+(H(XU2)-HXMM)**2)))*SQRT(1.0+(DH(
2 XU2)**2))
2+GM3*HAN2(G*SQRT(((XU3-XMM)**2)+(H(XU3)-HXMM)**2)))*SQRT(1.0+(DH(
2 XU3)**2))
2+GM4*HAN2(G*SQRT(((XU4-XMM)**2)+(H(XU4)-HXMM)**2)))*SQRT(1.0+(DH(
2 XU4)**2))
2+GM5*HAN2(G*SQRT(((XU5-XMM)**2)+(H(XU5)-HXMM)**2)))*SQRT(1.0+(DH(
2 XU5)**2)))
3361 CONTINUE
C THIS COMPLETES THE FILLIN OF THE MATRIX
C NCNSYMMETRIC CROUT
C FIRST COLUMN OK
C TOO GET FIRST ROW
DO 10 J=2,N
10 C(1,J)=C(1,J)/C(1,1)
C NOW WORK ON ROW AND COLUMN SET K
DO 11 K=2,N
KMD=K-1
KPD=K+1

```

```

C      TO GET DIAGONAL ELEMENT
      S=CMPLX(0.0,0.0)
      DO 12 IK=1,KMO
12     S=S+C(K,IK)*C(IK,K)
      C(K,K)=C(K,K)-S
C      TO GET ELEMENTS IN COLUMN K BELOW ROW K
      IF (KPO.GT.N) GO TO 17
      DO 13 IROW=KPO,N
      S=CMPLX(0.0,0.0)
      DO 14 JJ=1,KMO
14     S=S+C(IROW,JJ)*C(JJ,K)
13     C(IROW,K)=C(IROW,K)-S
C      TO GET ELEMENTS IN ROW K TO THE RIGHT OF COLUMN K
      DO 15 ICOL=KPO,N
      S=CMPLX(0.0,0.0)
      DO 16 JR=1,KMO
16     S=S+C(K,JR)*C(JR,ICOL)
15     C(K,ICOL)=(C(K,ICOL)-S)/C(K,K)
17     CONTINUE
11     CONTINUE
      WRITE (6,1222) N,WE
1222  FORMAT(3H N=,I3,4H WE=,E15.8)
      TH1=3.1415927*60.0/180.0
      THXD=TH1*180.0/3.1415927
      WRITE (6,9333) THXD
9333  FORMAT(9H INC ANG=,E15.8)
C      TH1 IS THE ANGLE OF INCIDENCE MEASURED FROM THE HORIZONTAL
C      I.E. THE POSITIVE X-AXIS
      STH=SIN(TH1)
      CTH=COS(TH1)
C      THIS FINDS THE INCIDENT FIELD ION THE NJTH SEGMENT
      DO 455 NJ=1,N
      XG=XM(NJ)
      F(NJ)=CEXP(CMPLX(0.0,G*(((XG*CTH)+(F(XG)*STH))))))
C
C
C      TAPERD ILLUMINATION
C
      IF(XG.LE.((WE*1.0)-EP)) F(NJ)=CMPLX(0.0,0.0)
      IF(XG.GE.(EP-(1.0*WE))) F(NJ)=CMPLX(0.0,0.0)
      IF((XG.GT.((1.0*WE)-EP)).AND.(XG.LE.((2.0*WE)-EP)))
2     F(NJ)=F(NJ)*(0.5+(0.5*SIN((G/2.0)*(XG -((1.5*WE)-EP))))))
      IF(XG .GE.(EP-(2.0*WE)).AND.(XG .LT.(EP-(1.0*WE))))
2     F(NJ)=F(NJ)*(0.5-(0.5*SIN((G/2.0)*(XG -(EP-(1.5*WE))))))
      ABSF=CABS(F(NJ))
      WRITE(6,83) NJ,ABSF
83    FCRMAT(' INC FIELD AT XM(,I4,')=,E15.8)
455   CONTINUE
C      THIS BEGINS THE BACK SUBSTITUTION
C      CONVERSION OF SOURCE SIDE
      F(1)=F(1)/C(1,1)
      DO 90 IJ=2,N
      S=CMPLX(0.0,0.0)
      IJMO=IJ-1
      DO 91 IK=1,IJMO
91     S=S+C(IJ,IK)*F(IK)
90     F(IJ)=(F(IJ)-S)/C(IJ,IJ)
C      NOW FOR FINAL BACK SUBSTITUTION

```

```

NMO=N-1
DO 160 L=1,NMO
K=N-L
KPO=K+1
S=CMPLX(0.0,0.0)
DO 175 JO=KPO,N
175 S=S+C(K,JO)*F(JO)
160 F(K)=F(K)-S
DO 425 KCURR=1,N
ABF=CABS(F(KCURR))
ANGF=180.0*ATAN2(AIMAG(F(KCURR)),REAL(F(KCURR)))/3.1415927
425 WRITE(6,553) KCURR,ABF,ANGF
553 FORMAT(' F(',I4,')=',E15.8,' AT. ANGLE',E15.8)
C THIS NDS THE BACK SUBSTITUTIONS
DC 439 KURR=1,N
IND=KURR-1
Y(1)=CABS(F(KURR))*4.0*WE/(6.28318*377.0)
XCRO=FLOAT(KURR)
439 CALL PLOT(XCRD,Y,1,IND,0.0200,0.0)
DO 440 KURR=1,N
IND=KURR-1
Y(1)=180.0*ATAN2(AIMAG(F(KURR)),REAL(F(KURR)))/3.1415927
XCRD=FLOAT(KURR)
440 CALL PLOT(XCRD,Y,1,IND,180.0,-180.0)
DC 317 JNX=1,360
TF=0.87266463 E-02*FLOAT(JNX)
T=CMPLX(0.0,0.0)
DO 310 I=1,N
XI=XH(I)
310 T=T+ ((F(I)*CEXP(CMPLX(0.0,G*((XN*(COS(TH))+H(XN)*SIN(TH))))))
T=T+DC*SQRT(WE)*CMPLX(-0.707107,-0.707107)/3.1415927
CM=CABS(T)
DB=20.0*ALOG10(CM)
CMC(JNX)=CM
CANG=57.296*ATAN2(AIMAG(T),REAL(T))
THD=TH+57.296
317 WRITE (6,312) CM,CANG,THD,DB
312 FORMAT (18H RELATIVE E FIELD=,E15.8,7H ANGLE=,E15.8,
2 23H ANGLE FROM HORIZONTAL=,E15.8,6H DB= ,E15.8)
DO 441 IES=1,360
IND=IES-1
Y(1)=CMC(IES)
THS=FLOAT(IES)/2.0
441 CALL PLOT(THS,Y,1,IND,50.0,0.0)
STOP
END

FUNCTION H(X)
C THIS DEFINES THE SURFACE
COMMON /PIG/ AONE,CONE,PONE,ATWO,CTWO,PTWO,N
H=AONE*SIN(CONE*X+PONE)+ATWO*SIN(CTWO*X+PTWO)
RETURN
END

FUNCTION HAN2(X)
C I DO THIS TO AVOID RETYPING THE WHOLE GAUSS INT. PART
COMPLEX HAN2
COMPLEX AHAN20
HAN2=AHAN20(X)
RETURN
END

FUNCTION DH(X)
C DH(X) IS THE DERIV. OF H(X)
COMMON /PIG/ AONE,CONE,PONE,ATWO,CTWO,PTWO,N
DH=AONE*CONE*COS(CONE*X+PONE)+ATWO*CTWO*COS(CTWO*X+PTWO)
RETURN
END

```

```

C THIS IS A METHOD OF MOMENTS SOLUTION FOR BISTATIC SCATT TM CASE
C USING TWO POINT INTERPOLATION
C GAUSSIAN INTEGRATION IS USED TO CALCULATE THE MATRIX ELEMENTS
C NSUB SEGMENTS HAVE N MIDPOINTS
C NSUB IS THE SUBSCRIPT WHICH COUNTS THE END POINTS
C N IS THE SUBSCRIPT WHICH COUNTS THE MIDPOINTS
C WATCH MAX SLOPE SO THAT THE X INCREMENTS ARE SMALL ENOUGH
C THE SURFACE UNDER CONSIDERATION LIES BETWEEN -EP AND +EP
C COMPLEX SNN,SST
C COMPLEX S,CO
C COMPLEX FSS.
C COMPLEX F(400),STS
C COMMON /PIG/ ADNE,CONE,PONE,ATWO,CTHO,PTWO,N
C COMMON /HOG/ XM(400),X(400),GA,G,DC
C COMMON/GASSN/ GU1,GU2,GU3,GU4,GU5,GW1,GW2,GW3,GW4,GW5
C COMPLEX C(150,150)
C COMPLEX F(400),FP(400),SS,T,CTEST
C COMPLEX FIN
C COMPLEX HANZ
C DIMENSION ABES(360),Y(10)
C WE IS THE ELECTRICAL WAVELENGTH
WE=25.0
C THE FOLLOWING CONSTANTS DESCRIBE THE SURFACE
ADNE=15.0
CONE=2.0*3.1415927/200.0
PONE=0.0
ATWO=0.0
CTHO=0.0
PTWO=0.0
DC=WE/10.0
DX=DC/1000.0
DC2=DC/2.0
DPIF=0.7853982
G=6.2831853 /WE
EE=2.71828
GA=G+DC/(2.0*EE)
C EP IS THE END POINT
EP=200.0
C CONSTANTS FOR GAUSSIAN INTEGRATION 5 TH ORDER
GU1=-0.9061798
GU2=-0.53846921
GU3=0.0
GU4=-GU2
GU5=-GU1
GW1=0.2369268
GW5=0.2369268
GW4=0.47862867
GW2=0.47862867
GW3=0.5688888
C CONSTANTS FOR GAUSSIAN INTEGRATION 5 TH ORDER
C THE FOLLOWING BREAKS THE SURFACE INTO SEGMENTS DC CENTIMETERS LONG
C BY LINE INTEGRATION USING STEPS OF LENGTH DX FOR THE INTEGRATION
NSUB=1
X(NSUB)=-EP
1002 AL=0.000
R=X(NSUB)
1001 R=R+DX
ALO=AL
AL=AL+(DX*SQRT(1.0+(DPIF)**2))
IF(((DC2-AL).LE.0.0).AND.(DC2-ALO).GT.0.0) XM(NSUB)=R
IF(AL.LT.DC)GO TO 1001
NSUB=NSUB+1
X(NSUB)=R
IF (R.LT.EP) GO TO 1002

```

```

N=NSUB-1
DO 1004 J=1,NSUB
IF (J.EQ.NSUB) XM(NSUB)=0.0
XXX=X(J)
XMD= XM(J)
1004 WRITE (6,1003) XXX,XMD,J
1003 FORMAT (6H X(J)=,E15.8,9H XM(J)=,E15.8,3H J=,I3)
C THIS ENDS THE SURFACE SUBDIVISION
C THIS INSURES THAT N IS ODD
KK=0
5733 KK=KK+1
IF ((2*KK-1).EQ.N) GO TO 5731
IF (2*KK.EQ.N) GO TO 5732
GO TO 5733
5732 N=N-1
5731 CONTINUE
WRITE (6,3728) N,KK
3728 FORMAT (' ', 'CORRECTED VALUE OF N=', I4, 'KK=', I4, '2*KK-1=N')
NMO=N-1
NM3=N-3
C DIMENSION OF FINC,F IS N
C MATRIX FILL IN
C DO BY COLUMNS
C FOR FIRST COLUMN
DO 3661 I=1,KK
3661 C(I,1)=CO(2*I-1,1)+(CO(2*I-1,2)/2.0)
C FOR LAST COLUMN
DO 3678 I=1,KK
3678 C(I,KK)=(CO(2*I-1,2*KK-2)/2.0)+CO(2*I-1,2*KK-1)
C FOR MIDDLE COLUMNS
DO 56 I=1,KK
II=2*I-1
KKM1=KK-1
DO 56 J=2,KKM1
JJ=2*J-1
C(I,J)=(CO(II,JJ-1)/2.0)+CO(II,JJ)+(CO(II,JJ+1)/2.0)
56 CONTINUE
C THIS COMPLETES THE FILLIN OF THE MATRIX
C NONSYMMETRIC CROUT
C FIRST COLLOM OK
C TO GET THE FIRST ROW
DO 10 J=2,KK
10 C(1,J)=C(1,J)/C(1,1)
C NOW WORK EM ROW AND COLUMN SET K
DO 11 K=2,KK
KMO=K-1
KPO=K+1
C TO GET DIAGONAL ELEMENT
S=CMLPX(0.0,0.0)
DO 12 IK=1,KMO
12 S=S+C(K,IK)*C(IK,K)
C(K,K)=C(K,K)-S
C TO GET ELEMENTS IN COLUMN K BELOW ROW K
IF(KPO.GT.KK) GO TO 17
DO 13 IROW=KPO,KK
S=CMLPX(0.0,0.0)
DO 14 JJ=1,KMO
14 S=S+C(IROW,JJ)*C(JJ,K)
13 C(IROW,K)=C(IROW,K)-S
C TO GET ELEMENTS IN ROW K TO THE RIGHT OF COLUMN K
DO 15 ICOL=KPO,KK
S=CMLPX(0.0,0.0)
DO 16 JR=1,KMO
16 S=S+C(K,JR)*C(JR,ICOL)
15 C(K,ICOL)=(C(K,ICOL)-S)/C(K,K)
17 CONTINUE
11 CONTINUE

```

```

WRITE (6,1222) KK,WE
1222 FORMAT(' ', ' KK=', I4, ' WE=', E15.8)
TH=3.1415927*60.0/180.0
THDEG=57.29578*TH
WRITE (6,9333) THDEG
9333 FORMAT(9H THC ANG=, E15.8)
C TH IS THE ANGLE OF INCIDENCE FROM THE HORIZONTAL
STH=SIN(TH)
CTH=COS(TH)
C THIS FINDS THE INCIDENT FIELD ION THE NJTH SEGMENT
DO 455 NJ=1, KK
XG=XM(2*NJ-1)
FP(NJ)=CEXP(CMPLX(0.0, G*((XG*CTH)+(H(XG)*STH))))
IF(XG.LE.((WE*1.0)-EP)) FP(NJ)=CMPLX(0.0,0.0)
IF(XG.GT.((EP-1.0*WE))) FP(NJ)=CMPLX(0.0,0.0)
IF((XG.GT.((1.0*WE)-EP)).AND.(XG.LE.((2.0*WE)-EP)))
2 FP(NJ)=FP(NJ)*(0.5+(0.5*SIN((G/2.0)*(XG-((1.5*WE)-EP))))
IF((XG.GE.(EP-(2.0*WE))).AND.(XG.LT.(EP-(1.0*WE))))
2 FP(NJ)=FP(NJ)*(0.5-(0.5*SIN((G/2.0)*(XG-(EP-(1.5*WE))))))
455 CONTINUE
WRITE(6,9410) (NJ,FP(NJ),NJ=1, KK)
9410 FORMAT(' ', ' INCIDENT FIELD FINC(' , I4, ') =', 2E15.8)
C THIS BEGINS THE BACK SUBSTITUTION
C CONVERSION OF SOURCE SIDE
FP(1)=FP(1)/C(1,1)
DO 90 IJ=2, KK
S=CMPLX(0.0,0.0)
IJMO=IJ-1
DO 91 IK=1, IJMO
91 S=S+C(IJ, IK)+FP(IK)
90 FP(IJ)=(FP(IJ)-S)/C(IJ, IJ)
C NOW FOR FINAL BACK SUBSTITUTION
NMO=KK-1
DO 160 L=1, NMO
K=KK-L
KPO=K+1
S=CMPLX(0.0,0.0)
DO 175 JD=KPO, KK
175 S=S+C(K, JD)+FP(JD)
160 FP(K)=FP(K)-S
KKM1=KK-1
C TO RECONSTRUCT THE CURRENTS
DO 47 IRA=1, KKM1
47 F(2*IRA)=(FP(IRA)+FP(IRA+1))/2.0
DO 48 IRA=1, KK
48 F(2*IRA-1)=FP(IRA)
WRITE (6,4970)((J,FP(J)),J=1, KK)
4970 FORMAT(' ', ' FP(' , I5, ') =', 2E15.8)
WRITE (6,553) (F(K),K=1, N)
553 FORMAT (6H F(K)=, 2E15.8)
C THIS ENDS THE BACK SUBSTITUTIONS
DO 439 KURR=1, N
IND=KURR-1
Y(1)=CABS(F(KURR))*4.0*WE/(6.28318*377.0)
XORD=FLOAT(KURR)
439 CALL PLOT(XORD, Y, 1, IND, 0.0200, 0.0)
DO 440 KURR=1, N
IND=KURR-1
Y(1)=180.0*ATAN2(AIMAG(F(KURR)), REAL(F(KURR)))/3.1415927

```

```

XORD=FLGAT(KURR)
440 CALL PLOT(XORD,Y,1,IND,180.0,-180.0)
DO 317 JNK=1,360
TH=0.01745329*FLOAT(JNK)/2.0
T=CMPLX(0.0,0.0)
DO 310 I=1,N
XN=XM(I)
310 T=T+ ((F(I)*CEXP(CMPLX(0.0,G*((XN*COS(TH))+(H(XN)*SIN(TH))))))
C ***** THIS CORRECTS THE OUTPUT TO TRUE ELE. FIELD
T=T+DC*SQRT(WE)*CMPLX(-0.707107,-0.707107)/3.1415927
CH=CABS(T)
DB=20.0*ALOG10(CH)
CANG=57.296*ATAN2(AIMAG(T),REAL(T))
THD=TH*57.296
ABES(JNK)=CM
317 WRITE (6,312) CH,CANG,THD,DB
312 FORMAT (18H RELATIVE E FIELD=,E15.8,7H ANGLE=,E15.8,
2 23H ANGLE FROM HORIZONTAL=,E15.8,6H DB=,E15.8)
DO 9500 JC=1,360
Y(J)=ABES(JC)
E=FLOAT(JC)/2.0
IND=JC-1
9500 CALL PLOT(E,Y,1,IND,50.0,0.0)
STOP
END

```

```

FUNCTION CO(MR,MC)
COMPLEX CO
COMPLEX AHAN20
COMMON/GASSN/ GU1, GU2, GU3, GU4, GU5, GW1, GW2, GW3, GW4, GW5
COMMON /HDG/ XM(400), X(400), GA, G, DC
IF(MR.NE.MC) GO TO 100
CO=DC*AHAN20(GA)
GO TO 200
100 CONTINUE
XMM=XM(MR)
HXMM=H(XMM)
EPL=X(MC)
EPU=X(MC+1)
DVDFEP=(EPU-EPL)/2.0
DVSMEP=(EPU+EPL)/2.0
XU5=GU5*DVDFEP+DVSMEP
XU1=GU1*DVDFEP+DVSMEP
XU2=GU2*DVDFEP+DVSMEP
XU3=GU3*DVDFEP+DVSMEP
XU4=GU4*DVDFEP+DVSMEP
CO=DVDFEP*(
2*GW1*AHAN20(G*SQRT(((XU1-XMM)**2)+((H(XU1)-HXMM)**2)))*SQRT(1.0
2+(DH(XU1)**2))
2*GW2*AHAN20(G*SQRT(((XU2-XMM)**2)+((H(XU2)-HXMM)**2)))*SQRT(1.0
2+(DH(XU2)**2))
2*GW3*AHAN20(G*SQRT(((XU3-XMM)**2)+((H(XU3)-HXMM)**2)))*SQRT(1.0
2+(DH(XU3)**2))
2*GW4*AHAN20(G*SQRT(((XU4-XMM)**2)+((H(XU4)-HXMM)**2)))*SQRT(1.0
2+(DH(XU4)**2))
2*GW5*AHAN20(G*SQRT(((XU5-XMM)**2)+((H(XU5)-HXMM)**2)))*SQRT(1.0
2+(DH(XU5)**2)))
200 CONTINUE
RETURN
END

```


C FUNCTION DH(X)
DH(X) IS THE DERIV. OF H(X)
COMMON /PI@/ ADNE, CONE, PONE, ATWO, CTWO, PTWO, N
DH=ADNE*CONE*COS(CONE*X+PONE)+ATWO*CTWO*COS(CTWO*X+PTWO)
RETURN
END

C FUNCTION H(X)
THIS DEFINES THE SURFACE
COMMON /PI@/ ADNE, CONE, PONE, ATWO, CTWO, PTWO, N
H=ADNE*SIN(CONE*X+PONE)+ATWO*SIN(CTWO*X+PTWO)
RETURN
END

```

C      TE CASE , GAUSSIAN INTEGRATION USED TO FILL IN MATRIX, INTEGRAL EQN:
C      NSUB SEGMENTS HAVE N MIDPOINTS
C      NSUB IS THE SUBSCRIPT WHICH COUNTS THE END POINTS
C      N      IS THE SUBSCRIPT WHICH COUNTS THE MIDPOINTS
C      WATCH MAX SLOPE SO THAT THE X INCREMENTS ARE SMALL ENOUGH
C      THE ARRAY XM(J) CONTAINS THE X COORDINATES OF THE MIDPOINTS OF THE
C      SURFACE SEGMENTS, X(I), X(I+1) ARE THE LOWER AND UPPER X COORDINATES
C      OF THE ENDPOINTS OF THE I' TH SEGMENT
C      THE SURFACE UNDER CONSIDERATION LIES BETWEEN -EP AND +EP
C      COMPLEX SNN, SST
C      COMPLEX S, CO
C      COMPLEX FSS
C      COMMON/GASSN/ GU1, GU2, GU3, GU4, GU5, GW1, GW2, GW3, GW4, GW5
C      COMPLEX FINC(20), STS
C      COMMON /PIG/ AGNE, CONE, PONE, ATWO, CTWO, PTWO, N
C      COMPLEX C(235, 235)
C      COMMON/HOG/ XM(400), G, X(400)
C      COMMON /DOG/ DJC
C      COMPLEX DJC
C      COMPLEX F(235), SS, T, CTEST
C      COMPLEX FIN
C      COMPLEX HAN2
C      DIMENSION      ABES(360), Y(10)
C      THE FOLLOWING CONSTANTS DESCRIBE THE SURFACE
C      AONE=40.0
C      CONE=6.28318/200.0
C      PONE=0.0
C      ATWO=0.0
C      CTWO=0.0
C      PTWO=0.0
C      WE IS THE ELECTRICAL WAVELENGTH
C      WE=25.0
C      G=6.2831853      /WE
C      DC=WE/10.0
C      DX=DC/1000.0
C      DC2=DC/2.0
C      EP=200.0
C      STS=-DC*CMPLX(0.707107, 0.707107)/(2.0*SQRT(WE))
C      DJC=CMPLX(0.0, 1.0)*G/4.0
C      CONSTANTS FOR GAUSSIAN INTEGRATION 5 TH ORDER
C      GU1=-C.9061798
C      GU2=-C.53846931
C      GU3=0.0
C      GU4=-GU2
C      GU5=-GU1
C      GW1=0.2369268
C      GW5=0.2369268
C      GW4=0.47862867
C      GW2=0.47862867
C      GW3=0.5688888
C      CONSTANTS FOR GAUSSIAN INTEGRATION 5 TH ORDER
C      THE FOLLOWING BREAKS THE SURFACE INTO SEGMENTS DC CENTIMETERS LONG
C      BY LINE INTEGRATION USING STEPS OF LENGTH DX FOR THE INTEGRATION
C      NSUB=1
C      X(NSUB)=-EP
1002 AL=0.000
C      R=X(NSUB)
1001 R=R+DX
C      ALO=AL
C      AL=AL+(DX*SQRT(1.0+(DH(R)**2)))
C      IF(((DC2-AL).LE.0.0).AND.((DC2-ALO).GT.0.0))      XM(NSUB)=R
C      IF(AL.LT.DC)GO TO 1001

```

```

WRITE(6,352) AL,NSUB
352 FORMAT(' AL=',E15.8,' NSUB=',I4)
NSUB=NSUB+1
X(NSUB)=R
IF (R.LT.EP) GO TO 1002
N=NSUB-1
WRITE(6,251) N,NSUB
251 FORMAT(' N=',I4,' NSUB=',I4)
DO 1004 J=1,NSUB
IF (J.EQ.NSUB) XM(NSUB)=0.0
XXX=X(J)
XMD= XM(J)
1004 WRITE (6,1003) XXX,XMD,J
1003 FORMAT (6H X(J)=,E15.8,9H XM(J)=,E15.8,3H J=,I3)
C THIS ENDS THE SURFACE SUBDIVISION
NMC=N-1
NM3=N-3
C DIMENSION OF FINC,F IS N
DPIF=0.7853982
C MATRIX FILL IN
DO 3661 IR=1,N
DO 3661 IC=1,N
3661 C(IR,IC)=CQ(IR,IC)
C THIS COMPLETES THE FILLIN OF THE MATRIX
C NCNSYMMETRIC CRQUT
C FIRST COLUMN OK
C TO GET THE FIRST ROW
DO 10 J=2,N
10 C(1,J)=C(1,J)/C(1,1)
C NOW WORK ON ROW AND COLUMN SET K
DO 11 K=2,N
KMC=K-1
KPO=K+1
C TO GET DIAGONAL ELEMENT
S=CMPLX(0.0,0.0)
DO 12 IK=1,KMC
12 S=S+C(K,IK)*C(1K,K)
C(K,K)=C(K,K)-S
C TO GET ELEMENTS IN COLUMN K BELOW ROW K
IF (KPO.GT.N) GO TO 17
DO 13 IROW=KPO,N
S=CMPLX(0.0,0.0)
DO 14 JJ=1,KMC
14 S=S+C(IROW,JJ)*C(JJ,K)
13 C(IROW,K)=C(IROW,K)-S
C TO GET ELEMENTS IN ROW K TO THE RIGHT OF COLUMN K
DO 15 ICOL=KPO,N
S=CMPLX(0.0,0.0)
DO 16 JR=1,KMC
16 S=S+C(K,JR)*C(JR,ICOL)
15 C(K,ICOL)=(C(K,ICOL)-S)/C(K,K)
17 CONTINUE
11 CONTINUE
C THIS ENDS THE MATRIX FACTORIZATION
WRITE (6,1222) N,NE
1222 FORMAT(3H N=,I3,4H NE=,E15.8)
THI=60.0*3.14159/180.0
WRITE (6,9333) THI
9333 FORMAT(9H INC ANG=,E15.8)
C THI IS THE ANGLE OF INC. MEAS. FROM THE +VE X AXIS
STH=SIN(THI)
CTH=COS(THI)
C THIS FINDS THE INCIDENT FIELD ION THE NJTH SEGMENT
DO 455 NJ=1,N
455 XG=XM(NJ)

```

```

C THE SIGN ON THE INCIDENT FIELD HAS BEEN ADJUSTED TO AGREE WITH
C THE INTEGRAL EQUATION.
F(NJ)=CEXP(CMPLX(0.0,G*{(XG*CTH)+(H(XG)*STH)}))*CMPLX(-1.0,0.0)
C
C
C TAPERED ILLUMINATION
IF(XG.LE.((WE*1.0)-EP)) F(NJ)=CMPLX(0.0,0.0)
IF(XG.GE.(EP-(1.0*WE))) F(NJ)=CMPLX(0.0,0.0)
IF((XG.GT.((1.0*WE)-EP)).AND.(XG.LE.((2.0*WE)-EP)))
2 F(NJ)=F(NJ)*(0.5+(0.5*SIN((G/2.0)*(XG -((1.5*WE)-EP))))))
IF((XG .GE.(EP-(2.0*WE))).AND.(XG .LT.(EP-(1.0*WE))))
2 F(NJ)=F(NJ)*(0.5-(0.5*SIN((G/2.0)*(XG -(EP-(1.5*WE))))))
455 CONTINUE
WRITE(6,2948) (NJ,F(NJ),NJ=1,N)
2948 FORMAT(' ', ' INC FIELD F(',I4,')='',2E15.8)
C THIS BEGINS THE BACK SUBSTITUTION
C CONVERSION OF SOURCE SIDE
F(1)=F(1)/C(1,1)
DO 90 IJ=2,N
S=CMPLX(0.0,0.0)
IJMO=IJ-1
DO 91 IK=1,IJMO
91 S=S+C(IJ,IK)*F(1K)
90 F(IJ)=(F(IJ)-S)/C(IJ,IJ)
C NOW FOR FINAL BACK SUBSTITUTION
NMC=N-1
DO 160 L=1,NMD
K=N-L
KPC=K+1
S=CMPLX(0.0,0.0)
DO 175 JQ=KPO,N
175 S=S+C(K,JQ)*F(JQ)
160 F(K)=F(K)-S
C THIS ENDS THE BACK SUBSTITUTIONS
DO 554 IKUR=1,N
AAF=CABS(F(1KUR))
ANF=57.296*ATAN2(AIMAG(F(1KUR)),REAL(F(1KUR)))
554 WRITE(6,553) IKUR,AAF,ANF
553 FORMAT (' ', ' F(',I4,')='', E15.8, ' AT ANGLE=',E15.8)
DO 9553 IRRO=1,N
IND=IRRO-1
Y(1)=CABS(F(1IRRO))
XRRO=FLOAT(IRRO)
9553 CALL PLOT(XRRO,Y,1,IND,5.00,0.0)
DO 9554 IRRO=1,N
IND=IRRO-1
Y(1)=57.2958*ATAN2(AIMAG(F(1IRRO)),REAL(F(1IRRO)))
XRRO=FLOAT(IRRO)
9554 CALL PLOT(XRRO,Y,1,IND,180.0,-180.0)
DO 317 JNX=1,360
THS=0.01745329*FLOAT(JNX)/2.0
T=CMPLX(0.0,0.0)
DO 310 I=1,N
XN=XH(I)
THN=1.5707963+ATAN(DH(XN))
310 T=T+ ((F(I))*CEXP(CMPLX(0.0,G*{(XN*COS(THS))+(H(XN)*SIN(THS))})))
2 *COS(THN-THS))
C ***** THIS CORRECTS THE OUTPUT TO TRUE MAG. FIELD
T=T*STS
CM=CABS(T)
DB=20.0*ALOG10(CM)
CANG=57.296*ATAN2(AIMAG(T),REAL(T))
THSD=THS*57.296
ABES(JNX)=CM
317 WRITE (6,312) CM,CANG,THSD,DB

```

```

312 FORMAT (18H RELATIVE H FIELD=,E15.8,7H ANGLE=,E15.8,
2 23H ANGLE FROM HORIZONTAL=,E15.8,6H DB=,E15.8)
DO 9500 JC=1,360
Y(1)=ADES(JC)
U=FLOAT(JC)/2.0
IND=JC-1
9500 CALL PLOT(U,Y,1,IND,50.0,0.0)
STOP
END

```

```

C      FUNCTION H(X)
      THIS DEFINES THE SURFACE
      COMMON /PIG/ AONE,CONE,PONE,ATWO,CTWO,PTWO,N
      H=AONE*SIN((CONE*X)+PONE)+ATWO*SIN((CTWO*X)+PTWO)
      RETURN
      END

```

```

C      FUNCTION DH(X)
      DH(X) IS THE DERIV. OF H(X)
      COMMON /PIG/ AONE,CONE,PONE,ATWO,CTWO,PTWO,N
      DH=AONE*CONE*COS((CONE*X)+PONE)+ATWO*CTWO*COS((CTWO*X)+PTWO)
      RETURN
      END

```

```

C      FUNCTION CO(MR,MC)
      THIS GIVES THE OLD MATRIX COEFFICIENTS
      COMPLEX CO
      COMPLEX DJC
      COMMON/GASSN/ GU1,GU2,GU3,GU4,GU5,GW1,GW2,GW3,GW4,GW5
      COMMON/HCG/ XM(400),G,X(400)
      COMMON /DOG/ DJC
      COMPLEX AHAN21
      IF(MR.NE.MC) GO TO 100
      CO=CMPLX(0.500,0.0)
      GO TO 200
100    CONTINUE
      XMP=X(MR)
      HXMM=H(XMM)
      EPL=X(MC)
      EPU=X(MC+1)
      DVDFEP=(EPU-EPL)/2.0
      DVSMEP=(EPU+EPL)/2.0
      XU5=GU5*DVSMEP+DVSMEP
      XU1=GU1*DVSMEP+DVSMEP
      XU2=GU2*DVSMEP+DVSMEP
      XU3=GU3*DVSMEP+DVSMEP
      XU4=GU4*DVSMEP+DVSMEP
      HXU1=H(XU1)
      HXU2=H(XU2)
      HXU3=H(XU3)
      HXU4=H(XU4)
      HXU5=H(XU5)
      DHXU1=DH(XU1)
      DHXU2=DH(XU2)
      DHXU3=DH(XU3)
      DHXU4=DH(XU4)
      DHXU5=DH(XU5)
      CO=DVDFEP*(
2+(GW1*AHAN21(G*SQRT(((XU1-XMM)**2)+((HXU1-HXMM)**2)))
2 *((-DHXU1*(XMM-XU1))+ (HXMM-HXU1))
2/SQRT(((XMM-XU1)**2)+((HXMM-HXU1)**2)))
2+(GW2*AHAN21(G*SQRT(((XU2-XMM)**2)+((HXU2-HXMM)**2)))
2 *((-DHXU2*(XMM-XU2))+ (HXMM-HXU2))

```

```
2/SQRT(((XMM-XU2)**2)+((HXMM-HXU2)**2)))
2+(GW3*AHAN21(G*SQRT(((XU3-XMM)**2)+((HXU3-HXMM)**2)))
2 *((-DHXU3*(XMM-XU3))+ (HXMM-HXU3))
2/SQRT(((XMM-XU3)**2)+((HXMM-HXU3)**2)))
2+(GW4*AHAN21(G*SQRT(((XU4-XMM)**2)+((HXU4-HXMM)**2)))
2 *((-DHXU4*(XMM-XU4))+ (HXMM-HXU4))
2/SQRT(((XMM-XU4)**2)+((HXMM-HXU4)**2)))
2+(GW5*AHAN21(G*SQRT(((XU5-XMM)**2)+((HXU5-HXMM)**2)))
2 *((-DHXU5*(XMM-XU5))+ (HXMM-HXU5))
2/SQRT(((XMM-XU5)**2)+((HXMM-HXU5)**2)))
CO=CO+DJC
-200 CONTINUE
RETURN
END
```

```

C      THIS IS THE CASE USING TWO POINT INTERPOLATION
C      THIS PROGRAM USES GAUSSIAN INTEGRATION TO GET MATRIX ELEMENTS
C      NSUB SEGMENTS HAVE N MIDPOINTS
C      NSUB IS THE SUBSCRIPT WHICH COUNTS THE END POINTS
C      N      IS THE SUBSCRIPT WHICH COUNTS THE MIDPOINTS
C      MATCH MAX SLOPE SO THAT THE X INCREMENTS ARE SMALL ENOUGH
C      EP IS THE END POINT
C      COMPLEX SNN,SST
C      COMPLEX S,CD
C      COMPLEX FSS
C      COMMON/GASSN/ GU1,GU2,GU3,GU4,GU5,GW1,GW2,GW3,GW4,GW5
C      COMPLEX FINC(20),STS
C      COMMON /PIG/ AONE,CONE,PUNE,ATWO,CTWO,PTWO,N
C      COMPLEX C(150,150)
C      COMMON/HDG/ XM(400),G,X(400)
C      COMMON /DOG/ DJC
C      COMPLEX DJC
C      COMPLEX F(400),FP(400),SS,T,CTEST
C      COMPLEX FIN
C      COMPLEX HAN2
C      DIMENSION      ABES(360),Y(10)
C      WE IS THE ELECTRICAL WAVELENGTH
C      WE=25.0
C      G=6.2831853      /WE
C      AONE=5.0
C      CONE=6.28318/200.0
C      PCNE=0.0
C      ATWO=0.0
C      CTWO=0.0
C      PTWO=0.0
C      DC=WE/15.0
C      DX=DC/1000.0
C      DC2=DC/2.0
C      EP=200.0
C      STS=DC*CMPLX(-0.70711,-0.70711)/(2.0*SQRT(WE))
C      DJC=CMPLX(0.0,1.0)*G/4.0
C      CONSTANTS FOR GAUSSIAN INTEGRATION 5 TH ORDER
C      GU1=-0.9061798
C      GU2=-0.53846931
C      GU3=0.0
C      GU4=-GU2
C      GU5=-GU1
C      GW1=0.2369268
C      GW2=0.2369268
C      GW3=0.47862867
C      GW4=0.47862867
C      GW5=0.5688888
C      CONSTANTS FOR GAUSSIAN INTEGRATION 5 TH ORDER
C      THE FOLLOWING BREAKS THE SURFACE INTO SEGMENTS DC CENTIMETERS LONG
C      BY LINE INTEGRATION USING STEPS OF LENGTH DX FOR THE INTEGRATION
C      NSUB=1
C      X(NSUB)=-EP
1002 AL=0.000
C      R=X(NSUB)
1001 R=R+DX
C      ALD=AL
C      AL=AL+(DX*SQRT(1.0+(DH(R)**2)))
C      IF(((DC2-AL).LE.0.0).AND.((DC2-ALD).GT.0.0)) XM(NSUB)=R
C      IF(AL.LT.DC)GO TO 1001
C      WRITE(6,352) AL,NSUB
352 FORMAT(' AL=',E15.8,' NSUB=',I4)

```

```

NSUB=NSUB+1
X(NSUB)=R
IF (R.LT.EP) GO TO 1002
N=NSUB-1
WRITE(6,251) N,NSUB
251 FORMAT(' ',N=' ',I4,' ',NSUB=' ',I4)
DO 1004 J=1,NSUB
IF (J.EQ.NSUB) XM(NSUB)=0.0
XXX=X(J)
XMD= XM(J)
1004 WRITE (6,1003) XXX,XMD,J
1003 FORMAT (6H X(J)=,E15.8,9H XM(J)=,E15.8,3H J=,I3)
C THIS ENDS THE SURFACE SUBDIVISION
C THIS INSURES THAT N IS ODD
KK=0
5733 KK=KK+1
IF ((2*KK-1).EQ.N) GO TO 5731
IF (2*KK.EQ.N) GO TO 5732
GO TO 5733
5732 N=N-1
5731 CONTINUE
WRITE (6,3728) N,KK
3728 FORMAT(' ', 'CORRECTED VALUE OF N=',I4,'KK=',I4,'2*KK-1=N')
NMO=N-1
NM3=N-3
C DIMENSION OF FINC,F IS N
DPIF=0.7853982
C MATRIX FILL IN
C DO BY COLUMNS
C FOR FIRST COLUMN
DO 3661 I=1,KK
3661 C(I,1)=C(2*I-1,1)+(C(2*I-1,2)/2.0)
C FOR LAST COLUMN
DO 3678 I=1,KK
3678 C(I,KK)=(C(2*I-1,2*KK-2)/2.0)+C(2*I-1,2*KK-1)
C FOR MIDDLE COLUMNS
DO 56 I=1,KK
II=2*I-1
KKM1=KK-1
DO 56 J=2,KKM1
JJ=2*J-1
C(I,J)=(C(II,JJ-1)/2.0)+C(II,JJ)+(C(II,JJ+1)/2.0)
56 CONTINUE
C THIS COMPLETES THE FILLIN OF THE MATRIX
C NONSYMMETRIC CROUT
C FIRST COLLOM OK
C TWO GET FIRST ROW
DO 10 J=2,KK
10 C(1,J)=C(1,J)/C(1,1)
C NOW WORK ON ROW AND COLUMN SET K
DO 11 K=2,KK
KMO=K-1
KPO=K+1
C TO GET DIAGONAL ELEMENT
S=CHPLX(0.0,0.0)
DO 12 IK=1,KMO
12 S=S+C(K,IK)*C(IK,K)
C(K,K)=C(K,K)-S
C TO GET ELEMENTS IN COLUMN K BELOW ROW K
IF(KPO.GT.KK) GO TO 17
DO 13 IROW=KPO,KK
S=CHPLX(0.0,0.0)
DO 14 JJ=1,KMO
14 S=S+C(IROW,JJ)*C(JJ,K)
13 C(IROW,K)=C(IROW,K)-S
C TO GET ELEMENTS IN ROW K TO THE RIGHT OF COLUMN K

```



```

DO 15 ICOL=KPO, KK
S=CMLX(0.0,0.0)
DO 16 JR=1, KMD
16 S=S+C(K, JR)*C(JR, ICOL)
15 C(K, ICOL)=(C(K, ICOL)-S)/C(K, K)
17 CONTINUE
11 CONTINUE
WRITE (6, 1222) KK, WE
1222 FORMAT(' ', ' KK=', I4, ' WE=', E15.8)
TH=3.1415927*60.0/180.0
THDEG=57.29578*TH
WRITE (6, 9333) THDEG
9333 FORMAT(9H INC ANG=, E15.8)
C TH IS THE ANGLE OF INCIDENCE FROM THE HORIZONTAL
STH=SIN(TH)
CTH=COS(TH)
C THIS FINDS THE INCIDENT FIELD ION THE NJTH SEGMENT
C
C TAPERED ILLUMINATION *****
C
DO 455 NJ=1, KK
XG=XM(2*NJ-1)
FP(NJ)=CEXP(CMLX(0.0, G*(XG*CTH)+(H(XG)*STH)))*CMLX(-1.0, 0.0)
C INCIDENT FIELD HAS BEEN ADJUSTED TO AGREE WITH INTEGRAL EQTN.
IF(XG.LE.((WE*1.0)-EP)) FP(NJ)=CMLX(0.0, 0.0)
IF(XG.GT.((EP-1.0*WE))) FP(NJ)=CMLX(0.0, 0.0)
IF((XG.GT.((1.0*WE)-EP)).AND.(XG.LE.((2.0*WE)-EP)))
2 FP(NJ)=FP(NJ)*(0.5+(0.5*SIN((G/2.0)*(XG-((1.5*WE)-EP))))
IF((XG.GE.((EP-2.0*WE))).AND.(XG.LT.((EP-1.0*WE))))
2 FP(NJ)=FP(NJ)*(0.5-(0.5*SIN((G/2.0)*(XG-(EP-(1.5*WE))))))
455 CONTINUE
WRITE(6, 9410) (NJ, FP(NJ), NJ=1, KK)
9410 FORMAT(' ', ' INCIDENT FIELD FINC(' ', I4, ')=' ', 2E15.8)
C THIS BEGINS THE BACK SUBSTITUTION
C CONVERSION OF SOURCE SIDE
FP(1)=FP(1)/C(1, 1)
DO 90 IJ=2, KK
S=CMLX(0.0, 0.0)
IJMO=IJ-1
DO 91 IK=1, IJMO
91 S=S+C(IJ, IK)*FP(IK)
90 FP(IJ)=(FP(IJ)-S)/C(IJ, IJ)
C NOW FOR FINAL BACK SUBSTITUTION
NMO=KK-1
DO 160 L=1, NMO
K=KK-L
KPB=K+1
S=CMLX(0.0, 0.0)
DO 175 JD=KPB, KK
175 S=S+C(K, JD)*FP(JD)
160 FP(K)=FP(K)-S
KKM1=KK-1
C TO RECONSTRUCT THE CURRENTS
DO 47 IRA=1, KKM1
47 F(2*IRA)=(FP(IRA)+FP(IRA+1))/2.0
DO 48 IRA=1, KK
48 F(2*IRA-1)=FP(IRA)
WRITE (6, 4970)((J, FP(J)), J=1, KK)
4970 FORMAT(' ', ' FP(' ', I5, ')=' ', 2E15.8)
WRITE (6, 553) (F(K), K=1, N)
553 FORMAT (6H F(K)=, 2E15.8)
DO 553 IRRO=1, N
IND=IRRO-1
Y(1)=CABS(F(IRRO))
XRPO=FLOAT(IRRO)

```

```

9553 CALL PLOT(XRRD,Y,1,IND,5.00,0.0)
DO 9554 IRRD=1,N
IND=IRRD-1
Y(1)=57.2958*ATAN2(AIMAG(F(IRRD)),REAL(F(IRRD)))
XRRD=FLOAT(IRRD)
9554 CALL PLOT(XRRD,Y,1,IND,180.0,-180.0)
C THIS ENDS THE BACK SUBSTITUTIONS
DO 317 JNX=1,360
THS=0.01745329*FLOAT(JNX)/2.0
T=CMPLX(0.0,0.0)
DO 310 I=1,N
XN=XM(I)
THN=1.5707963+ATAN(DH(XN))
310 T=T+((F(I)*CEXP(CMPLX(0.0,G*((XN*COS(THS))+(H(XN)*SIN(THS))))))
2 *COS(THN-THS))
C ***** THIS CORRECTS THE OUTPUT TO TRUE ELE. FIELD
T=T*STS
CM=CABS(T)
DB=20.0*ALOG10(CM)
CANG=57.296*ATAN2(AIMAG(T),REAL(T))
THSD=THS*57.296
ABES(JNX)=CM
317 WRITE (6,312) CM,CANG,THSD,DB
312 FORMAT (10H RELATIVE E FIELD=,E15.8,7H ANGLE=,E15.8,
2 23H ANGLE FROM HORIZONTAL=,E15.8,6H DB=,E15.8)
DU 9500 JC=1,360
Y(1)=ABES(JC)
U=FLOAT(JC)/2.0
IND=JC-1
9500 CALL PLOT(U,Y,1,IND,50.0,0.0)
STOP
END

```

```

C FUNCTION H(X)
THIS DEFINES THE SURFACE
COMMON /PIG/ AONE,CONE,PONE,ATWO,CTWO,PTWO,N
H=AONE*SIN(CONE*X)+PONE+ATWO*SIN((CTWO*X)+PTWO)
RETURN
END

```

```

C FUNCTION DH(X)
DH(X) IS THE DERIV. OF H(X)
COMMON /PIG/ AONE,CONE,PONE,ATWO,CTWO,PTWO,N
DH=AONE*CONE*COS((CONE*X)+PCONE)+ATWO*CTWO*COS((CTWO*X)+PTWO)
RETURN
END

```

```

C FUNCTION CO(MR,MC)
THIS GIVES THE OLD MATRIX COEFFICIENTS
COMPLEX CO
COMPLEX DJC
COMMON/GASSN/ GU1,GU2,GU3,GU4,GU5,GH1,GH2,GH3,GH4,GH5
COMMON/HOG/ XM(400),G,X(400)
COMMON /DOG/ DJC
COMPLEX AHAN21
IF(MR.NE.MC) GO TO 100
CO=CMPLX(0.500,0.0)
GO TO 200
100 CONTINUE
XMM=XM(MR)
HXMM=H(XMM)

```

```

EPL=X(MC)
EPU=X(MC+1)
DVDFEP=(EPU-EPL)/2.0
DVSMEP=(EPU+EPL)/2.0
XU5=GU5*DVDFEP+DVSMEP
XU1=GU1*DVDFEP+DVSMEP
XU2=GU2*DVDFEP+DVSMEP
XU3=GU3*DVDFEP+DVSMEP
XU4=GU4*DVDFEP+DVSMEP
ATDH1=ATAN(DH(XU1))
ATDH2=ATAN(DH(XU2))
ATDH3=ATAN(DH(XU3))
ATDH4=ATAN(DH(XU4))
ATDH5=ATAN(DH(XU5))
HXU1=H(XU1)
HXU2=H(XU2)
HXU3=H(XU3)
HXU4=H(XU4)
HXU5=H(XU5)
CO=DVDFEP*(
2*GW1*AHAN21(G*SQRT(((XU1-XMM)**2)+((H(XU1)-HXMM)**2)))*SQRT(1.0+(
2DH(XU1)**2))*((-SIN(ATDH1)*(XMM-XU1))+COS(ATDH1)*(HXMM-HXU1))
2/SQRT(((XMM-XU1)**2)+((HXMM-HXU1)**2))
2*GW2*AHAN21(G*SQRT(((XU2-XMM)**2)+((H(XU2)-HXMM)**2)))*SQRT(1.0+(
2DH(XU2)**2))*((-SIN(ATDH2)*(XMM-XU2))+COS(ATDH2)*(HXMM-HXU2))
2/SQRT(((XMM-XU2)**2)+((HXMM-HXU2)**2))
2*GW3*AHAN21(G*SQRT(((XU3-XMM)**2)+((H(XU3)-HXMM)**2)))*SQRT(1.0+(
2DH(XU3)**2))*((-SIN(ATDH3)*(XMM-XU3))+COS(ATDH3)*(HXMM-HXU3))
2/SQRT(((XMM-XU3)**2)+((HXMM-HXU3)**2))
2*GW4*AHAN21(G*SQRT(((XU4-XMM)**2)+((H(XU4)-HXMM)**2)))*SQRT(1.0+(
2DH(XU4)**2))*((-SIN(ATDH4)*(XMM-XU4))+COS(ATDH4)*(HXMM-HXU4))
2/SQRT(((XMM-XU4)**2)+((HXMM-HXU4)**2))
2*GW5*AHAN21(G*SQRT(((XU5-XMM)**2)+((H(XU5)-HXMM)**2)))*SQRT(1.0+(
2DH(XU5)**2))*((-SIN(ATDH5)*(XMM-XU5))+COS(ATDH5)*(HXMM-HXU5))
2/SQRT(((XMM-XU5)**2)+((HXMM-HXU5)**2))
CO=DJC*CO
200 CONTINUE
RETURN
END

```

```

FUNCTION AHAN21(X)
THIS IS THE HANKEL FUNCTION OF TYPE 2 AND OF ORDER 1
DOUBLE PRECISION XD,DX,A1,A2,A3,A4,A5,A6,HJ1,B1,B2,B3,B4,B5,AHJ1,
2TDX,A1,A2,A3,A4,A5,A6,T1,T2,T3,T4,T5,T6,T7,DSQX,B6
COMPLEX AHAN21
DX=DBLE(X)
IF (X.GT.3.0) GO TO 200
XU=DX*DX/9.0D+00
A1=-0.31761D-03+0.11C9D-04*XU
A2=0.00443319U+00+A1*XU
A3=-0.03954289U+60+A2*XU
A4=0.21093573D+00+A3*XU
A5=-0.56249985U+00+A4*XU
A6=0.5D+00+A5*XU
HJ1=A6*DX
B1=-0.040C976D+00+0.0027873D+00*XU
B2=0.3123951D+60+B1*XU
B3=-1.3164827D+00+B2*XU
B4=2.1682709D+00+B3*XU
B5=0.2212091D+00+B4*XU
B6=-0.6366198D+00+B5*XU
AHJ1=(B6/DX)+HJ1*DLOG(DX/2.0)*0.63661977
AHAN21=CMPLX(SNGL(HJ1),-SNGL(AHJ1))
GO TO 300
200 TDX=3.0/DX
A1=0.00113653D+00-0.00020033*TDX
A2=-0.00249511D+00+A1*TDX
A3=0.00017105U+00+A2*TDX
A4=0.01659667U+00+A3*TDX
A5=0.156D-05+A4*TDX
A6=0.79788456U+00+A5*TDX
T1=0.00079824D+00-0.00029166D+00*TDX
T2=0.00074348D+00+T1*TDX
T3=-0.00637879D+00+T2*TDX
T4=0.00005650D+00+T3*TDX
T5=0.12499612U+00+T4*TDX
T6=-2.35619449D+00+T5*TDX
T7=DX+T6
DSQX=A6/DSQRT(DX)
AHAN21=CMPLX(SNGL(DSQX*DCOS(T7)),-SNGL(DSQX*DSIN(T7)))
300 CONTINUE
RETURN
END

```

```

FUNCTION AHANZO(X)
C THIS IS THE HANKEL FUNCTION OF ORDER 0 AND OF TYPE 2
DOUBLE PRECISION XSQ,B10,B8,B6,B4,B2,C10,C8,C6,C4,C2,D5,D4,D3,
2D2,D1,E5,E4,E2,E1,E0,XD,DX,FO,E3,HJ,DSX
COMPLEX AHANZO
DX=DBLE(X)
IF (X.GT.3.0) GO TO 100
XSQ=DX*DX/C.9D+01
B10=-0.39444D-02+XSQ*0.21D-03
B8=0.0444479D+00+XSQ*B10
B6=-0.3163866D+00+XSQ*B8
B4=1.2656208D+00+XSQ*B6
B2=-2.249997D+00+XSQ*B4
HJ=1.0D+00+XSQ*B2
C10=0.427916D-02-XSQ*0.24846D-03
C8=-0.4261214D-01+XSQ*C10
C6=0.25300117D+00+XSQ*C8
C4=-0.74350384D+00+XSQ*C6
C2=0.60559366D+00+XSQ*C4
HY=SNGL(0.36746691D+00+0.6366198D+00*HJ*DLOG(DX/2.0)+XSQ*C2)
AHANZO=CMPLX(SNGL(HJ),-HY)
GO TO 200
100 YD=3.0/DX
L5=-0.72805D-03+XD*0.14476D-03
D4=0.137237D-02+D5*XD
D3=-0.9512D-04+D4*XD
D2=-0.55274CD-02+D3*XD
D1=-0.77D-06+D2*XD
FO=0.79788456D+00+XD*D1
E5=-0.29333D-03+XD*0.13558D-03
E4=-0.54125D-03+E5*XD
E3=0.262573D-02+E4*XD
E2=-0.3954D-04+E3*XD
E1=-0.4166397D-01+E2*XD
E0=(-0.78539816D+00+XD*E1)+DX
DSX=DSQRT(DX)
AHANZO=CMPLX(SNGL(FO*DCOS(E0)/DSX),-SNGL(FO*DSIN(E0)/DSX))
200 CONTINUE
RETURN
END

```

```

SUBROUTINE PLOT( X, Y, N, IND, YMAX, YMIN)
  DIMENSION M(119), YLABEL(6), Y(10), MARK(10)
  DATA MARK(1), MARK(2), MARK(3), MARK(5), MARK(6), MARK(7), MARK(8),
2 MARK(9), MARK(10), MARK(4) / 1H*, 1H., 1H!, 1H0, 1HN, 1HH, 1H1, 1HZ, 1H-, 1HX /
  DATA IBLANK, NOPT, IPLUS / 1H , 1Hs, 1H+ /
  IF (IND) 1, 1, 11
1  WRITE(6, 3)
3  FORMAT(1H1//25X, 48HORDER IN WHICH PLOT SYMBOLS ARE USED *.IXONHIZ
  *-//30X, 39HTHE SYMBOL (S) INDICATES OFF-SCALE DATA//)
  DC7J=9, 119
7  M(J)=MARK(10)
  NCCOUNT=10
  SCALE=100.0/(YMAX-YMIN)
  LLL=(-YMIN*SCALE)+11.5
  DO8J=1, 6
  R=J-1
8  YLABEL(J)=R*20.0/SCALE+YMIN
  WRITE(6, 9) (YLABEL(I), I=1, 6)
9  FORMAT(6X, 1PE9.2, 5(1PE20.2) / )
  GOTO 132
11  NCCOUNT=NCCOUNT+1
  DO99J=1, 119
99  M(J)=IBLANK
  IF(LLL.GE.11.AND.LLL.LE.110)M(LLL)=MARK(10)
  IF(NCCOUNT-10)133, 132, 133
132  DC89J=11, 111, 20
89  M(J)=IPLUS
133  DO20J=1, N
  L=(Y(J)-YMIN)*SCALE+0.5
  IF(L)14, 17, 17
14  IF(L+10)15, 16, 16
15  M(1)=NOPT
  GOTO 20
16  LL=L+11
  M(LL)=MARK(J)
  GOTO 20
17  IF(L-108)18, 19, 19
18  LL=L+11
  M(LL)=MARK(J)
  GOTO 20
19  M(119)=NOPT
20  CONTINUE
  IF(NCCOUNT-10)21, 25, 21
21  WRITE(6, 24) (M(J), J=1, 119)
24  FORMAT(1X, 119A1)
  GOTO 27
25  WRITE(6, 26) (X, (M(J), J=9, 119))
26  FORMAT(1X, F7.3 , 111A1)
  NCCOUNT=0
27  CONTINUE
  RETURN
  END

```

APPENDIX B

SOLUTION OF SYSTEMS OF SIMULTANEOUS LINEAR EQUATIONS

Several direct methods exist which find the solution vector, $[X]$, when the system of equations

$$(99) \quad [C] [X] = [B]$$

is given. The two methods used here were the square root (or Cholesky) method for symmetric systems, and the Crout method for non-symmetric systems (Ref. [35]). Both methods take advantage of the fact that a non-singular matrix $[C]$ is equivalent to $[L][U]$, where $[L]$ is a lower triangular matrix and $[U]$ is an upper triangular matrix. So

$$(100) \quad \begin{bmatrix} l_{11} & 0 & 0 & \dots & 0 \\ l_{21} & l_{22} & 0 & \dots & 0 \\ l_{31} & l_{32} & l_{33} & 0 & 0 \\ \vdots & \vdots & \vdots & \vdots & \vdots \\ l_{N1} & \cdot & \cdot & \dots & l_{NN} \end{bmatrix} \begin{bmatrix} u_{11} & u_{12} & \dots & u_{1N} \\ 0 & u_{22} & \dots & u_{2N} \\ \vdots & \vdots & \vdots & \vdots \\ 0 & \cdot & 0 & u_{NN} \end{bmatrix} = \begin{bmatrix} c_{11} & c_{12} & \dots & c_{1N} \\ c_{21} & c_{22} & \dots & \cdot \\ \cdot & \cdot & \cdot & \cdot \\ c_{N1} & \cdot & \dots & c_{NN} \end{bmatrix}$$

or

$$(101) \quad \sum_{k=1}^{\min(i,j)} l_{ik} u_{kj} = c_{ij}$$

since

$$(102) \quad l_{ik} \equiv 0 \quad \text{if } k > i \quad \text{and}$$

$$(103) \quad u_{kj} \equiv 0 \quad \text{if } k > j.$$

In order to specify $[L]$ and $[U]$, $N^2 + N$ unknowns must be determined. Since there are only N^2 equations, (values of c_{ij}), N unknowns may be specified. In the square root method the diagonal elements are assumed equal, i.e.,

$$u_{ii} = l_{ii} \quad \text{for } i = 1, \dots, N$$

which gives the N extra conditions; in the Crout method one set of diagonals is specified, namely

$$(104) \quad u_{kk} = 1 \quad \text{for } k = 1, \dots, N.$$

Suppose that $[C]$ has been broken up into $[L][U]$, then

$$(105) \quad [L][U][X] = [B]$$

whence by defining

$$(106) \quad [R] = [U][X]$$

there results

$$(107) \quad [L][R] = [B]$$

which has the solution

$$(108) \quad r_i = (b_i - \sum_{k=1}^{i-1} l_{ik} x_k) / l_{ii} \quad \text{for } i=1, \dots, N$$

and the sum is omitted, if i equals 1. Once the $[R]$ vector is known the system

$$(109) \quad [U][X] = [R]$$

is solved by

$$(110) \quad x_i = (r_i - \sum_{k=i+1}^N u_{ik} x_k) / u_{ii} \quad \text{for } i=1, \dots, N$$

where the sum is omitted if i equals N . Wilkinson (Ref. [36]) has shown that most of the error in a solution of Eq. (99) by triangularization methods comes from the decomposition of $[C]$ into $[L][U]$ and not in the double back substitution (Eqs. (108) and (110)).

The details of the decomposition of $[C]$ into $[L][U]$ will now be considered. For Crout factorization the diagonal elements of $[U]$ are set equal to unity leaving N^2 equations and N^2 unknowns in the set of Eqs. (101), (102) and (103), which can be solved as follows:

$$(111) \quad l_{ik} = c_{ik} - \sum_{m=1}^{k-1} l_{im} u_{mk} \quad \text{for } i=k, \dots, N$$

$$(112) \quad u_{kj} = \frac{1}{l_{kk}} \left(c_{kj} - \sum_{m=1}^{k-1} l_{km} u_{mj} \right) \quad \text{for } j=k+1, \dots, N$$

$$(113) \quad l_{ik} = 0 \quad \text{if } i < k$$

$$(114) \quad u_{kj} = 0 \quad \text{if } j < k.$$

These equations are used in the order: first column of [L], first row of [U]; second column of [L], second row of [U]; third column of [L], ect. In a computer solution the elements of [U] and [L] may be written over the original matrix [C] as they are generated. Once this is done the matrix becomes

$$\left[\begin{array}{c} C \\ \end{array} \right] \xrightarrow[\text{AND STORED}]{\text{FACTORED}} \left[\begin{array}{ccc} l_{11} & u_{12} & u_{1N} \\ \cdot & \cdot & \cdot \\ \cdot & \cdot & l_{22} & \cdot \\ \cdot & \cdot & \cdot & \cdot \\ l_{N1} & \dots & \cdot & l_{NN} \end{array} \right]$$

and the fact that the diagonal elements of [U] are unity is used only in the previously described back substitution portion of the solution.

If [C] is symmetric then [C] can be factored into

$$(115) \quad [C] = [U]^T [U]$$

where $[U]^T$ is the transpose of [U]. Equation (101) becomes

$$(116) \quad \sum_{k=1}^{\min \text{ of } (i,j)} u_{ki} u_{kj} = c_{ij}$$

The $u_{i,j}$'s are found from

$$(117) \quad u_{11} = \sqrt{c_{11}}$$

$$(118) \quad u_{1j} = c_{1j}/u_{11} \quad \text{for } j=2, \dots, N$$

$$(119) \quad u_{ii} = (c_{ii} - \sum_{k=1}^{i-1} u_{ki}^2)^{1/2} \quad \text{for } i=2, \dots, N$$

$$(120) \quad u_{ij} = (c_{ij} - \sum_{k=1}^{i-1} u_{ki} u_{kj})/u_{ii} \quad \text{for } \begin{cases} j=i+1, \dots, N \\ i=2, \dots, N \end{cases}$$

and

$$(121) \quad u_{ij} = 0 \quad \text{if } i > j.$$

The value of this method lies in the reduction of storage space required for a given N . With the usual Crout method N^2 storage locations are required, but the square root method requires $N(N+1)/2$ storage locations since only the upper triangular portion of $[C]$ need be stored and $[U]$ can be found using only the upper triangular part of $[C]$.

A small trick is required if this saving is to be realized in practice, since in FORTRAN IV the use of the dimension statement "COMPLEX C(N,N)" would set aside N^2 complex storage locations for

the elements of $[C]$ even if only the upper triangular part of $[C]$ were to be filled in and manipulated. To economize on storage a way was found to load the elements of the upper triangular part of $[C]$ into a linear array $N(N+1)/2$ positions long. It was convenient to preserve the double subscript notation for the matrix manipulations and use a simple formula to access the proper location in the singly subscripted linear array. A symmetric matrix $[C]$ is shown in Fig. 42 with the elements of the linear array S inserted into the corresponding locations of $[C]$. The order of the matrix is chosen to be 6 for this example.

s_1	s_2	s_3	s_4	s_5	s_6
	s_7	s_8	s_9	s_{10}	s_{11}
		s_{12}	s_{13}	s_{14}	s_{15}
			s_{16}	s_{17}	s_{18}
				s_{19}	s_{20}
					s_{21}

Fig. 42.--Storing a symmetric matrix in a linear array.

Element c_{11} is stored in position s_1 , a_{12} in c_2 , etc. The element c_{ij} ($i \leq j$) can be accessed in the following way. The rows above the i -th row contain $N(i-1) - ((i-1)(i-2)/2)$ elements and in the i -th row there are $j - i + 1$ elements up to and including the one to be accessed, hence

$$\begin{aligned}
 (122) \quad c_{ij} &= s(N(i-1) - \frac{(i-1)(i-2)}{2} + j - i + 1) \\
 &= sN \cdot i - [\frac{i(i-1)}{2} + N - j].
 \end{aligned}$$

In the programs the subscript manipulations are performed directly in the subscript or accessed by calling a function named ISUB(i,j) [Integer Subscript corresponding to i,j]. If, for example, c_{15} were needed in a computation the element $s(\text{ISUB}(1,5))$ is used. Once the factorization is completed, the back substitutions are performed.

Notice that in either the Crout method or the square root method there are two distinct steps. The first is factoring the matrix and the second is the back substitution. The first step is independent of the driving column [B] and hence need be done only once for any given matrix [C] so any number of driving columns may be considered without re-factoring [C].

REFERENCES

1. Wright, J.W., "Backscattering from capillary waves with applications to sea clutter," IEEE Trans. on Antennas and Propagation, vol. AP-14, pp. 749-754, (November 1966).
2. Valenzuela, G.R., "Scattering of EM waves from a tilted slightly rough surface," Radio Science, Vol. 3, pp. 1057-1064, (July 1968).
3. Guinard, N.W., et al., "An Experimental Study of a Sea Clutter Model," Proc. IEEE, Vol. 58, pp. 543-550, (April 1970).
4. Stogryn, A., "The Apparent Temperature of the Sea at Microwave Frequencies," IEEE Trans. on Antennas and Propagation, Vol. AP-15, pp. 278-285, (March 1967).
5. Barrick, D.E. and Peake, W.H., "A review of scattering from surfaces with different roughness scales," Radio Science, Vol. 3, pp. 865-868, (August 1968).
6. Semenov, B., "An approximate calculation of scattering of electromagnetic waves from a rough surface," Radiotekh. Elektron., Vol. 11, pp. 1351-1361, (August 1966).
7. Fuks, I., "Contribution to the theory of radio wave scattering on the perturbed sea surface," Izv. Vyssh. Ucheb. Zaved. Radiofiz., Vol. 9, pp. 876-887, (May 1966).

8. Phillips, O.M., The Dynamics of the Upper Ocean, Cambridge University Press, (1966).
9. Barrick, D.E., "Unacceptable height correlation coefficients and the quasi-specular component in rough surface scattering," Radio Science, Vol. 5, pp. 647-654, (April 1970).
10. Silver, S., Microwave Antenna Theory and Design, pp. 138-143, Dover, New York, (1965).
11. Kay, I. and Keller, J.B., "Asymptotic evaluation of the field at a caustic," J. Appl. Physics, Vol. 25, pp. 876-883, (July 1954).
12. Kouyoumjian, R.G., "Asymptotic high frequency methods," Proc. IEEE, Vol. 53, pp. 864, 876 (August 1965).
13. Beckmann, P., and Spizzichino, A., The Scattering of Electromagnetic Waves from Rough Surfaces, Pergamon, New York, pp. 9-16, (1963).
14. Harrington, R.F., Time Harmonic Electromagnetic Fields, McGraw-Hill, p. 127, (1961).
15. Kouyoumjian, R.G., "Asymptotic High-Frequency Methods," Proceedings of the IEEE, Vol. 53, pp. 864-876.
16. Kodis, R.D., "A Note on the Theory of Scattering from an Irregular Surface," IEEE Trans. on Antennas and Propagation, Vol. AP-14, pp. 77-82, (January 1966).
17. Silver, S., Microwave Antenna Theory and Design, Dover, New York, p. 121, (1965).

18. Van Bladel, J., Electromagnetic Field, McGraw-Hill, New York, pp. 360-361, (1964).
19. Van Bladel, J., op.cit., p. 413.
20. Van Bladel, J., op.cit., pp. 360-361.
21. Beckman, Petr, Depolarization of Electromagnetic Waves, Golem, pp. 82-86, (1968).
22. Harrington, R.F., Field Computation by Moment Methods, MacMillan, New York, 1968.
23. Mei, K.K., "Scattering of Radio Waves by Rectangular Cylinders," University of Wisconsin Dissertation, (1962).
24. Harrington, R.F., Field Computation by Moment Methods, MacMillan, New York, (1968), p. 42.
25. Abramowitz M. and Stegun, I.A., Ed., Handbook of Mathematical Functions, National Bureau of Standards, Appl. Math. Series 55, (1964), p. 916.
26. Richmond, J.H., private communications.
27. Rudduck, R.C., "Application of Wedge Diffraction Theory to Antenna Theory," Ohio State University Antenna Laboratory Report, N.A.S.A. Grant Number NsG-448, (1965), pp. 1-6.
28. Poggio, A.J. and Miller, E.K., "Integral Equation Solutions of Three Dimensional Scattering Problems," Computer Techniques for Electromagnetics and Antennas, Part 2, University of Illinois Short Course, (1970).
29. Van Bladel, J., op. cit., p. 220.

30. Rudduck, R.C., op.cit., pp. 1-6.
31. Zaki, K.A. and Neureuther, A.R., "Scattering from a Perfectly Conducting Surface with a Sinusoidal Height Profile: TE Polarization," IEEE Trans. on Antennas and Propagation, Vol. AP-19, (March 1971), pp. 208-214.
32. Lysanov, Iu.P., "One Approximation for the Problem of the Scattering of Acoustic Waves by an Uneven Surface," Soviet Physics - Acoustics, Vol. 2, pp. 190-197.
33. Leporskii, A.N., "Experimental Investigation of Diffraction of Acoustic Waves by Periodic Structures," Soviet Physics - Acoustics, Vol. 1, pp. 50-59.
34. Phillips, O.M., op. cit.
35. Westlake, J., A Handbook of Numerical Matrix Inversion and Solution of Linear Equations, Wiley, (1968), pp. 10-14.
36. Wilkinson, J.H., Rounding Errors in Algebraic Processes, Prentice-Hall, New Jersey, (1963).